Chapter 1: Introduction

1.1. Summary

Thiol:disulphide oxidoreductases (TDORs) are essential for the correct insertion and/or removal of disulphide bonds. This thesis will concentrate on the role that TDORs play in the maturation of cytochromes *c* and in particular the role of a disulphide bond reducing TDOR, ResA, from the Gram positive soil bacteria *Bacillus subtilis* and *Streptomyces coelicolor*. ResA is responsible for the reduction of disulphide bonds present in the CXXCH haem binding motif of apo-cytochrome *c* prior to haem attachment. In many organisms cytochromes *c* are essential but, due to the presence of alternative terminal oxidases, *B. subtilis* is a perfect model organism for the study of cytochrome *c* maturation (CCM) system II.

1.2. Thiol:disulfide oxidoreductases (TDORs)

The *in vivo* formation of disulfide bonds is essential for the stability and/or activity of many proteins. TDORs belong to a superfamily of proteins, many of which are related to thioredoxin, that catalyse the reduction and oxidation of disulphide bonds and cysteine thiols, respectively. Families of proteins related to thioredoxin include glutaredoxins, glutathione S-transferases, alkylhydroperoxidases and TDORs (1).

1.2.1. Thioredoxin

Thioredoxin is a small (~12 kDa) protein found in cells of all types and is responsible for a range of functions. It protects the cell from oxidative damage,

helps maintain a reducing potential in the cytosol, donates reducing equivalents to ribonucleotide reductase, is a good indicator of intracellular redox status and can reduce protein disulphides (1). It is very stable and can remain folded at temperatures up to 80 ^{o}C. The structural template of thioredoxin has been adopted by many different proteins involved in disulphide bond reduction and oxidation for their function (1).

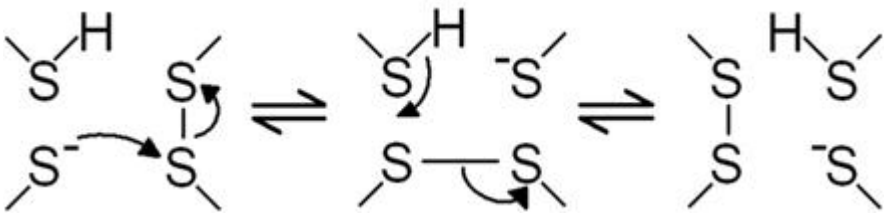

Figure 1.1. Schematic depiction of the accepted mechanism of disulphide exchange.

1.2.2. Structure of thioredoxin

The structure of thioredoxin consists of five β-strands encircled by four α-helixes. The active site of Cys-Pro-Gly-Cys is located at the C-terminus of the second β-sheet at the start of an α-helix (2). Thioredoxin has a standard redox potential of -270 mV at pH 7 versus the standard hydrogen electrode (SHE) (1), which indicates that the protein prefers to be in an oxidised state, with the disulphide bond between the cysteines of the active site (3). The N-terminal cysteine has a pK_a in the range of 6.7-7.5, significantly lower than a typical value observed for cysteine residues (8.2-9.0) and the C-terminal cysteine, which has a pK_a estimated to be more than 9 (4-6). The low pK_a of the N-terminal cysteine allows it to attack disulphide bonds within target proteins. This results in a mixed disulphide complex between thioredoxin and the target protein. This

disulphide is then resolved by the C-terminal cysteine. In this way thioredoxin acts to reduce proteins. Thioredoxin is then reduced by thioredoxin reductase, with NADPH as the reductant (1). This method of disulphide exchange appears to be universal across the entire thioredoxin-like superfamily and is shown schematically in Figure 1.1 and the structure of *E. coli* thioredoxin can be seen in Figure 1.2.

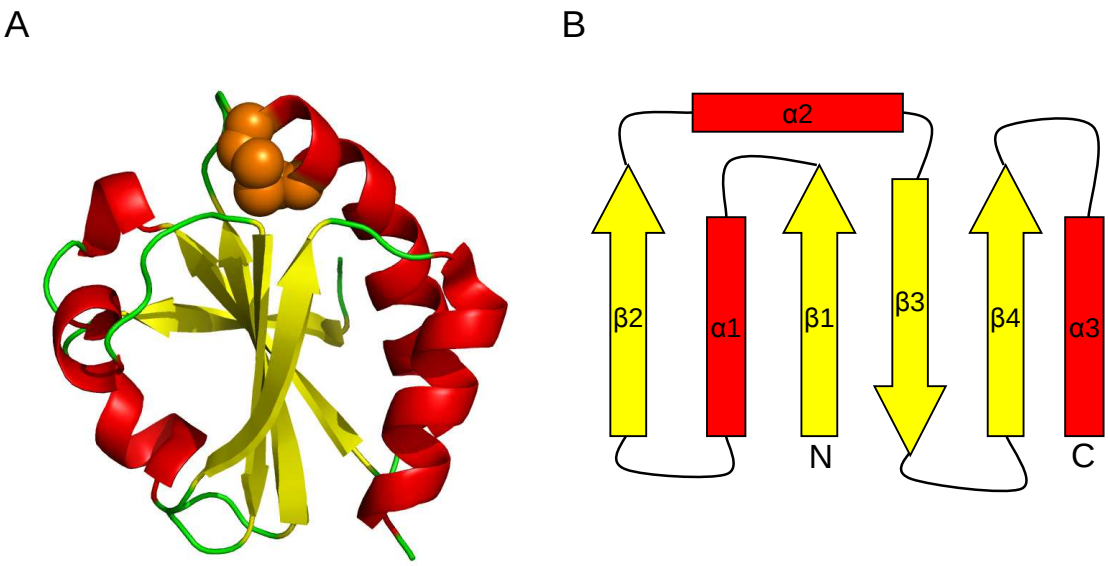

Figure 1.2. Structure of thioredoxin from *E. coli*. A, crystal structure of *E. coli* thioredoxin showing five β-strands (in yellow) encircled by four α-helixes (red), the active site cysteines are shown as orange spheres. Image created using Pymol with PDB file 2TRX and labelled using Adobe Photoshop 7. B, Connectivity diagram of the thioredoxin core, α-helices are shown in red and β-sheets in yellow.

1.2.3. Thioredoxin in *B. subtilis*

Although the *trxA* gene (encoding thioredoxin) in *B. subtilis* is regarded as essential, the roles of thioredoxin in *B. subtilis* and other Gram positive bacteria remains largely unknown. Inactivation of the *trxA* gene in *B. subtilis* results in

its inability to produce deoxyribonucleoside and cysteine or methionine (7). This mutation will also result in defects in cytochrome *c* maturation and endospore synthesis (7). Both processes (discussed below) require electrons passed from the integral membrane TDOR CcdA (8-10) as CcdA passes electrons to other more specific membrane bound TDORs, ResA for CCM and StoA for endospore synthesis (11,12), although it must be noted that direct exchange between thioredoxin and CcdA and between CcdA and ResA or StoA has not yet been observed.

1.3. TDORs of *B.subtilis*.

B. subtilis is a Gram positive bacterium, meaning that (unlike Gram negative bacteria such as *E. coli*) it has no periplasmic space. Therefore, all proteins positioned on the external side of the cytoplasm are required to be attached to the cytoplasmic membrane by one or more transmembrane segments. Eight membrane associated TDORs have been identified within the *B. subtilis* proteome: ResA, StoA, BdbA, BdbB, BdbC, BdbD, CcdA, YneN. These each assume a different role within the cell, though sometimes their functions are overlapping and often interrelated. ResA and StoA are both reducing TDORs, similar in structure with highly specific and dedicated, but different, roles. CcdA is not a thioredoxin-like protein, but is a reducing TDOR that is more general in its substrate specificity. BdbD also appears to have a broad range of substrates, but it is highly oxidising. BdbA and BdbD have a high level of sequence similarity and although BdbD has several potential substrates, no role has been determined for BdbA. BdbB and BdbC are responsible for the reoxidation of

BdbA and BdbD, respectively. Each of these *B. subtilis* TDORs is discussed in more detail below. As yet there has been no role identified for YneN.

1.3.1. ResA

B. subtilis ResA is a membrane bound reducing TDOR which is involved in cytochrome *c* maturation. Deletion of the *resA* gene results in the loss of mature cytochromes *c*, a phenotype that can be recovered by the addition of reductant to the growth medium, or the inactivation of the oxidising TDOR, BdbD (12). ResA is maintained as a reducing protein by CcdA (most likely via a direct interaction) before directly reducing the disulphide bond in the CXXCH haem binding site of apo-cytochromes *c*, although, as yet, no complexes between ResA and its redox partners have been observed.

1.3.1.1. Function of ResA

ResA functions within the cell to reduce the disulphide bond of apo-cytochrome *c* molecules. After translocation across the cytoplasmic membrane into the extracytoplasmic space, the oxidising TDOR BdbD introduces a disulphide bond at the CXXCH haem binding motif. It is essential for the cysteines of the apo-cytochrome *c* to be in the reduced state for the covalent attachment of haem to occur. When the *resA* gene is interrupted and transcription prevented no mature cytochromes *c* can be detected in *B. subtilis*. Site directed mutagenesis of the CXXC active site of ResA demonstrated that both cysteines are essential for reduction of the apo-cytochrome *c* (13).

1.3.1.2. Structure of ResA

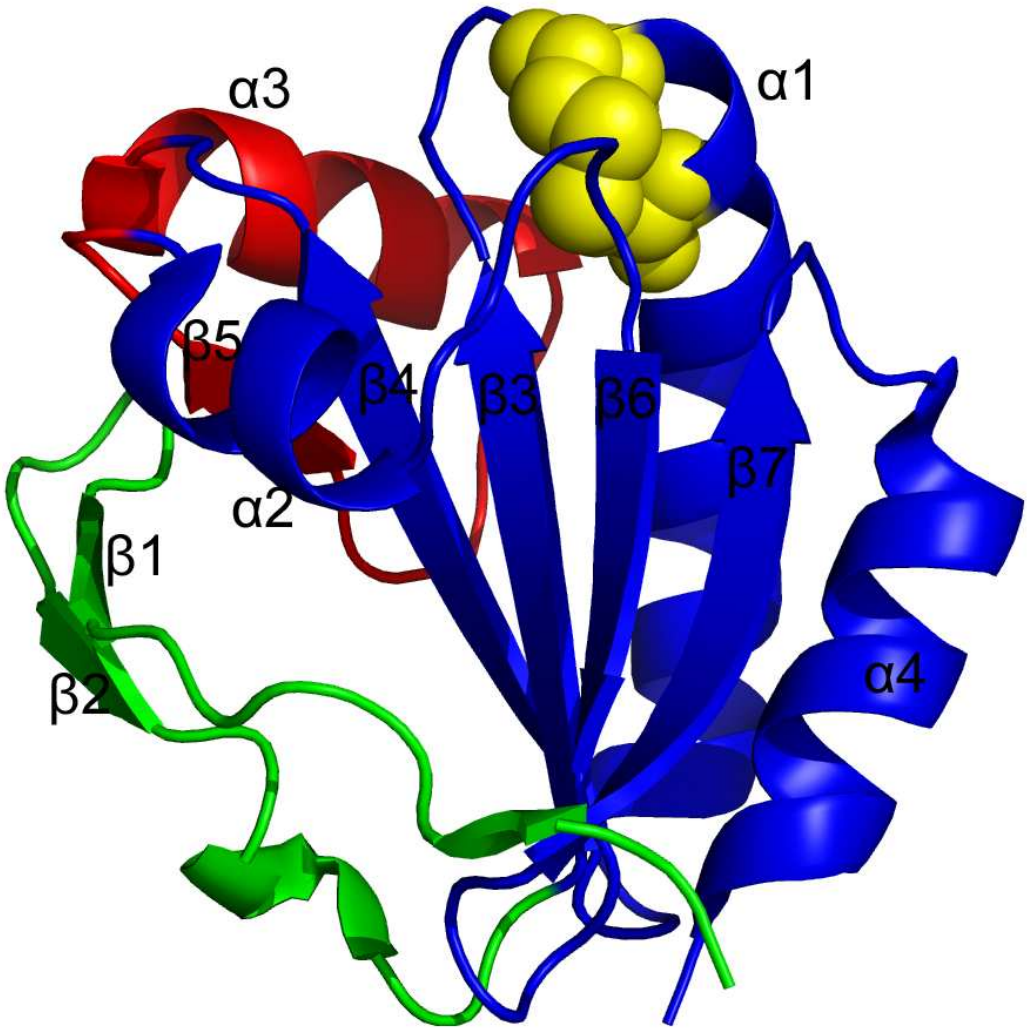

Figure 1.3. Ribbon structure of the oxidised form of *B. subtilis* ResA. α-helices and β-sheets are numbered in the order they appear in the amino acid sequences The structure demonstrates a typical thioredoxin fold (blue) with an additional N-terminal β-hairpin (green) and a central insert (red). The two cysteine residues of the active site are shown as yellow spheres. Image created using pymol with PDB file 1ST9 and labelled using Adobe Photoshop 7.

The structure of ResA includes the typical thioredoxin-like fold containing a mixed beta sheet of five strands surrounded by four alpha helices (Figure 1.3). The active site containing a CXXC motif is located at the terminus of alpha helix

1. There is a hydrophobic cavity near the active site which is thought to be involved in the recognition of apocytochromes *c* (14). ResA is an extracytoplasmic protein, anchored to the outer membrane by a single cross membrane segment (12). Note that the structure of the transmembrane segment of ResA has not been determined; structural studies employed a form of the protein containing only the soluble domain.

In the oxidised state the distance between the cysteines is about 2.16 Å, typical for a disulphide bond. Upon reduction this distance increases to 4.5 Å which is the longest intercysteine for any thioredoxin-like TDOR so far measured (14). This change is brought about by a 228^{o} rotation of the C74 side chain from the oxidised to reduced states, which partially exposes the thiolate to the solvent, potentially poising it for nucleophilic attack on the disulphide of the substrate polypeptide (14). As well as the active site cysteines, several other residues have been found to be important for reactivity, structural conformation and substrate recognition. Glu80, a residue that is buried in the oxidised structure, moves upon reduction exposing one of its carboxyl oxygen groups to the surface (14). This shift causes other residues to move in order to accommodate the new position of Glu80, which creates a hydrophobic cavity that is exposed to the solvent. This cavity is in immediate proximity of the active site and access to the partially exposed Cys74 is possible from the side of the cleft (14). It is very likely that the hydrophobic cavity and the glutamate at its base (Glu80) are important for substrate recognition by ResA. The conformational changes of the surface of ResA as it shuffles between the oxidised and reduced states determine which substrate it will bind to. Thus, when ResA is reduced the hydrophobic cavity

opens allowing specific recognition of a substrate. This allows the nucleophilic attack on that substrate disulphide, but, after the substrate is released, ResA resumes its closed, oxidised state ready to be reduced by CcdA (14). When this glutamate was replaced by a glutamine in a soluble version of ResA (sResA-E80Q) several intermolecular contacts were revealed, some of these close to the active site, which resulted in conformational changes to the active site cysteines (15). The protein did appear to be folded correctly although was less stable at a higher pH than wild type (15). The negative charge of Glu80 also appears to be important for regulating the reactivity of the active site thiols. The cysteines in the active site of sResA-E80Q were more reactive than those of the wild type protein (15).

Pro141 was also identified as being potentially important. This proline is absolutely conserved amongst thioredoxin-like TDORs. It adopts the *cis* configuration and has varying roles and importance for protein structure and substrate interactions depending on species. The vast majority of residues in any polypeptide will adopt the *trans* configuration, but proline is more likely to be found in the *cis* configuration than other residues. An estimated 6% of prolines in polypeptides adopt the *cis* configuration and, when this is observed, it often points to an important function for that residue. For example, in the *Escherichia coli* TDOR DsbA, it was shown that the conserved *cis* proline was important for substrate recognition and release (16). When the proline was replaced with either a threonine or a serine it was possible to trap DsbA in a complex with substrate polypeptides (16). It was also shown that when this residue was replaced with an alanine it strongly destabilised the structure of DsbA and *in vivo*

this variant, although oxidised, exhibited less than half the activity of the wild type protein in respect to its ability to fold alkaline phosphatase (17). Alanine is not prone to adopt the *cis* configuration and this was observed in the crystal structure of this DsbA variant; the loop between residues 149-152 adopted a new backbone configuration with Ala151 in the *trans* configuration (17).

The equivalent residue in CcmG (also known as DsbE), P144, is a key residue of the region near the active site of this protein. Studies of the crystal structure of the wild type protein and a P144A variant showed the *cis* configuration allows van der Waals interactions with the active site cysteines and allows the formation of a hydrogen bond with Thr82, which helps to stabilise the active site. The *cis* configuration also exposes the backbone nitrogen and oxygen of Ala143, which is favourable for interacting with binding proteins (18).

The residue Glu80 of ResA has previously been shown to play a key role in controlling the acid/base properties of the active site (15). Substitution of this residue led to a significant decrease in pK_a values of both active site cysteine residues, leading to the proposal that a role of Glu80 might be to ensure that ResA is unreactive towards non-substrate proteins, presumably because the deprotonated form of the cysteines is required for reactivity (15). In order to investigate the importance of the residues Pro141 and E80 of *B. subtilis* ResA *in vivo*, PCR mutagenesis was employed to engineer three ResA variants, P141S, P141T and E80Q, to be expressed and produced in a ResA deficient strain of *B. subtilis*.

1.3.1.3 Biophysical properties of ResA

The pK_a values of the cysteines of the active site are 8.8 and 8.2 for Cys74 and Cys77 respectively (15). The pK_a value for Cys74 is an average pK_a of a two proton dissociation event. It is likely that Cys74 is cooperatively coupled to another residue, possibly Glu105, which binds and releases protons simultaneously with Cys74 (15). Its redox potential was originally reported to be -340 mV at pH 7 versus SHE (12) but more recent studies have corrected this value to be -256 mV (19). The low reduction potential of ResA and high pK_a values of its active site cysteines are consistent with ResA being a reducing TDOR, as a disulphide formed between two cysteines with high pK_a values will more easily give up their electron to reduce the disulphide of their substrate protein. The pK_a value for Cys77 in sResA-E80Q was found to be 7.4, lower than in the wild-type protein (15). Although an accurate determination of the pK_a value of Cys74 was not possible in sResA-E80Q, due to its instability at high pH, it was estimated to be less than 8, again lower than Cys74 in the wild type protein (15). *In vitro* studies have demonstrated that the glutamate and the proline that lie between the two cysteines of the ResA active site (Glu75 and Pro76, respectively) are important to maintain the low reduction midpoint potential of ResA by maintaining the pK_a values of the active site cysteines, see Table 3.1 (19). When the active site of ResA was altered by mutagenesis to resemble the active site of *E. coli* DsbA, an oxidising TDOR, the pK_a values of the active site cysteines were significantly reduced and the reduction potential of the protein increased, see Table 1.1. Although the midpoint potentials were clearly defined, in the case of the ResA CEHC and CPHC variants, fits of the data indicated the involvement of four electrons (19). The reason for this is not

yet known. One possibility is that two variant ResA molecules associate in a co-operatively coupled electron-transfer process, although no evidence of a ResA-ResA association has been found in either the oxidised or reduced states (19). It is also possible that DTT interacts in an unexpected way with these variants but this was not supported by structural analysis (19). Changes in the reduction potential of the active site cysteines upon alteration of the residues that lie between the active cysteines have also been reported for other thioredoxin-like proteins, including *E. coli* thioredoxin (20), *E. coli* DsbA (21,22) and *Staphylococcus aureus* thioredoxin (23).

Table 1.1. Changes in active site cysteine pK_a and redox midpoint potential of ResA with the active site altered to that of *E. coli* DsbA.

ResA active site	pK_a value		ΔpK_a value		Midpoint redox potential (mV)	Number of electrons (n)
	Cys 74	Cys 77	Cys 74	Cys 77		
CEPC (wild type)	8.8 ± 0.2*	8.2 ± 0.1	-	-	-256 ± 1	2.2 ± 0.1
CPPC	7.02 ± 0.05	6.6 ± 0.1*	-1.8	-1.6	-232 ± 1	1.9 ± 0.2
CEHC	7.4 ± 0.1	7.5 ± 0.2	-1.4	-0.7	-229 ± 1	4 ± 1
CPHC	6.33 ± 0.07	5.71 ± 0.05	-2.5	-2.5	-221 ± 2	4 ± 1

*This pK_a is an average of two coupled pK_a values. ΔpK_a values report the differences from the properties of the wild type protein. Data taken from Lewin *et al* (2008) (19)

1.3.2. BdbD/BdbC

BdbD is an extracytoplasmic, membrane bound TDOR that functions to introduce disulphide bonds to several known substrate proteins and peptides. Its catalytic cycle is completed by its re-oxidation by BdbC, an integral membrane TDOR (24-27).

1.3.2.1. Function of BdbD

BdbD is proposed to be a general oxidiser of cysteine thiols of proteins and peptides transported across the cytoplasmic membrane. The BdbC/BdbD system of *B. subtilis* is homologous to the well described DsbA/DsbB system of *E. coli* and other Gram negative bacteria. DsbA is a soluble periplasmic TDOR that introduces disulphide bonds to the di-thiol motifs of a range of substrates (16,28,29). DsbA is rapidly re-oxidised by DsbB (16,30), a membrane bound TDOR that channels electrons in the membrane to the quinol pool (30).

Evidence exists to suggest BdbD will also oxidise substrates that do not require disulphide bonds to be active, leading to the requirement for proteins to specifically re-reduce them. For example, BdbD will oxidise the CXXCH haem binding motif of apo-cytochromes *c* which then must be reduced by ResA (12,15,27). This is also the case for an as yet unknown sporulation factor that requires the presence of another specific reducing TDOR, StoA. It seems unlikely that the oxidation of the apo-cytochrome *c* haem binding site is random, so it is likely this process serves to protect the cysteines of the apo-cytochrome from non-specific reactions until it is ready for haem insertion.

BdbD is also required for natural competence development facilitating DNA uptake into *B. subtilis* (25). It has been shown that the introduction of a disulphide is required for the stability of several proteins required to allow the transport of DNA across the cytoplasmic membrane and into the cell (25,31). ComCG, a surface localised pilin-like protein required for DNA binding, contains an intermolecular disulphide bond and a mutation in either the *bdbC* or

bdbD genes significantly reduces the presence of this bond, which renders ComCG unstable (25). Also involved in DNA uptake is ComEC, a large (776 residues) integral membrane protein containing a disulphide between Cys131 and Cys172, which is required for protein stability (31). Another competence protein, ComGG, has also been reported to have been found in small amounts in a dimeric form linked via a disulphide, also introduced by BdbD (25). Further evidence to support the importance of the BdbC/BdbD system for introducing disulphide bonds to substrates is that *B. subtilis* strains with a *bdbC* and/or a *bdbD* knockout mutation are unable to secrete *E. coli* alkaline phosphatase (PhoA) (25,32). *E. coli* PhoA is a good reporter of the activity of DsbA-like proteins as it requires two intramolecular disulphide bonds for stability and activity and when fused to the signal peptide and pro region of a lipase from *Staphylococcus hyicus*, it is efficiently secreted from *B. subtilis* into the growth medium where it is easily detected (32,33). Levels of secreted *B. subtilis* PhoA or *B. amyloliquefaciens* AmyQ were not affected in *bdbC*/*bdbD* mutants as neither of these proteins contain disulphide bonds (25,32). *Staphylococcus aureus* DsbA (SaDsbA) can complement a BdbC/BdbD deficient strain of *B. subtilis* in both PhoA excretion and for competence (34). *S. aureus* contains no homologue of BdbC or DsbB to work with SaDsbA as a cooperative redox pair. Therefore, SaDsbA must be reoxidised by an alternative pathway (34).

1.3.2.2. Structure of BdbD

Structural studies of the solvent-exposed soluble domain of BdbD demonstrated that it has a typical DsbA-like composition consisting of a thioredoxin domain and an α-helical domain (27). BdbD is most similar to SaDsbA, but exhibits

different features from both SaDsbA and EcDsbA. BdbD and SaDsbA both have a loop between helices α-3 and α-4 which is much longer than the equivalent observed in EcDsbA, but SaDsbA lacks the hydrophobic groove observed for both BdbD and EcDsbA (Figure 1.4B) (27). The most striking feature that stands BdbD apart from all other known DsbA-like proteins is the presence of a unique calcium site between the helical domain and the central β-sheet of the thioredoxin-like domain (Figure 1.4A). The calcium is coordinated by residues Gln49, Glu115 and Asp180 and unfolding studies showed that it is not required for the stability of the protein (27).

BdbD has a typical CXXC TDOR active site, located at the N-terminus of the long α-1 helix with the sequence Cys69-Pro70-Ser71-Cys72. Other features include the conserved *cis*-proline loop that lies directly opposite the active site cysteines and an unusual buried glutamate (Glu63) that lies in close proximity to the C-terminal cysteine (27).

1.3.2.3. Biopysical properties of BdbD

Like DsbA, BdbD is an oxidising TDOR. It has a very high reduction midpoint potential of -75 mV at pH 7 versus SHE, compared to that of reducing TDORs, such as thioredoxin and ResA. This high midpoint reduction potential is decreased by 20 mV when the calcium ion is removed from the protein indicating that the low potential is in part maintained by the calcium (27).

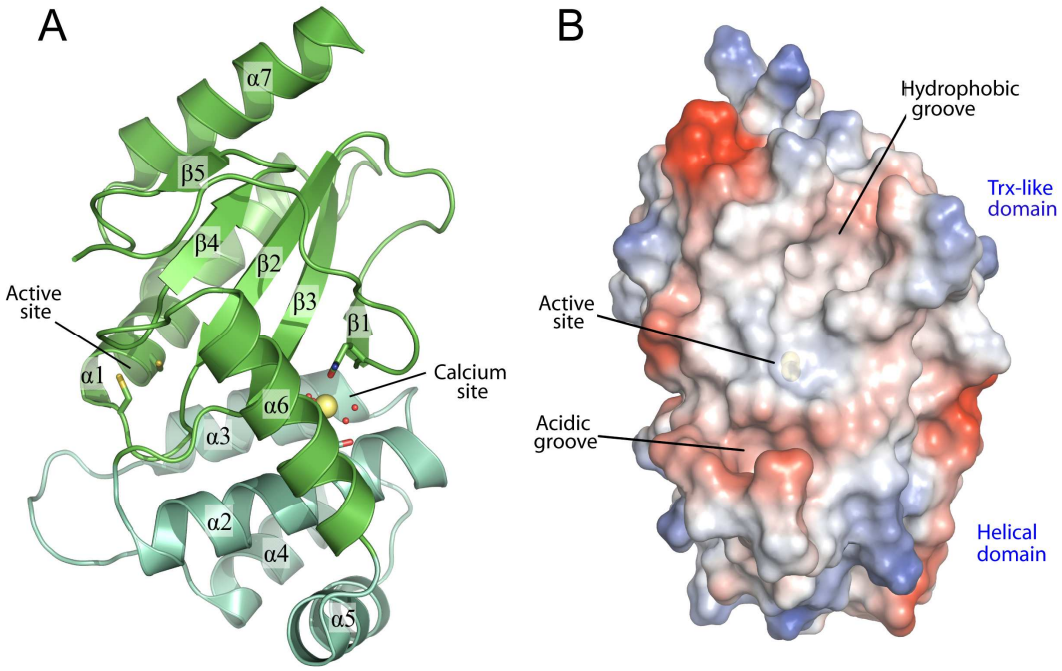

Figure 1.4. Structure of *B. subtilis* BdbD. A, ribbon structure showing the typical DsbA-like composition with the thioredoxin domain (green) and α-helical domain (teal), α-helices and β-sheets are labelled in the order they appear in the amino sequence of the protein. The calcium binding site and active site are also labelled. B, surface representation of BdbD. Thioredoxin-like (Trx-like) and helical domains are labelled as are the active site, acidic groove ans hydrophobic groove. The structure was solved from a soluble variant of BdbD so does not show the membrane anchor. Figure adapted from Crow *et al*, 2009 (27).

Although the exact pK_a values of the active site cysteines are not known, data indicate that they are both below 4.5. BdbD will unfold at pH 4.5, which makes it impossible to obtain an accurate pK_a below this pH value (27). The oxidising power of BdbD is based on the instability introduced to the protein by the disulphide bond in the oxidised form (27).

1.3.3. BdbA and BdbB

Like *B. subtilis* BdbC/BdbD, *B. subtilis* BdbB/BdbA is thought to homologous to the *E. coli* DsbB/DsbA system (24). BdbB is a paralogue of BdbC. As with *B. subtilis bdbC* mutants, strains lacking BdbB secreted a stable, active *E. coli*

PhoA, but only about four-fold less than the wild type. Mutants defective in *bdbC* exhibit a 15-fold decrease in active PhoA when compared to wild type, showing that although BdbC is more prominent, the two proteins are partially redundant (32). Cells lacking BdbA were unaffected in their ability to mature *E. coli* alkaline phosphatase (32). In fact, to date no role has been assigned to BdbA. It was originally thought that BdbA worked in redox partnership with BdbB to mature sublancin 168 due to the proximity of *bdbA* and *bdbB* to the *sunT* gene but is has since been demonstrated that this is not the case. This point is discussed further below (24,26,32,34). Sequence analysis shows it to be 43% identical to Bdb of *B. brevis*, a TDOR which is capable of complementing a DsbA mutation in *E. coli* (32,35).

BdbB is involved in the maturation of sublancin 168, a dehydroalanine containing lantibiotic produced by *B. subtilis* 168. It has 56 residues consisting of a 19 residue leader sequence and a 37 residue mature segment (36). The mature segment contains four cysteine residues which form two disulphide bridges (Figure 1.5). BdbC is able to partially complement a BdbB deficient strain of *B. subtilis* with regard to sublancin 168 production but BdbB is unable to complement BdbC deficiency with regard to the correct folding of proteins involved in genetic competence (26). It appears that BdbA is not essential for the folding of sublancin 168 as a mutation in the *bdbA* gene has no effect on its production (26). Originally it was assumed that BdbA was not needed because it could be replaced by BdbD, but a strain of *B. subtilis* deficient in both BdbA and BdbD but with functioning BdbB and BdbC was able to produce wild type levels of sublancin (34). It is possible that BdbB (and to a lesser extent BdbC) works

with SunT, a protein that belongs to a large family of ATP-binding cassette transporters, which is also required for sublancin secretion (26). SaDsbA was able to partially complement a knockout of all four *bdb* genes in *B. subtilis* with regard to sublancin production (34). SaDsbA has a reduction midpoint potential of -131 mV (37), which may explain why it only partially rescues the phenotype of BdbD deficient *B. subtilis* strains, as BdbD has a reduction midpoint potential of -75 mV (27).

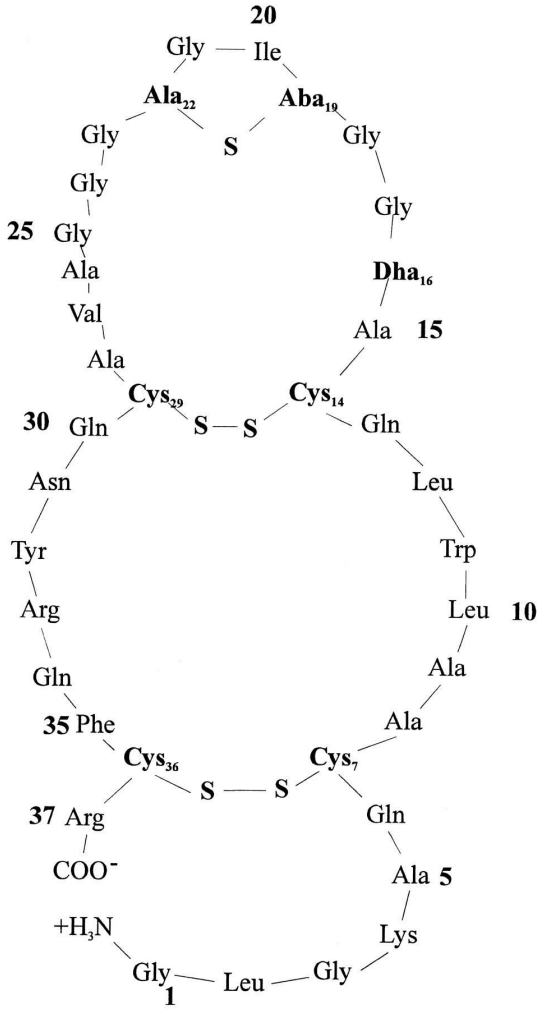

Figure 1.5. The locations of thioether and disulfide bonds in sublancin. The position of the disulfide bridges (between Cys7-Cys36 and Cys14-Cys29) and the lanthionine residue (Aba19-Ala22) were inferred by NMR. Figure from Paik *et al*, 1998 (36).

1.3.4. StoA

B. subtilis is able to form endospores when growth resources become depleted. Endospores are resilient to conditions of extreme heat and pH and are capable of remaining dormant for many years, until growth resources become available, where upon the spore will germinate and *B. subtilis* will return to normal vegetative growth. Many genes and their protein products have been identified as being involved, if not essential, to this process (38). StoA, also known as SpoIVH and YkvV, has a reductive role in endospore formation in *B. subtilis* (11,39).

It is expressed both in the mother cell and in the forespore under the regulation of σ^E and σ^G, respectively (40,41). It has recently been shown to have a very similar structure to ResA but there are some important differences: StoA contains an extended loop between strand β4 and helix α2 and whereas the third alpha helix of ResA is negatively charged, it is positively charged for StoA (Figure 1.6). ResA and StoA have separate functions that do not overlap. StoA cannot complement ResA deficiency or *vice versa* (11,39). Like ResA, it has a low midpoint potential, -248 mV at pH 7 versus SHE, but unlike ResA the pK_a values of the two cysteines of the active are significantly different, 5.5 and 7.8 for Cys65 and Cys68, respectively (39) whereas the pK_a values for ResA are very similar, 8.8 and 8.2 for Cys74 and Cys77, respectively (15).

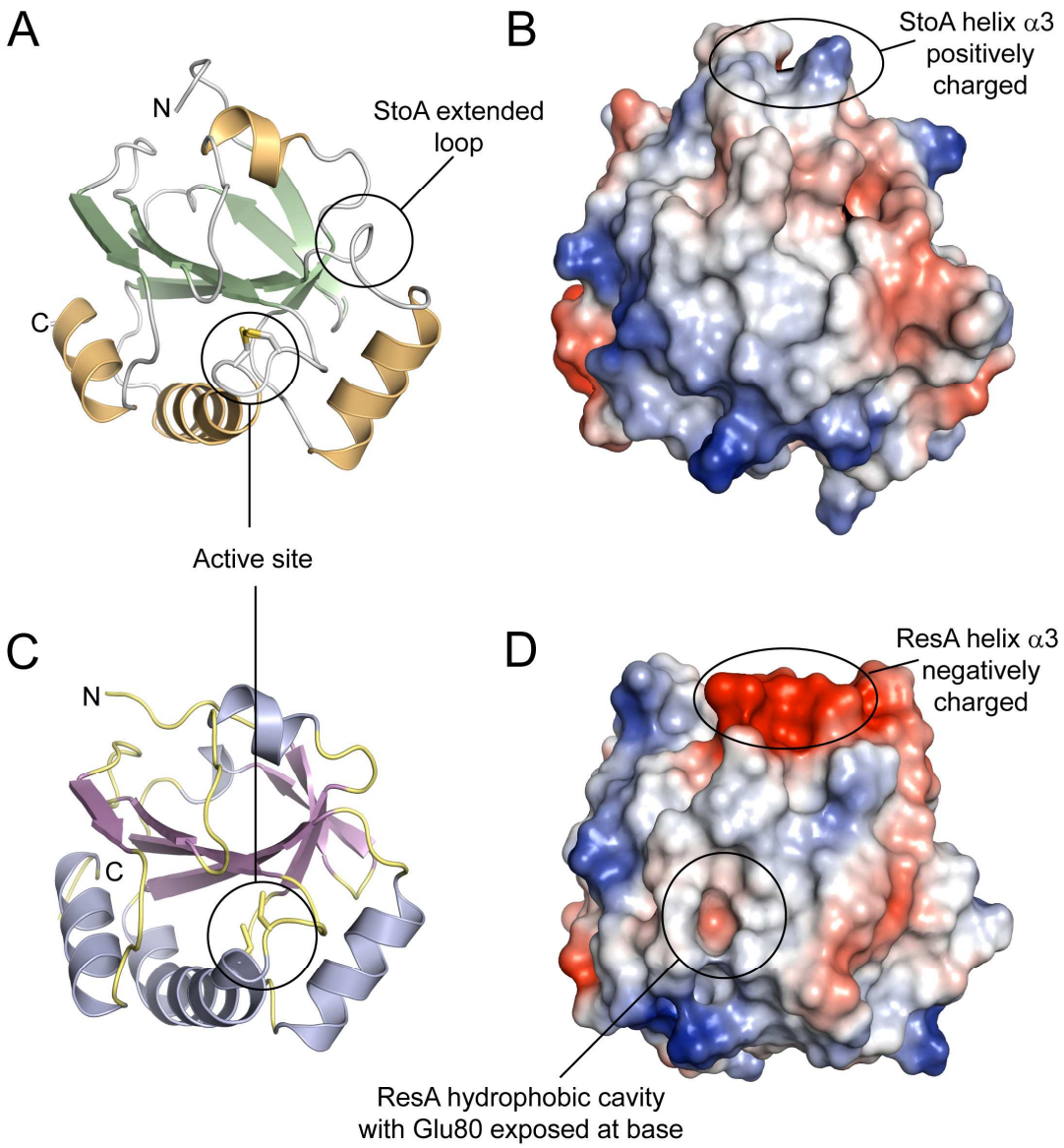

Figure 1.6. Comparison of the structure of sStoA and sResA from *B. subtilis*. *A* and *C* show the three-dimensional structures of sStoA and sResA, respectively, in schematic representation. *B* and *D* are surface representations of sStoA and sResA, respectively. Regions colored *red* indicate areas of high negative electrostatic potential, whereas *blue* areas indicate areas of high positive potential. Neutral regions are shown in *white*. Figure taken from Crow *et al*, 2009 (39).

The Trx-like domain is likely located in the intermembrane compartment in the forespore during endospore maturation (11). Deletion of *stoA* results in endospores being deficient in the cortex layer, meaning that the spores are much more susceptible to heat, lysozyme and chloroform treatment than the wild-type

spores (11). This spore cortex deficient phenotype can be suppressed by the deletion of *bdbD*. Deletion of *bdbD* also rescued the *resA* phenotype, indicating a connection between the reductive and oxidative branches of disulphide bond management systems. If BdbD is not active, StoA and ResA substrates are not oxidised so do not need to be reduced. In contrast to the ResA deficiency, a StoA deficiency cannot be complemented by the addition of DTT to the growth medium (11). Like ResA, it is very likely that StoA is re-reduced by CcdA, as a CcdA deficient strain of *B. subtilis* is also sporulation deficient (8,11). As with ResA, *in vivo* studies showed that both cysteines of the active site are essential for function (39). A conserved glutamate was identified as important in both ResA and StoA, Glu80 and Glu71, respectively. In ResA, Glu80 is likely to be important for substrate recognition and variations of this residue impair protein function (13,15,19) (discussed in detail in chapter 3). Likewise, replacement of Glu71 in StoA with a glutamine significantly reduced the number of viable spores (39). It is unlikely that this residue is involved directly in substrate specificity because it is completely buried (39).

1.3.5. CcdA

The integral membrane protein CcdA is a reducing TDOR that is functionally related to *E. coli* DsbD, which catalyses the transport of electrons from thioredoxin in the cytoplasm to periplasmic substrate proteins (42). *E. coli* DsbD has eight transmembrane segments (I-VIII) and a large periplasmic domain, which has a TDOR CXXC active site motif (Figure 1.7). *B. subtilis* CcdA transmembrane segments appear to be homologous to *E. coli* DsbD segments I-

VI but it does not contain a CXXC motif normally associated with TDORs, so it apparently has a different mode of function (9).

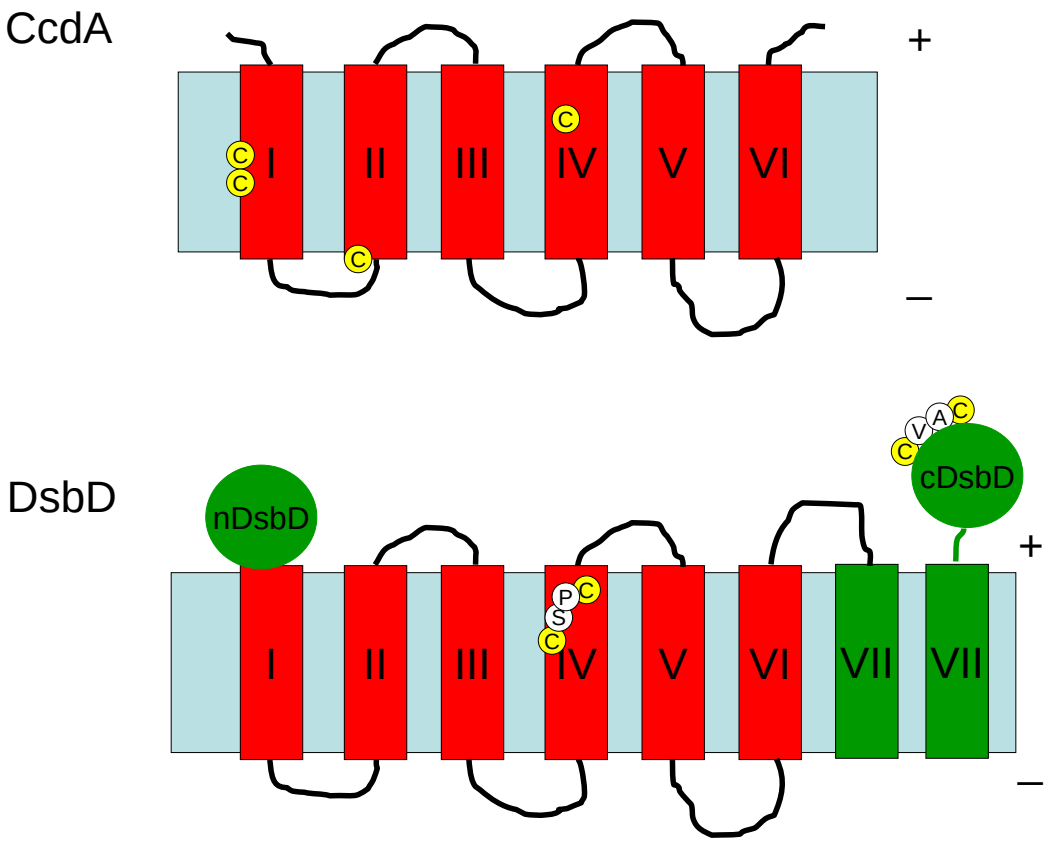

Figure 1.7. Comparison of the predicted topology of *B. subtilis* CcdA and *E. coli* DsbD. CcdA, the six predicted transmembrane segments are shown in red and the cysteine residues are shown as yellow circles, the transmembrane segments are numbered to correspond with the homologous segments in *E. coli* DsbD. DsbD, the transmembrane segments homologous to to CcdA are shown in red, the non-corresponding domains are shown in green. The positive and negative side of the cytoplasmic memebrane are depicted by the '+' and '-' symbols respectively. This diagram shows the DsbD transmembrane in a linear fashion for comparison with CcdA but the helices are predicted to form a circular channel through the membrane.

CcdA appears to have multiple substrate proteins, including ResA and StoA, to maintain their more substrate specific reducing abilities and like DsbD in *E. coli*, it receives electrons from thioredoxin (7). It is known to be important for the

efficient endospore synthesis and cytochrome *c* synthesis due to its function in passing the reducing equivalent to StoA and ResA, respectively (8,9,11,12). CcdA deficient strains were shown to only have 3.7% sporulation efficiency compared to 90% in the 1A1 wild type strain (8). The promoter for *ccdA* was found to be weak but activity increased during the transition from the exponential to stationary growth phases (8). As CcdA is known to be important for the production of cytochromes *c*, which are also primarily expressed in the late exponential phase, it is likely that CcdA production is stepped up to coincide with this and its involvement of spore synthesis (43).

1.4. Cytochromes *c*

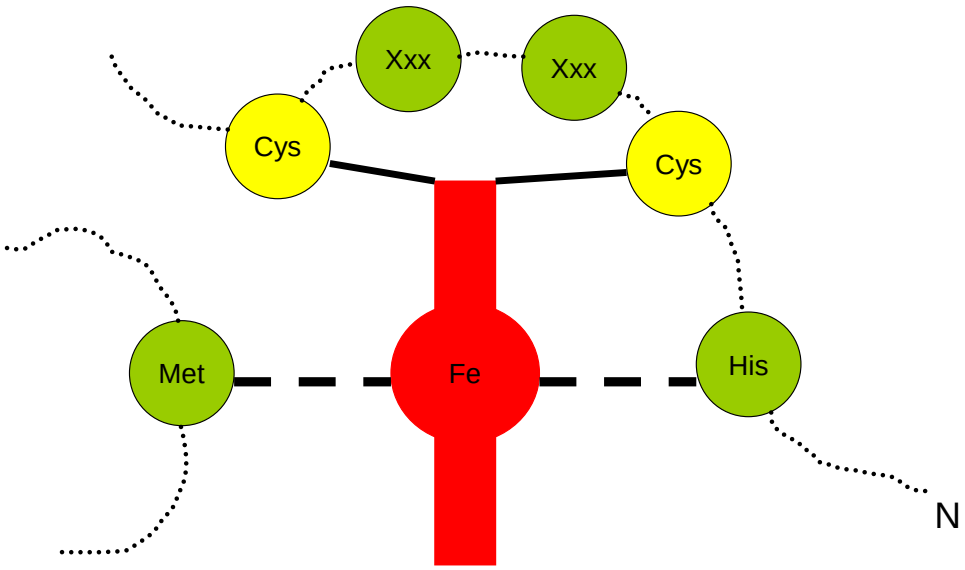

Figure 1.8 Haem attachment to cytochrome *c*. The haem (red) is covalently bound (solid lines) to the two cysteines and axial ligands (dashed lines) from the histidine and methionine residues position the haem.

Cytochromes are redox active haem-containing proteins. The iron of the haem cofactor can either be oxidised or reduced, which enables them to receive and donate electrons as part of respiratory pathways (44).

*C*ytochromes *c* differ from other types of cytochrome as they bind haem covalently via thioether bonds formed between vinyl groups of the haem and the two cysteine residues in a CXXCH motif, with the histidine side-chain serving as an axial ligand, positioning the haem iron, Figure 1.8 (45).

1.4.1. Haem C

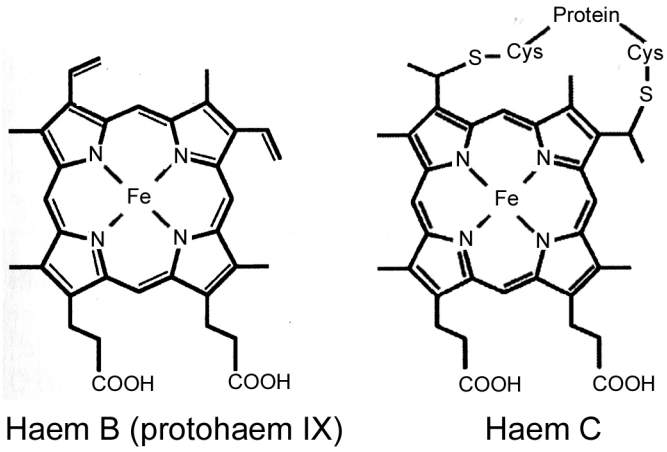

Figure 1.9. Haem B (protohaem IX) and haem C. Unlike haem B, haem C is covalently bound to protein via thioether bonds between the porphyrin ring of the haem and the cysteine thiols of the CXXCH motif present on the polypeptide.

Haem C consists of porphyrin (a cyclic tetrapyrrole) with an iron ion ligated at its centre, Figure 1.9. The haem iron is the most reactive part of the haem molecule and can cycle between the oxidised and reduced states ($Fe^{3+} + e^{-} \leftrightarrow Fe^{2+}$). Haem has several variations, as well as haem C, which have the same common precursor, haem B (or protohaem IX). Haem C is essentially a haem B that has been covalently attached via thioether bonds between the cysteine side chains of

the polypeptide and the vinyl groups of the porphyrin ring. In most cases the haem is attached to the cytochrome via two cysteine thiols in a CXXCH motif, although in some rare cases the haem will bind to a CXXXCH, CXXXXCH or CXXCK motif or be attached via only one thioether bond to a A/FXXCH motif (46).

1.4.2. Cytochromes *c*

Cytochrome *c* has been documented as having various roles. In eukaryotes cytochrome *c* is involved in electron transport for aerobic respiration in mitochondria and photosynthesis in chloroplasts (47). Cytochromes *c* can also act as signalling molecules within these two organelles. They are involved in apoptosis in mitochondria and electron transport in chloroplasts (48). In prokaryotes cytochromes *c* are involved in respiration (both aerobic and anaerobic electron transport), photosynthesis (oxygenic and anoxygenic), detoxification (via electron transport) and signalling (haem intermediate biosynthesis) (48). The location of cytochromes *c* varies depending on function and the organism in which they are found. For example, in prokaryotes *c*-type cytochromes are located outside the cytoplasmic membrane; in mitochondria, they are located in the intermembrane space, and in chloroplasts they are found in the lumen (48). *B. subtilis* has four cytochromes *c* (CtaC, QcrC, CccA and CccB, discussed in detail below) all of which are attached to the membrane either via a transmembrane anchor or as a lipoprotein (43,49-52).

1.4.3. Cytochromes *c* of *B. subtilis*

B. subtilis has four true cytochromes *c*: CtaC, QcrC, CccA and CccB, (Figure 1.10). A fifth protein called QcrB is a cytochrome *b* but unusually it has a covalently bound haem, although it is matured outside of the cytochrome *c* maturation system (53,54). All *B. subtilis* cytochromes *c* are membrane bound and none of them are essential for growth in rich or minimal media due to the presence of two quinol oxidases, cytochrome aa_3 (which is likely to be the major oxidase) and cytochrome *bd*, neither of which rely on cytochromes *c* (50,52). The aerobic respiratory pathways of *B. subtilis* are illustrated in Figure 1.11.

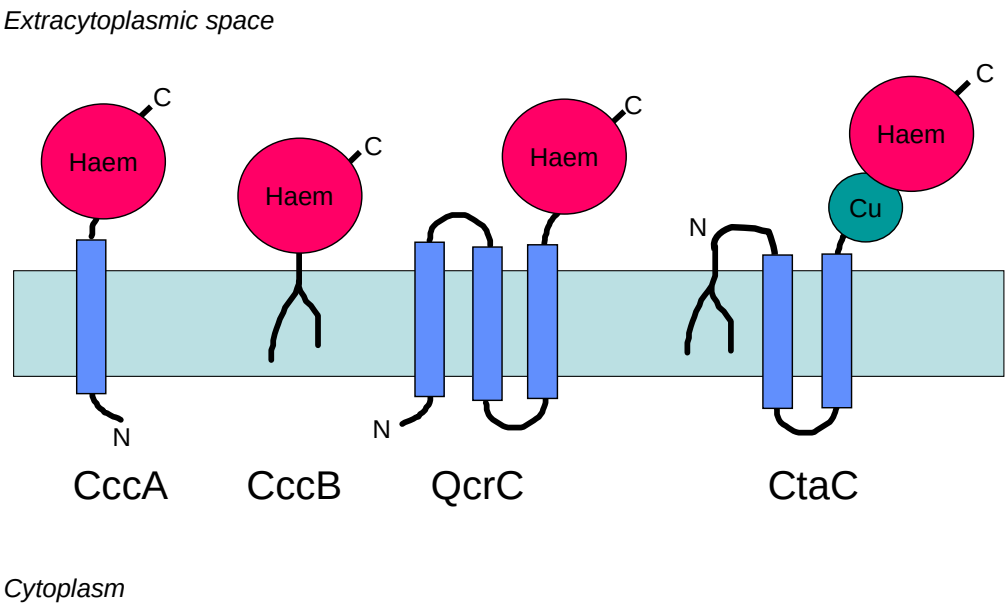

Figure 1.10. Schematic topology of *B. subtilis* cytochromes *c*. Details of each cytochrome *c* are discussed in the text. Briefly, CccA is cytochrome c_{550}, CccB is a cytochrome c_{551}, QcrC is the cytochrome *c* subunit of the *bc* complex and CtaC is subunit II of cytochrome *c* oxidase.

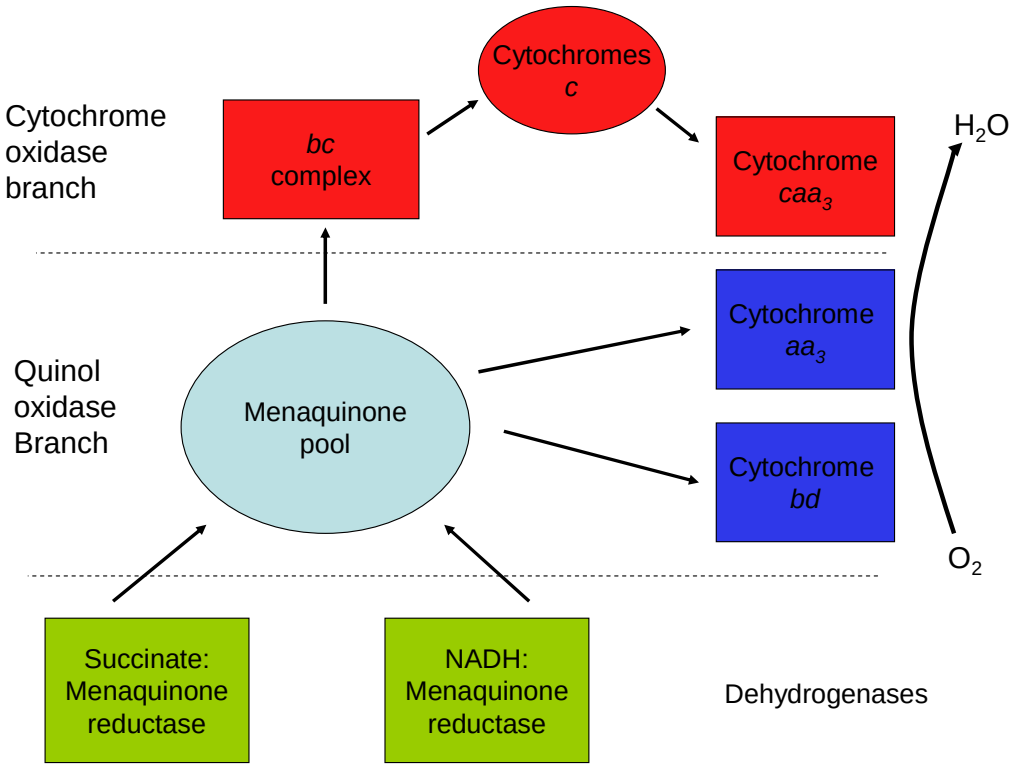

Figure 1.11. Aerobic respiratory chains of *B. subtilis*. Dehydrogenases reduce menaquinone which passes electrons to the terminal oxidases, either directly to the two quinol oxidases or via the *bc* complex and small cytochromes *c* to the cytochrome *c* oxidase.

1.4.3.1. QcrC

The 29 kDa protein QcrC is the cytochrome *c* subunit of the cytochrome *bc* complex (menaquinone:cytochrome *c* reductase) that transfers electrons from low potential quinol in the membrane to cytochrome *c* and adds to the transmembrane proton gradient (55,56). A typical bc_1 complex contains three protein subunits, which contain four prosthetic redox groups between them. These are the cytochrome *b* which contains two low spin haem *b* groups; a cytochrome c_1, which contains one type *c* haem; and a Rieske type iron-sulphur protein (55). Due to the cytochrome *b* of the *B. subtilis* complex being similar to that of a b_6f complex and the organisation of the cytochrome *c* subunit, the

complex encoded by the *qcr* operon is called a *bc* complex, with no subscript (56).

QcrC has a structure that resembles a b_6f complex subunit IV fused to a cytochrome *c* and is predicted to have three transmembrane helices (56). The predicted structures of the putative protein products encoded by the *qcr* operon suggest a distinct protein complex that is closely related to known bc_1 and b_6f complexes (56). It is the C-terminal end of QcrC that contains the CXXCH motif and sequence comparison demonstrated that this region is more similar to *B. subtilis* CccA than to the equivalent regions of other bc_1 and b_6f complexes (56). The cytochrome *b* of this *bc* complex, QcrB, is a 22 kDa protein and is novel among cytochromes *b* as it can covalently bind haem, most likely via Cys43 (53). The cytochrome bc_1 complex will liberate two electrons from quinol: one is passed along a high potential chain of the Rieske iron-sulphur protein to a cytochrome *c* and then the terminal oxidase; the second is passed down a chain of lower potential *b*-type haems across the membrane to contribute to the electrical and chemical work of the transmembrane proton gradient (57). The complex has been isolated from mitochondria and several bacterial species and the very similar b_6f complex has been isolated from plant chloroplasts and from cyanobacteria (57).

1.4.3.2. CccA

B. subtilis CccA, also known as cytochrome c_{550}, is a 13 kDa membrane bound protein. It is predicted to consist of an N-terminal membrane anchor, which spans the membrane in the form of an alpha helix, and the C-terminal haem

domain, which is exposed to the extracytoplasmic side of the membrane (50). The deletion of the *cccA* gene showed that CccA is not essential for the growth of *B. subtilis*. This deletion also led to the discovery that *B. subtilis* has another small cytochrome *c*, CccB (50). The expression of *cccA* has been linked to the onset of sporulation, possibly playing a role in the initiation of sporulation through regulation of *spo0A* (58). When *cccA* was over-expressed in *B. subtilis*, sporulation was significantly accelerated and in a *cccA* defective mutant sporulation was delayed (58). Several sporulation associated factors were detected in higher level in the CccA over-expressing mutant, including higher levels of *spo0A* transcripts and higher levels of stage-II-specific alkaline phosphatase and stage-III-specific glucose dehydrogenase activities (58). Although CccA is not essential for sporulation, the expression of *cccA* may play an important role in the initiation of sporulation, possibly by aiding the activation of Spo0A (58). In *B. anthracis*, the causative agent of anthrax, CccA and CccB (discussed below) have been shown to be involved in the regulation of toxin gene expression by affecting the expression of the master virulence regulator AtxA (59). The loss of CccA and CccB resulted in deregulated AtxA-mediated gene expression and, therefore, an increase in the expression of the toxin genes (59).

1.4.3.3. CccB

This second small protein, CccB or cytochrome c_{551}, is a lipoprotein that is expressed at a low level during exponential growth along with the gene *yvjA*, which encodes a 29.8 kDa polypeptide with no known function (51). The C-terminus of CccB is very similar to that of CccA, consisting of a single haem domain. The N-terminal domains are clearly different. While CccA has a 32 residue non-cleaved signal sequence membrane insertion that acts as a membrane anchor for the haem domain (50), CccB contains at its N-terminus a bacterial lipoprotein consensus sequence (Leu-Ala-Ala-Cys) that is modified by the addition of a diacylglycerol moiety at the cysteine residue. The N-terminal peptide is then cleaved by type II signal peptidase allowing the modified cysteine residue at the N-terminus to become anchored to the membrane by the fatty acid residues (51). Due to the size and other similarities to CccA, CccB is hard to distinguish on SDS-PAGE gels stained for haem or with Coomassie.

1.4.3.4. CtaC

CtaC is subunit II (SU II) of *B. subtilis* cytochrome *c* oxidase and, like CccB, is a lipoprotein (52). *B. subtilis* has three different respiratory oxidases in the cytoplasmic membrane. Cytochrome aa_3 and cytochrome *bd* are both quinol oxidases and cytochrome caa_3, of which CtaC is part, is a cytochrome *c* oxidase (52). Of these three systems, only a deficiency in cytochrome aa_3 significantly affects cell growth (60). Due to its close similarity to *Paracoccus denitrificans* cytochrome aa_3 the following structural information has been inferred; the two haem A groups are harboured by CtaD (SU I); CtaC contains the Cu_A di-copper centre and the cytochrome *c* domain (both domains are exposed to the

extracytoplasmic side of the membrane). CtaC is anchored in the membrane by two transmembrane alpha-helixes towards the N-terminus of the polypeptide. Both the N-terminal and C-terminal domains are located on the extracytoplasmic side of the membrane (52). The cytochrome caa_3 oxidase is part of a well characterised family of haem-Cu oxidases. They are membrane bound enzymes involved in electron transfer reactions, reducing dioxygen to water and pumping protons across the membrane (61). *B. subtilis* cytochrome caa_3 is comprised of four subunits encoded by *ctaC, ctaD, ctaE* and *ctaF* (subunits SUII, SUI, SUIII and SUIV, respectively) (62). *B. subtilis* caa_3 is similar to aa_3 in respect to amino acid and structure, with only SUII (the substrate binding subunit) differing to accommodate cytochrome *c* in the caa_3 and menaquinol in aa_3 (60,62). The *cta* genes encoding *B. subtilis* cytochrome caa_3 is an operon *ctaCDEFG,* which is part of a gene cluster *ctaABCDEFG*. The *ctaA* and *ctaB* genes encode for a haem A and heam O sythase, respectively, and *ctaG* codes for a caa_3 assembly factor (62-64). SUI is 621 residues and about 69 kDa and is larger than its mitochondrial or *Paracoccus denitrificans* homologues due to it having two extra transmembrane segments (62). It contains a bimetallic cytochrome a_3/Cu_B centre and the bisimidazole cytochrome *a* haem and several residues thought to be important for proton translocation (62). SUII, encoded by *ctaC*, contains the di-copper centre and a haem C, discussed above. SUIII in *B. subtilis* has a shorter N-terminus than the mitochondrial or *P. denitrificans* subunits, having two less transmembrane segments, but is similar in size to the *E. coli* cytochrome *bo* subunit III (62). It does not contain any redox centres and is not an important element of the enzyme with regard to proton pumping (65). SUIV is a unique small, 12.6 kDa, protein that does not appear to be well conserved among

Bacillus sp. but may be a novel *Bacillus* oxidase subunit (62). Electrons are passed from the substrate cytochrome *c* to the SUII Cu via the SUII haem C, then through the haem A group of SUI to the haem A_3-Cu centre (61). *B. subtilis* caa_3 is not a major oxidase and is mainly produced when cells are grown on non-glucose based media at the onset of the stationary growth phase and it is required for sporulation in the absence of cytochrome aa_3 (60,66,67)

1.4.4. Cytochrome *c* maturation

Cytochromes *c* are found in nearly all forms of life, usually as part of respiratory electron transport chains. They differ from other cytochromes in the way they have a type C haem covalently bound via two sulphur groups of two cysteine residue side chains. Although it has been demonstrated that haem can bind to an apo-cytochrome *c in vitro* in the absence of accessory proteins, nature has developed several systems to ensure this occurs quickly and with the correct stereochemistry *in vivo* (68). To date, five different systems for the maturation of cytochromes *c* have been identified. They are designated cytochrome *c* maturation (CCM) systems I-V and, apart from a few rare exceptions, only one of these is found in any particular cell type (46). System I, II and III have been studied in some detail, although there is still much to learn, but very little is known about the recently proposed systems IV and V. Although these systems appear very different in the numbers of proteins involved, they all share a common end result, the covalent attachment of haem to cytochromes.

1.4.4.1. CCM System I

CCM system I is the best studied of the CCM systems. It is commonly found in Gram-negative bacteria and the mitochondria of plant cells. It is seemingly the most complex of the systems with many dedicated proteins: in *E. coli*, CCM system I has eight dedicated proteins. The roles of many of the components involved in CCM system I are still not fully understood.

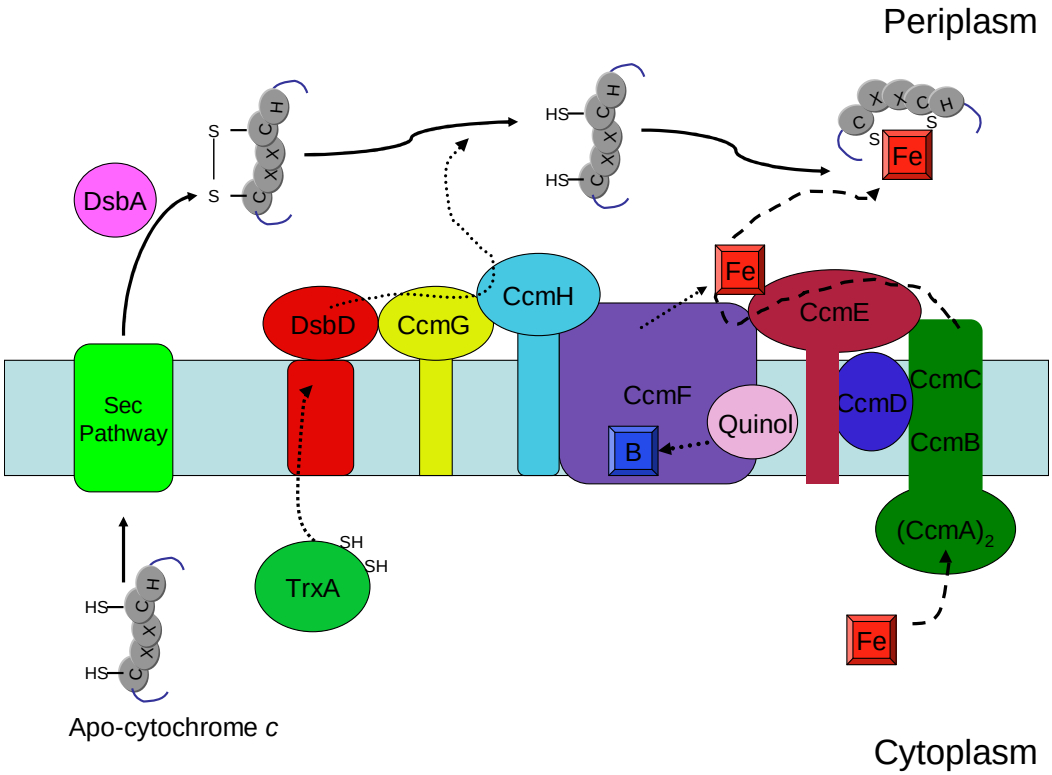

Figure 1.12. CCM system I from *E. coli*. This system is typical of most Gram negative bacteria. Variations can found in plant and red algal mitochondria as well as α, β, and γ proteobacteria and deinococci. Apo-cytochrome *c* enters the periplasm from the cytoplasm via the Sec pathway where the cysteine thiols are oxidised by DsbA. Haem C (red box labelled 'Fe') is likely to be transported to the periplasm via a complex formed by CcmA, CcmB, CcmC, CcmD and CcmE. Electrons are passed from TrxA in the cytoplasm through DsbD (also known as DipZ), to CcmG, to CcmH which reduces the disulphide of the apo-cytochrome. The haem C is likely reduced by CcmFH, by e^- received from quinol via a haem B (blue box labelled 'B'). The covalent binding of the haem to the apo-cytochrome *c* is also likely carried out by CcmFH. Solid arrows denote the path of the apo-cytochrome *c*, dotted arrows denote the path of electrons (e^-) and dashed denote the path of the haem. The roles of each of the proteins involved are discussed in detail in the text.

Ccm proteins, responsible for the covalent attachment of haem to the apocytochrome in the periplasm, are all localized to the cytoplasmic membrane (Figure 1.12) (69). The *ccm* genes are commonly arranged in most γ- and β-proteobacteria as a single cluster and transcribed at the same time and in the same direction (69). The spaces between the genes are usually very short, except for the region between *ccmB* and *ccmC*. Some organisms vary from this general rule, for example *Shewanella oneidensis* has two clusters, *ccmABCDE* and *ccmFGHI*, which are transcribed divergently and separated by two genes, one of which codes for a cytochrome *c* (69).

Maturation of the cytochromes *c* occurs in the periplasm. The apo-cytochrome *c* has an N-terminal signal sequence, which allows it to pass through the cytoplasmic membrane via the Sec pathway (70). This leader sequence was found to be removed from apocytchrome *c* located in the periplasm in a *Paracoccus denitrificans* mutant unable to synthesise mature cytochrome *c* (70). Other evidence supporting the periplasmic maturation of *c*-type cytochrome includes the finding that, in *E. coli*, if the apocytochrome *c* is translated without the leader sequence, only apocytochrome *c* is found in the cytoplasm, and that the products of many of the genes required for cytochrome *c* biogenesis are found on the periplasmic side of the cytoplasmic membrane (70).

For simplicity, the CCM system I described here is based on the current knowledge of the *E. coli* system, with details from systems from other organisms where differences are thought to occur. Sequence analysis identified CcmA and CcmB as an ABC transport complex with CcmB being membrane bound with the

associated CcmA bearing an ATP-binding cassette (46,69). Little is known about how haem is transported into the periplasm from the cytosol where it is synthesised but it is possible that CcmA and CcmB act in conjunction with CcmC and CcmD to do this (46). Haem C has been detected in the oxidised form covalently attached to CcmE in a purified CcmCDE complex with CcmC providing the fifth and sixth axial ligands (71). It is possible that, due to the hydrophobic nature of haem, it can partition into the cytoplasmic membrane and reach the protein in the periplasm; however, free haem is potentially toxic to the cell, which makes this idea unlikely (46). CcmE is anchored to the cytoplasmic membrane and is a haem chaperone. It is thought that the haem is transferred to CcmE from CcmC (69,72), an integral membrane protein with six transmembrane helices, which is thought to bind haem from the periplasm (69). Haem becomes covalently attached to CcmE but only in the presence of CcmC; this attachment occurs in the absence of CcmFGH showing that these three proteins are not involved in transporting haem from the cytoplasm (73).

CcmF is a large integral membrane protein with 11 transmembrane helices that receives haem from CcmE (69). CcmF contains a haem B that is reduced by quinols and is likely to reduce the haem C prior to covalent attachment (71). It is thought that CcmE shuffles between CcmC and CcmF transferring haem between them (72) or these three proteins may be bound as a super-complex (46). CcmD is a small monotopic membrane protein, which stabilizes the interaction between CcmC and CcmE (69,72). The haem-lyase complex that mediates the covalent attachment of haem to the apocytochrome is thought to be formed by the association of CcmF with CcmH, which possibly serves to keep apo-cytochrome

c cysteines in the reduced form (69). In *Rhodobacter capsulatus* the N-terminal, membrane spanning segment of CcmI, which is not found in *E. coli*, is thought to be involved with CcmF-CcmH dependent haem ligation and the C-terminal periplasmic domain of it is thought to be involved in the CcdA- and CcmG-dependent reduction of the thiol groups of apo-cytochrome *c* (74).

CcmG (also known as DsbE) is a membrane bound TDOR that faces the periplasm. Deletion of the *ccmG* gene results in the complete loss of cytochromes *c* in *E. coli* (75). The CXXC motif of the active site is located at the bottom of a cleft, which is capped by the *cis*-Pro144 (18). Cys80 is solvent exposed and Cys83 is buried (18). When one or both of the cysteine residues of the active site (CPTC) were changed to serine, low levels of *B. japonicum* holocytochrome c_{550} were detected when expressed in *E. coli*, suggesting these residues are not essential for the maturation of all cytochromes *c* (75). The conserved GVXGXPETF sequence has been identified as the fingerprint of the CcmG subfamily (18). Two important residues within the fingerprint region have been identified, the conserved *cis*-Pro144 and Glu145, which are believed to stabilise the structure of the active site (18). Three acidic residues around the redox-active centre of CcmG (Glu86, Glu145 and Asp162) are thought to be important for maturation of cytochromes *c*. Single substitutions of these residues to an alanine demonstrated a wild-type phenotype, but double and triple mutations of these residues were less able to mature cytochomes *c* (76). Electrons are channelled from thioredoxin in the cytoplasm via DsbD to CcmG (77). Direct disulphide exchange has been demonstrated between the N-terminal periplasmic domain of DsbD and CcmG. This was achieved by trapping active

site cysteine variants of these proteins in a mixed disulphide and determining a crystal structure for this complex (78). The disulphide exchange between wild-type DsbD and CcmG is fast, $k = 3.9 \times 10^5\ M^{-1}\ s^{-1}$ (78). The redox potential of CcmG is between -203 and – 220 mV at pH 7 versus SHE (78). When the *E. coli* CcmABCDEFGH proteins were over produced in a Δ*dsbD E. coli* strain some cytochrome *c* maturation activity was restored, although not to wild type levels (79). This could suggest a way of reducing CcmG independently of DsbD or simply show that reduced CcmG will occur in the oxidising periplasmic environment but can only be observed when over-expressed.

A soluble monomeric 21.1 kDa protein called DsbA is responsible for oxidising the two cysteine residues of the haem binding site of the apo-cytochrome *c* (42,48). It contains a single catalytic dithiol/disulfide pair within the CXXC active site motif (42). DsbA is known to catalyse the oxidation of reduced, unfolded proteins. DsbA contains a helical insertion that forms a hydrophobic patch on the surface of the protein as well as a hydrophobic groove near the active site (80). The oxidising power of DsbA is in some way related to the residues that lie between the cysteines of the active site. When the active site of *E. coli* thioredoxin was altered to resemble that of *E. coli* DsbA, a decrease in pK_a of the N-terminal cysteine from 7.1 to 6.1 was recorded (21) and when the active site of DsbA was altered to resemble that of thioredoxin, the opposite was found resulting in an increase in pK_a from 3.3 to 6.2 in the N-terminal cysteine (22). The redox process for TDORs such as ResA involves two electrons ($n = 2$).

The precise mechanism of substrate introduction and release by DsbA is not yet known. A conserved *cis*-proline has been shown to be involved in the resolution of DsbA-substrate intermediates (16,29). DsbA is reoxidised by DsbB (30). DsbB has four transmembrane helices with both the C- and N-termini located in the cytoplasm. The first periplasmic loop (P1) contains the well conserved CXXC motif, the second periplasmic loop (P2) has two cysteines separated by 25 amino acid residues (42). Despite the fact that the reduction potential is far below that of DsbA, it is the disulphide of P2 between Cys104-Cys130 that is most likely donated to DsbA (80). DsbB contains a ubiquinone co-factor that oxidises the CXXC motif in P1 that may promote the oxidation of DsbA, although ubiquinone-free DsbB will still oxidise DsbA to about 40% efficiency (80). The crystal structure of the DsbA-DsbB complex showed that the hydrophobic groove of DsbA captures the Pro100-Cys104-Phe106 region of the DsbB P2, which causes the two cysteines of the P2 loop to be out of range for a disulphide bond and allows a mixed disulphide between Cys30 of DsbA and Cys104 of DsbB (81). A likely model of the reoxidation of DsbA by DsbB starts with the nucleophilic attack by the Cys30 thiol on the disulphide formed between Cys104 and Cys130 of the DsbB P2 leading to the formation of a mixed disulphide between DsbA-Cys30 and DsbB-Cys104 (82). The DsbB-Cys130 thiol then attacks the disulphide between Cys41 and Cys44 of DsbB P1 forming an interdomain mixed disulphide between DsbB-P2-Cys130 and DsbB-P1-Cys41 leaving DsbB-P1-Cys44 reduced (82). At this point the two periplasmic domains of DsbB and DsbA are locked in a ternary complex. DsbA-Cys33 attacks the mixed disulphide between DsbA-Cys30 and DsbB-Cys104 resolving the complex leaving DsbA oxidised, driving the resolution of the intradomain

disulphide of DsbB and the donation of two electrons to the quinone pool leaving both DsbA and DsbB in the oxidised state (82,83).

1.4.4.2. CCM System II

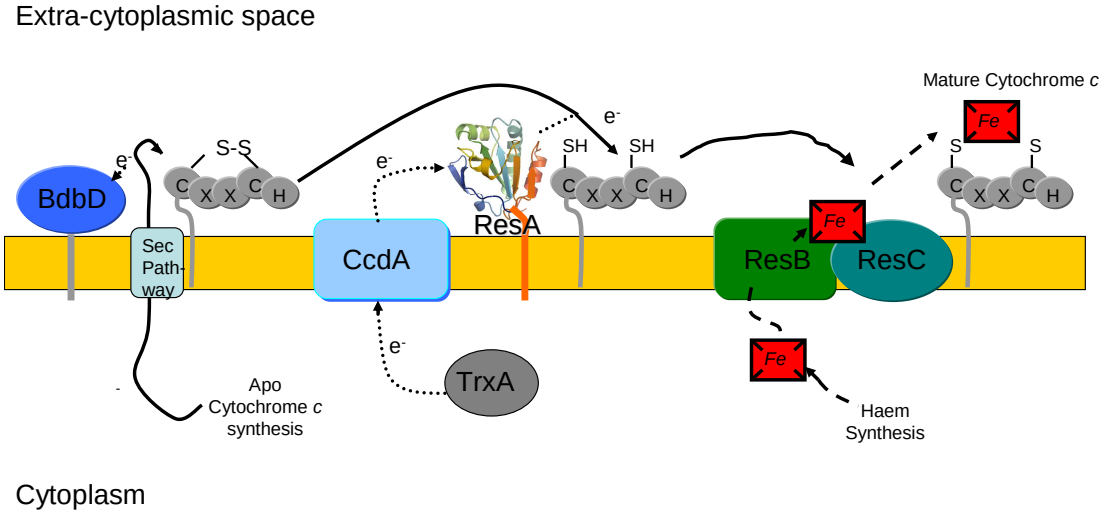

Figure 1.13. CCM system II from *B. subtilis*. This system is typical of many Gram positive bacteria as well as chloroplast thylakoid membranes. The apo-cytochrome *c* is transported from the cytoplasm via the sec pathway, and the cysteine thiols are oxidised by BdbD. The newly inserted apo-cytochrome *c* disulphide is reduced by ResA. ResA receives electrons (e^-) from CcdA, which receives e^- from thioredoxin (TrxA) in the cytoplasm. Haem (Red box labelled 'Fe') is transported across the membrane by ResB. It is likely that the covalent binding of the haem to apo-cytochrome c is catalysed by ResC. Solid arrows show the path of the apo-cytochrome *c*, dotted arrows show the path of e^- and the dashed arrows show the path of the haem.

Although CCM system II is less complex than CCM system I, there are some similarities (Figure 1.13). *B. subtilis* has four genes that are required for the maturation of cytochromes *c*: *ccdA*, *resA*, *resB* and *resC* (9,12,54). Of the products encoded by these genes, ResA, ResB and ResC all appear to be dedicated to CCM. Neither CcdA nor ResA are absolutely essential for CCM as the CCM negative phenotype achieved by their inactivation can be reversed by

the introduction of reductant to the growth medium or by the inactivation of *bdbD*, as discussed above (24).

The *resABC* genes are encoded by an operon, which also encodes a typical two-component regulatory system from *resDE* (66) (Figure 1.14). Several genes involved in both aerobic and anaerobic respiration in *B. subtilis* are regulated by ResD and ResE, including genes encoding the *bc* complex, the cytochrome *c* oxidase and genes required for haem sythesis, as well the *res* operon itself (66,84).

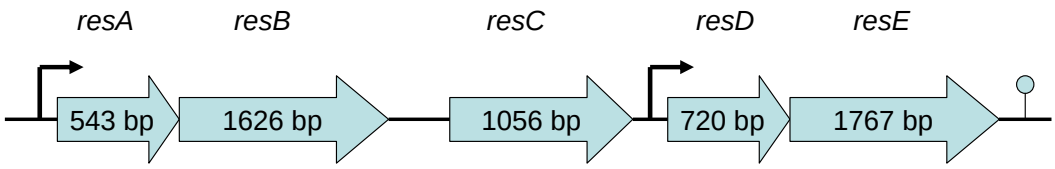

Figure 1.14. The *res* operon from *B. subtilis*. The block arrows represent open reading frames, promoters by the thin arrows and transcription stop by stem-loop symbol. *resD* and *resE* are transcribed from their own promoter as well as in an operon with the other *res* genes.

As with CCM system I, CCM system II starts with the translocation of apo-cytochrome *c* from the cytoplasm. Like all Gram positive bacteria, *B. subtilis* has no periplasm so all components are membrane bound and located in the extra-cytoplasmic space between the cytoplasmic membrane and the exterior cell wall. Once translocated the two thiol groups in the haem binding site of the apo-cytochromes *c* are oxidised by BdbD to a disulphide bond (24,27). It is still unclear as to why in both CCM systems I and II a disulphide is introduced to the apo-cytochrome *c* upon translocation. Both BdbD and DsbA are general

catalysts of disulphide bond formation so this event could be an evolutionary artefact or it could serve to provide some sort of secondary structure important for the stability of apo-cytochrome *c* outside of the cytoplasm, protecting it from forming heterodisulphides up until the point when haem attachment occurs.

The role of the integral membrane protein CcdA is to pass the reducing equivalents to the membrane bound protein ResA (and also to StoA which is involved in sporulation, discussed above). ResA is proposed to reduce the disulphide bond in the apo-cytochrome *c* in preparation for covalent haem attachment (12), although no ResA-substrate or ResA-CcdA complexes have yet been reported, probably due to the short lived nature of any such complex (78). A constructed ResA deficient strain of *B. subtilis* was found to lack cytochromes *c*, showing that the protein is required for maturation. Cytochrome *c* maturation was subsequently restored by a deficiency of BdbD (in this case the apo-cytochrome *c* is not oxidised and thus does not need to be reduced) (12). The addition of the reducing agent dithiothreitol (DTT) also restored cytochrome *c* synthesis, further supporting the role of ResA in reducing the apo-cytochrome *c* (12). Structures of the soluble domain of ResA from *B .subtilis* in both its oxidised and reduced states illustrate how the redox state causes conformational changes in the protein surface, which pre-determine which substrates it will bind (14): ResA is discussed in more detail above.

The precise roles of ResB and ResC are yet to be determined. ResB (542 aa) and ResC (352 aa) are both integral membrane proteins and share similarity to proteins known to be involved in cytochrome *c* biogenesis in other organisms

(54,85). ResB has four cysteine residues. Two of these form a thioredoxin motif and could have a redox function (54). By analogy to *B. pertussis* CcsB (a ResB homologue) and membrane topology prediction, ResB has four predicted transmembrane segments with the N-terminus exposed to the cytoplasm (85). ResB has been shown to covalently bind haem via Cys138, located at the N-terminus, although Cys138 has been shown to be non-essential for the protein's function (85). CcsBA of *Helicobacter pylori* can be thought of as a naturally fused homologue of ResBC. The CcsA domain (ResB homologue) will bind haem in a non-covalent fashion (86). *H. pylori* CcsBA can replace the functions of *E. coli* CcmA-H in CCM system I but expression of the *B. subtilis res* genes in CCM deficient *E. coli* will not recover the CCM phenotype (85,87). It is very likely that ResB, like CcsB, is involved in the translocation of haem across the membrane (85,87,88). Neither ResA nor ResC are required for ResB to bind haem which supports the conclusion that ResB is the haem transporter and ResA and ResC are involved in only haem attachment (85). ResC contains a tryptophan rich sequence motif which could be involved in haem binding (54). When ResC was over expressed in *B. subtilis* it was shown to bind haem but it is unclear as to whether this is natural or a result of the over-expression (85). From sequence analysis ResC was predicted to be ~44 kDa, but when *resC* was over-expressed in *B. subtilis* the resulting ResC was found to be only ~27 kDa, suggesting the protein may be truncated after translocation. Interestingly, ResC appears as a ~36 kDa protein when expressed in *E. coli*, which matches neither the predicted size of the protein from sequence analysis nor the size of the protein when expressed in *B. subtilis* (85). *H. pylori* CcsBA contains two conserved hisidine residues (His77 and His858), which have been shown to be

required for the traffic of haem from the cytoplasm to the haem binding domain. These residues correspond to *B. subtilis* ResB-His207 and ResC-His350, respectively, so it is likely these residues are also important for haem transport in *B. subtilis* (85,86). It is thought that ResBC forms a complex to transport haem from the cytoplasm and attach it to apo-cytochrome *c* (85).

1.4.4.3. CCM System III

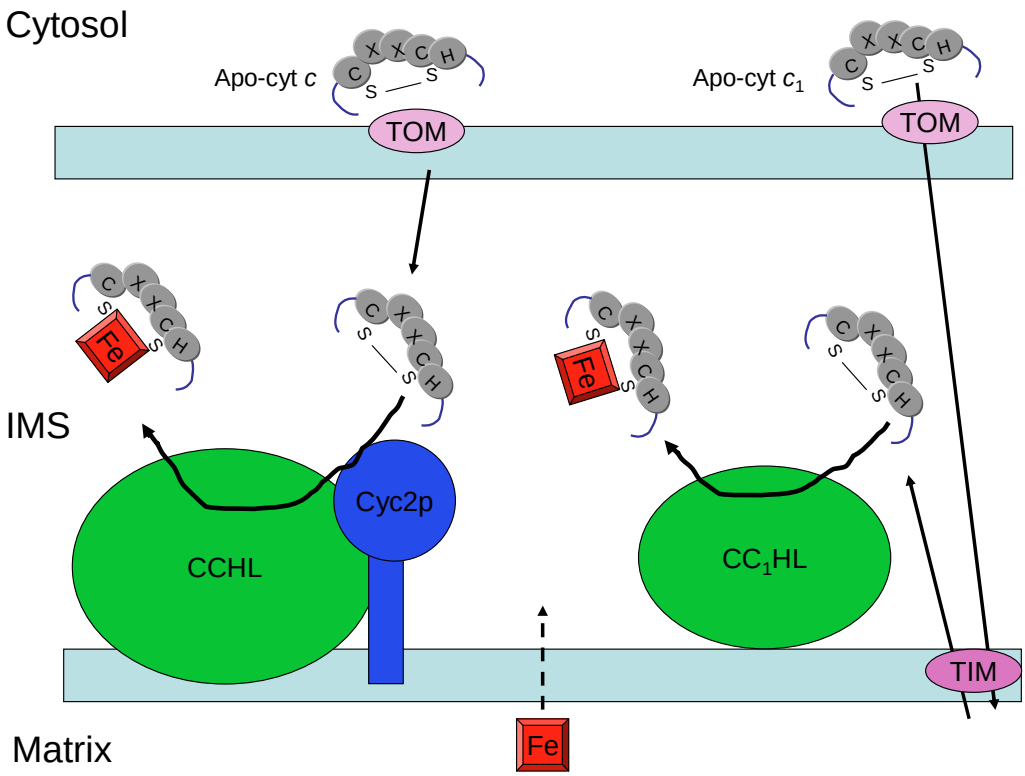

Figure 1.15. CCM biogenesis system III from *Saccharomyces cerevisiae*. There are two very similar systems for the maturation of cytochrome (cyt) *c* and cytochrome c_1, cytochrome *c* haem lyase (CCHL) and cytochrome c_1 haem lyase (CC_1HL). Both systems operate within the intermembrane space (IMS). It is thought that CCHL mediates the import of apo-cytochrome *c* into the IMS, requiring elements of the TOM machinery on the cytosol side. Cyc2p then reduces the CXXCH disulphide prior to haem attachment by haem lyase. CC_1HL is not involved with the import of apo-cytochrome c_1 but both the TOM and TIM translocation machinery are required. CC_1HL does not require Cyc2p to reduce the apo-cytochrome c_1 disulphide. There are several proteolytic steps involved in the maturation cytochrome c_1 (discussed in the text) that have been left

out of this schematic for simplicity. Cyc2p is restricted to organisms where both CCHL and CC_1HL are present; in animals only one haem lyase is present.

CCM system III appears to be incredibly simple compared to the other two studied systems (Figure 1.15). It is thought that either a single cytochrome *c* lyase or a pair of very similar cytochrome *c* and cytochrome c_1 lyases are the major components involved in CCM system III (46). CCM system III is utilised in the mitochondria of several organisms (often alongside a CCM system I, described above) including yeast, animals, apicomplexan parasites, diatoms and green algae, as determined by genomic analysis (89).

The yeast *Saccharomyces cerevisiae* uses the two lyases: cytochrome *c* haem lyase (CCHL) and cytochrome c_1 haem lyase (CC_1HL) to mature cytochrome *c* and cytochrome c_1, respectively, whereas in mammals it appears that a single haem lyase is sufficient for the maturation of both *c* and c_1 cytochromes and is referred to as holocytochrome *c* lyase (HCCL) (89). Several important differences have been uncovered in *S. cerevisiae* CCHL and CC_1HL systems. Aswell as being essential for the covalent attachment of haem to the apo-cytochrome *c*, CCHL is also required for the translocation of the apo-cytochrome *c* from the cytosol into the intermembrane space (IMS) of the mitochondrion along with the protease resistant part of the TOM complex (outer-membrane translocation machinery). TOM directs the apo-cytochrome *c* to the outer-membrane and CCHL acts as the receptor in the IMS (90). Unlike other proteins transported via the TOM machinery, apo-cytochromes *c* do not have an N-terminal signal sequence for mitochondrial targeting; instead they possess internal signals (89). Upon import to the IMS any apo-cytochrome *c* with an

oxidised haem binding motif is required to be reduced by a membrane bound flavoprotein, Cyc2p, before CCHL can insert the haem. It is probable that the majority of apo-cytochrome *c* is reduced upon entry to the IMS as cytochrome *c* maturation is only partially affected in the absence of Cyc2p (89,91).

Pre-apo-aytochrome c_1 is imported into the mitochondrial IMS via the TOM and TIM (inner membrane translocation) translocation machinery by virtue of a bipartite N-terminal signal sequence that is processed on entry into the organelle (89). It is unclear as to why both the TOM and TIM machinery are required for the import of pre-apo-cytochrome c_1 as there is still no consensus as to the sorting of the bipartite signal (89). Two models to the involvement of TIM currently exist. First, it may be that the entire bipartite sequence in imported to the matrix then "pulled-back" into the inner membrane. Secondly, the hydrophobic domain of the sequence acts to stop pre-apo-cytochrome c_1 being translocated into the matrix and anchors the pre-apo-cytochrome c_1 to the IMS side of the inner membrane (89). However, there is agreement on the processing of the pre-apo-cytochrome c_1, starting with the pre-sequence of the peptide being proteolytically removed by the MPP (the mitochondrial general processing peptidase) in the mitochondrial matrix (89). This generates an intermediate sized apo-cytochrome c_1, which is acted on by Imp2, an IMS-localised protease, to generate the apo-cytochrome c_1 (89). Covalent attachment of haem is carried out by CC_1HL before a final cleavage step by the Imp2 protease (89).

Only CCHL was identified in genetic screens in yeast and, when it was expressed in *E. coli* with mitochondrial apo-cytochrome *c*. A good yield of mature

cytochrome *c* indistinguishable from the same protein matured in yeast was produced (92). It is possible that this system is so simple when compared to systems I and II because system III only has to attach haem to two cytochromes that have very similar folds, whereas systems I and II have varying apo-cytochrome *c* substrates (46). It has not yet been possible to demonstrate that system III haem lyase can attach haem to bacterial apo-cytochrome *c*, which suggests a high level of specificity toward the apo-cytochromes *c* it will reduce. Unlike system I, system III is able to attach haem to apo-cytochrome *c* with a mutated AXXCH motif, which suggests a lack of specificity towards the active site alone (46). There is no evidence for a system III precursor in any prokaryotes so it seems likely that haem lyase evolved once and came to replace CCM system I in many organisms (93).

1.4.4.4. Systems IV and V

Apart from the existence of cytochromes *c* (and other cytochromes with atypical covalently bound haem) that are matured in the absence of CCM systems I, II and III, very little is yet known about alternative systems for the covalent ligation of haem to peptides. As discussed above, some cytochromes *c* have a non-CXXCH motif and are able to bind haem via a CXXXCH, CXXXXCH or CXXCK motif or are attached via only one thioether bond to a A/FXXCH motif. Each of these motifs must require a system of haem attachment (46).

The CCM system IV machinery (also known as CCB) has been identified in chloroplasts as being involved in the maturation of the b_6f complex (94). The b_6f complex is closely related to bc_1 complexes both in its structure and function

(discussed above), the main difference being the b_6f complex has an additional haem cofactor covalently bound to the backbone of the cytochrome *b* (94). Four genes, *CCB1-4*, have been identified as being involved in the covalent attachment of a *c*-type haem to cytochrome b_6 (94). This *c*-type haem is attached by only one thioether bond and there does not appear to be a second axial ligand. This type of haem *c* is called a *c*' haem (94). Each of the CCB proteins are predicted to be integral membrane proteins spanning the thylakoid membrane, but as yet no specific role has been assigned to the individual protein (94). Disruption of genes involved in CCM system II, also found in chloroplasts, does not affect the attachment of haem *c*' to cytochrome b_6 (94). QcrB, of the *B. subtilis bc* complex (homologous to the b_6f complex, discussed above) also has a haem covalently bound via one thioether bond, but aside from the fact that this occurs outside of CCM system II, very little is known about its maturation (53). A *CCB3* homologue has been identified in *B. subtilis* but the other three components appear to be absent (85,94).

CCM system V has been identified as being involved in the maturation of cytochrome *c* and cytochrome c_1 in the mitochondria of protist phylum Euglenozoa, which includes *Leishmania* species and *Trypanosoma brucei*, a parasitic protist that causes African sleeping sickness (95). The cytochromes *c* of these organisms have haem covalently attached via one cysteine thiol to a (A/F)XXCH motif (95,96). The *E. coli* CCM system I machinery was not able to mature *T. brucei* cytochrome *c* and cytochrome c_1 unless the genes were mutated to encode the proteins so that they had a CXXCH motif (95). The CCM system III of *S. cerevisiae* was not able to mature *T. brucei* cytochrome *c* and

cytochrome c_1 even if the haem binding motif was altered to a CXXCH even though the overall structure of the *T. brucei* cytochromes *c* is remarkably to similar to those found to *S. cerevisiae* (96).

1.4.4.5. CCM in *S. coelicolor*

Streptomyces coelicolor is a Gram positive, spore forming soil bacterium, belonging to the sporoactinomycetes group. The *Streptomyces* family are different from other bacteria as they exhibit complex multicellular development, with the differentiation of cells into distinct tissues. The *Streptomyces* family is also responsible for producing most of the naturally occurring antibiotics used today in human and veterinary medicine. *S. coelicolor* has the largest number of predicted genes of any bacterium, to date, on its linear, eight million base pair chromosome (97). They grow as branching hyphae that form vegetative mycelia that disperse through spores that form on aerial hyphae. These are specialised reproductive structures, that emerge from the colony surface into the air (98).

Relatively little is known about respiration in *S. coelicolor*. It is classed as an obligate aerobe although it possesses three copies of the *narGHJI* operon, which encodes nitrate reductase, an enzyme complex involved with anaerobic respiration. *S. coelicolor* is capable of aerobic growth on a wide range of carbon sources and, although it can survive anaerobic conditions, it is incapable of growth (99).

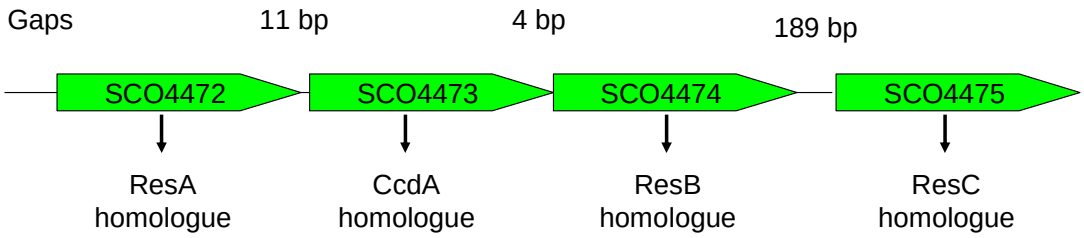

Figure 1.16 Gene organisation of the predicted *S. coelicolor res* operon. The SCO numbers refer to the order of genes on the *S. coelicolor* genome. The genes are apparently arranged as an operon with a likely promoter upstream of the *resA* gene (SCO4472). 'Gaps' refers to the number of base pairs between the 'stop' codon of one gene and the start codon of the next. The genes are very close together with the largest gap of 189 bps being between *resB* (SCO4474) and *resC* (SCO4475); as yet no additional promoter has been identified in this region.

The *S. coelicolor* genome sequencing project identified 7825 predicted genes in the 8,667,507 bp chromosome, many of which remain completely uncharacterised (100). Sequence analysis identified four genes, potentially arranged in an operon, that are predicted to encode proteins homologous to *B. subtilis* ResA, CcdA, ResB and ResC (Figure 1.16). The *Streptomyces* data base (StrepDB, http://strepdb.streptomyces.org.uk/) designates all *S. coelicolor* genes by 'SCO' numbers. The gene predicted to encode a homologue of *B. subtilis* ResA is designated SCO4472. The rest of the operon, predicted to encode homologues of CcdA, ResB and ResC, are designated SCO4473, SCO4474 and SCO4475, respectively. For clarity, in this thesis, these genes will be referred to by the product they are expected to encode, for example, SCO4472 will be referred to as *resA* as it is expected to encode a homologue of *B. subtilis* ResA.

Membrane bound TDORs have remained largely unstudied in *S. coelicolor*. The bacterium does not synthesise glutathione (GSH), which is considered to be important for protecting the cell against oxygen toxicity. *S. coelicolor* along, with many other Actinomycetes, produces mycothiol (MSH) which is more resistant to heavy-metal ion-catalysed oxygenation than GSH (101). With the existence of thioredoxin (Trx) in the cytoplasm of *S. coelicolor* established (102,103) and with a likely homologue of *ccdA* found in the same operon as the *res* genes it is clear that *S. coelicolor* possesses a system II cytochrome *c* maturation pathway similar to that of *B. subtilis* where the reducing equivalents are passed from Trx in the cytoplasm to CcdA to ResA and finally to the apocytochrome *c*.

```
BsResA          MKKKRRLFIRTG------------------------------ILLVLICALGYTIYN-- 27
ScResA          MSAASRAPLRSNRTAERFTERTADARARVRSRAARAAVGAAAAALLVSACSSGGTSGGGG 60
                                                          -----

BsResA          --AVFAGKESIS-----EGSDAPNFVLEDTNGKRIELSDLKGKGVFLNFWGTWCEPCKKE 80
ScResA          QTGFITGSDGIATAKKGERADAPELSGETVDGGQVDVADYKGKVVVLNVWGSWCPPCRAE 120

BsResA          FPYMANQYKHFKSQGVEIVAVNVGE-SKIAVHNFMKSYGVNFPVVLDTDRQVLDAYDVSP 139
ScResA          AKNFEKVYQDVKDQGVQFVGINTRDTSTGPARAFEKDYGVTYPSLYDPAGRLMLRFEKGT 180

BsResA          L-----PTTFLINPEGKVVKVVTGTMTESMIHDYMNLIKPGETSG 179
ScResA          LNPQAVPSTLIIDREGKVAARTLQALSEEKLRKMLAPYLQPEK-- 223
```

Figure 1.17 Sequence alignment of BsResA and ScResA. Generated using CLUSTAL 2.0.10 (http://www.ebi.ac.uk/Tools/clustalw2/index.html). Residues highlighted yellow represent an exact match and residues highlighted green represent a compatible substitution. The 'lipobox' region is underlined in red.

B. subtilis ResA (BsResA) is membrane bound by a transmembrane anchor whereas analysis suggests that *S. coelicolor* ResA (ScResA) is a lipoprotein as it contains an N-terminus 'lipobox' consensus sequence (LVSAC) between residues 46-50 (104). Although *B. subtilis* ResA has this same consensus

sequence previous studies have demonstrated that it is not a lipoprotein. A sequence alignment between BsResA and ScResA can be seen in (Figure 1.17).

The *ccdA* and *res* system in *B. subtilis* represents a model for CCM system II, which is found in a wide variety of organisms including Gram positive bacteria. Sequence analysis of the *S. coelicolor* genome predicts there to be only one cytochrome *c*, homologous to the *B. subtilis* cytochrome *c* QcrC . The gene, designated SCO2150 by the Streptomyces database, is located in a cluster with other genes also encoding proteins that are homologous to other components of a cytochrome bc_1 quinol oxidase complex, as well as several genes expected to encode homologues of protein subunits of a cytochrome *c* oxidase (Figure 1.18). As the *S. coelicolor* quinol oxidase complex bares sequence homology to the *B. subtilis* complex it too will be referred to as a *bc* complex, with no subscript.

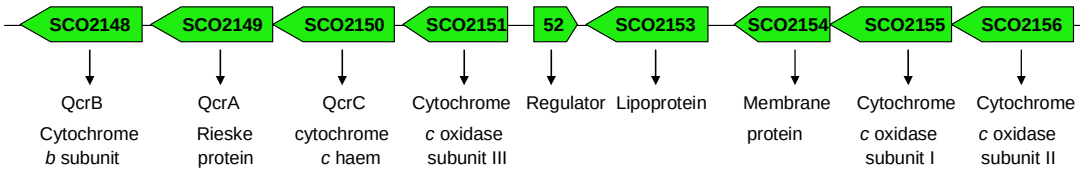

Figure 1.18. The *qcr* and cytochrome *c* oxidase gene cluster of *S. coelicolor*. SCO2148, SCO2149 and SCO2150 are predicted to encode proteins that make up a quinol oxidase bc_1 complex. SCO2151, SCO2155 and SCO2156 are predicted to encode subunits of a cytochrome *c* oxidase complex. The cluster also includes a regulator, a lipoprotein and a membrane protein of no predicted function, 52 (SCO2152), SCO2153 and SCO2154, respectively.

QcrC in *B. subtilis* forms part of the *bc* complex, which transfers electrons from relatively low potential quinol to cytochromes *c* and contribute to the transmembrane proton gradient (53,56). The cytochrome *bc* complex also

requires a cytochrome *b* and a Rieske-type iron-sulphur protein; genes encoding homologues of these proteins are located in an operon with the gene encoding the QcrC homologue on the *S. coelicolor* chromosome (Figure 1.18). Currently it is not known what the terminal oxidase is for the electron from the *S. coelicolor bc* complex. Although *S. coelicolor* does encode homologues of a cytochrome *c* oxidase, there is apparently no homologue of a small cytochrome *c* to shuttle electrons from the *bc* complex to it. It could be that the *bc* complex is able to pass electrons directly to the cytochrome *c* oxidase without the need of a small cytochrome *c*. The role of cytochrome *bc* complexes is discussed in detail in above.

BLAST searches of the *S. coelicolor* genome also identified a homologue of the *B. subtilis* cytochrome *bd* ubiquinol oxidase, encoded by SCO3935 and SCO3964. Searches were also made for homologues of the *B. subtilis* cytochrome aa_3 quinol oxidase against the *S. coelicolor* genome but the closest matches found had already been identified as being more closely related to the *B. subtilis* cytochrome *c* oxidase, parts of which are missing in the M145Δ*qcr* strain, discussed above. It is also possible that *S. coelicolor* has homologues of other terminal oxidases not identified here.

The presence of genes encoding homologues of the CcdA and Res proteins in *S. coelicolor* means that it is highly likely that the only predicted cytochrome *c* of *S. coelicolor*, a homologue of *B. subtilis* QcrC, is matured by the CCM II pathway.

1.5. Project Aims

This project was centred around three main aims; first, using *B. subtilis* as a model organism, this project aimed to explore the *in vivo* function of predicted key residues in the ResA amino sequence by expressing variant ResA protein in a ResA deficient *B. subtilis* strain and investigating the affects of these mutations on CCM activity. In this fashion the cysteines, glutamate and the proline of the CEPC active site as well as the near active site glutamate and *cis* proline residues were investigated. The importance of the transmembrane anchor of ResA was also explored in a similar manner by replacing the transmembrane region of ResA with the anchor from the *B. subtilis* cytochrome *c*, CcdA. The second aim of this project was to study the importance, *in vivo*, of key amino acid residues previously identified from biophysical/structural studies in the highly oxidising TDOR BdbD from *B. subtilis*. The final aim of this project was to identify and investigate a homologue of *B. subtilis* ResA found in another Gram positive bacterium in order to compare and contrast the CCM systems from two different organisms. *S. coelicolor* ResA was identified and investigated, both in its *in vivo* function in terms of CCM in *S. coelicolor* and its biophysical properties *in vitro*.

Chapter 2: Materials and Methods

2.1 Introduction

Many different experimental techniques and procedures have been employed throughout the work presented in this thesis, including protein purification, molecular biology, genetics and spectroscopy. The aim of this chapter is to describe experimental procedures commonly used throughout this work. Many of the techniques used are specific to a later chapter and will therefore be described there.

2.2 Bacterial strains

Various strains of *E. coli*, *B. subtilis* and *S. coelicolor* were used throughout this work. These strains are listed in Table 2.1.

2.3 Growth media

E. coli strains were grown on Luria-Bertani (LB) medium or on LB/agar plates. *B. subtilis* strains were grown in nutrient sporulation medium with phosphate (NSMP), minimal glucose (MG) or tryptose blood agar base (TBAB) and *S. coelicolor* were grown on LB or soya flour mannitol (SFM). All media were sterilised by autoclave or filtration before use. The ingredients used to make growth media are listed in Table 2.2.

Table 2.1. Bacterial strains used and/or generated throughout the course of this study

Strain	Genotype and/or relevant properties[a]	Origin and/or reference[b]
B. subtilis		
1A1	*trpC2*	BGSC[c]
LUL7	*trpC2* Δ*ccdA::ble, bdbD*Ω*Tn10*; Pm^R Sp^R	(24)
LUL9	*trpC2 resA*Ω*pLLE36*; Em^R	(12)
LUN1	*trpC2 resA*Ω*pLLE36*, *amyE*::P_{spac}-*resA*; Em^R Cm^R	This study; pALR12 → LUL9
LUN2	*trpC2 resA*Ω*pLLE36*, *amyE*::P_{spac}-*resA (C74A)*; Em^R Cm^R	This study; pALR34 → LUL9
LUN3	*trpC2 resA*Ω*pLLE36*, *amyE*::P_{spac}-*resA (C77A)*; Em^R Cm^R	This study; pALR35 → LUL9
LUN4	*trpC2 resA*Ω*pLLE36*, *amyE*::$_{Pspac}$-*resA (C74A/C77A)*; Em^R Cm^R	This study; pALR39 → LUL9
LUN5	*trpC2 resA*Ω*pLLE36*, *amyE*::Pspac-*resA (E80Q)*; Em^R Cm^R	This study; pALR40 → LUL9
LUN6	*trpC2 resA*Ω*pLLE36*, *amyE*::Pspac-*resA (P141S)*; Em^R Cm^R	This study; pCHN2 → LUL9
LUN7	*trpC2 resA*Ω*pLLE36*, *amyE*::Pspac-*resA (P141T)*; Em^R Cm^R	This study; pCHN4 → LUL9
LUN8	*trpC2 resA*Ω*pLLE36*, *amyE*::$_{Pspac}$-*resA (P76H)*; Em^R Cm^R	This study; pCHN6 → LUL9
E. coli		
JM109	*recA1 supE44 endA1 hsdR17 gyrA96 relA1 thi Δ(lac-proAB)* F'[*traD36 proAB*$^+$ *lacI*^{q} *lacZΔM15*]	(105)
DH5α	*fhuA2 Δ(argF-lacZ)U169 phoA glnV44 Φ80 Δ(lacZ)M15 gyrA96 recA1 relA1 endA1 thi-1 hsdR17*	Invitrogen
BW25113	K-12 derivative: Δ*araBAD*, Δ*rhaBAD*	(106)
ET12567	*dam*, *dcm*, *hsdM*, *hsdS*, *hsdR*, *cat*, *tet*	(107)
BT340	DH5α/pCP20	(108)
BL21 DE3	F^- *omp*T *hsd*S_B($r_B^-m_B^-$) *gal dcm* (DE3)	Promega
BL21 Star™ (DE3)	F^- ***omp***T ***hsd***S_B(r_B^-, m_B^-) ***gal dcm rne***131 (DE3)	Invitrogen
BL21 Rosetta	F^- *ompT hsdS*$_B$(r_B^- m_B^-) *gal dcm* (DE3) pRARE (Cam^R)	Novagen
BL21 CodonPlus(DE 3)-RP	F– *ompT hsdS* (r_B^- m_B) *dcm*$^+$ Tet^R *gal endA* Hte *argU proL* Cam^R	Stratagene
S. coelicolor		
M145	$SCP1^-$, $SCP2^-$	(100)
M145 Δ*qcr*	*qcr::apr*	This work[d]

[a] Ap^R, resistance to ampicillin; Cm^R, resistance to kanamycin; Em^R, resistance to erythromycin; Sp^R, resistance to spectinomycin

[b] An arrow indicates transformation of the strain

[c] BGSC, Bacillus Genetic Stock Centre, Ohio State University, Columbus, OH, USA

[d] Donatated by Matt Hutchings, School of Biological Sciences, UEA, Earlham Road, Norwich

Table 2.2. Growth media used in this work.

Media	Ingredients
LB	10 g/L Sodium chloride; 10 g/L Tryptone; 5 g/L yeast extract, in distilled H_2O (for LB/agar plates 1.5 g/100ml agar was added to LB).
NSMP	8 g/L nutrient broth; 0.1 M potassium phosphate pH 6.5 (added after autoclaving); 0.7 mM $CaCl_2$; 0.05 mM $MnCl_2$; 1 mM $MgCl_2$**;** 1 µM $FeCl_2$ (for NSMP/agar plates 1.5 g/100ml agar was added to NSMP).
2 x MG (diluted as needed)	4 g/L ammonium sulphate; 14 g/L potassium sulphate (dibasic); 6 g/L potassium phosphate (monobasic); 1 g/L sodium citrate; 0.2 g/L magnesium sulphate; 0.5% glucose added after autoclaving (for MG agar, 15 g/L agar added). Additional growth factor can be added after autoclaving; Bott and Wilson (B&W) solution: 5 mg/ml of each of the following: arginine, asparagine, glycine, histidine, lysine, methionine, threonine and tryptophan (filter sterilised before use).
TBAB	33 g/L TBAB; 5 g/L agar, made up to 1 L with dH_2O
Starch-TBAB	As TBAB with the addition of 1% starch
SFM	20 g/L agar, 20 g/L mannitol, soya flour, made up to 1 L with tap water.
2 x YT medium	16 g/L Difco bacto tryptone; 10 g/L Difco bacto yeast extract; 5 g/L NaCl, made up to 1 L with dH_2O

2.4. Molecular biology techniques

A wide range of molecular biology techniques were used throughout this project as the manipulation of DNA was essential for the preparation of samples and the generation of bacterial strains and vectors. Described below are the most commonly used techniques; variations to these methods are discussed in the results Chapters where relevant.

2.4.1 Polymerase chain reaction (PCR)

PCR was used to amplify DNA fragments from chromosomal DNA from *B. subtilis* and cosmid DNA libraries from *S. coelicolor* for ligation into and expression from plasmids or for the confirmation of gene insertion and/or interruption. The components of a typical amplification reaction are listed in

Table 2.3 and the reaction conditions are described in Table 2.4. The sequences of the DNA oligonucleotide primers used throughout this study are listed in Table 2.7.

Table 2.3. Typical components of a PCR amplification reaction

Component	Stock concentration	Volume
Template DNA	1-100 ng μl^{-1}	1 µl
Forward primer	100 µM	0.5 µl
Reverse primer	100 µM	0.5 µl
dNTPs	40 mM (10 mM each)	1 µl
Roche High-Fidelity Expand polymerase	2.5 U/µl	0.5 µl
Roche High-Fidelity Expand polymerase 10 x buffer (+$MgSO_4$)	As supplied	5 µl
H_2O (sterile, deionised)	-	To make up to 50 µl

Table 2.4. Typical conditions of a DNA amplification PCR reaction

Process	Temp ^oC	Time	Repeat
Initial denaturation	94	2 min	1
Cycle 1			
Denaturation	94	15 s	
Primer annealing	58	30 s	10
Extension	72	45 s	
Cycle 2			
Denaturation	94	15 s	
Primer annealing	62	30 s	20
Extension	72	45 s – 2 min 25 s	
Final Extension	72	5 min	1

Reaction carried out in a Techne thermocycler. Extension time for 'Cycle 2' increases from 45 sec to 2 min 25 s as per enzyme manufacturers' recommendations depending on fragment size.

2.4.2. Site directed PCR mutagenesis

PCR was also employed to generate genes encoding ResA and BdbD variants. The full length wild type *resA* gene in pUC18 was used as template DNA. Components of a typical PCR mutagenesis reaction are in Table 2.5 and the reaction conditions are outlined in Table 2.6. Each PCR reaction was carried out in triplicate using 1, 2 or 4 µl of template DNA.

Table 2.5. Typical reaction mixture used for a PCR mutagenesis reaction.

Component	Stock concentration	Volume
Template DNA	1-100 ng μl^{-1}	1-4 µl
Forward primer	100 µM	2 µl
Reverse primer	100 µM	2 µl
dNTPs	40 mM (10 mM each)	1.5 µM
PWO polymerase	2.5 U/µl	0.5 µl
PWO polymerase 10 x buffer (+$MgSO_4$)	As supplied	5 µl
dH_2O (sterile, deionised)	-	To make up to 50 µl

PWO polymerase from Roche, primers purchased Sigma Genosys.

Table 2.6. Typical conditions of a site directed PCR mutagenesis reaction.

Process	Temp ^oC	Time	Repeat
Initial denatuation	94	3 min	1
Denaturation Primer annealing Extension	94 57 70	30 s 30 s 10 min	20
Final extension	70	10 min	1

Reaction carried out within a Techne thermocycler.

The wild type template DNA was removed from the PCR reaction mixture product by incubation with 1 µl *Dpn*I (which specifically digests methylated DNA) for 1 hour at 37 ^oC. *Dpn*I was denatured by incubation for 30 min at 72 ^oC. PCR products were ligated to circular plasmids by incubation with T4 DNA

ligase at 37 °C for 1 hour, and were then used to transform *E.coli* JM109 (see below for protocol). Successful transformants were screened by plating on to LB agar containing 100 µg/ml ampicillin. Single colonies were used to inoculate 5 ml LB containing 100 µg/L ampicillin, and cultures were incubated overnight at 37 °C and 200 rpm. Plasmid DNA was extracted from 5 ml culture using QIAprep mini prep kit (QiaGen, protocol as manufacturer's instructions). Mutations were verified by DNA sequencing (MWG-Biotech).

Table 2.7. Primers used in this study

Variant	Primer	For use with template
B. subtilis resA primers		
Wild type	fwd: GATAAGCTTGAATGGATCTGCAATAGGGG rev: ACTCTAGACTTGCTTCATCCCGAAGTCTC	*B. subtilis* 1A1 genomic DNA
C74A	GGGGTACATGGGCTGAACCGTGCAAAAAAG[a]	pALR9[b]
C77A	ATGGTGTGAACCGGCCAAAAAAGAGTTTCC[a]	pALR9[b]
C74A/C77A	ATGGGCTGAACCGGCCAAAAAAGAGTTTCC[a]	pALR33[c]
P76H	GGTACATGGTGTGAACACTGCAAAAAAGAG[a]	pALR9[b]
P141S	GTATCTCCGCTTTCGACAACCTTTTTG[a]	pALR9[b]
P141T	GTATCTCCGCTTACGACAACCTTTTTG[a]	pALR9[b]
E80Q	CCGTGCAAAAAACAATTTCCTTATATG[a]	pALR9[b]
pVK1	TTTGAGGTAGCCCTTGCCTACC	*B. sutilis* pVK48 insert genomic DNA
pVK2	GTACGTACGATCTTTCAGCCG	*B. sutilis* pVK48 insert genomic DNA
B. subtilis bdbD primers		
Wild type	For: AAGCTTCTTTTTTAATTTTAAAACGATGAGG Rev: AGCATGCAAAAATACGATTCTATTTTTC	*B. subtilis* 1A1 genomic DNA
D180A	CAAGTGGAAAAGGCTTCTGACCTTAATC[a]	
E63Q	GTAACTGTAGTACAATTCGGAGATTAC[a]	
E115A	GCTCTTGCATCTGCAGAAGTATGGAAG[a]	
P193T	CATACAGGCAACAACGACGATTTACGTC[a]	
P193S	CATACAGGCAACATCGACGATTTACGTC[a]	
Q49A	CTATCAAAGGGGCGCCTGTGCTTGGC[a]	
S. coelicolor resA primers		
ScResA1	CATATGACCGGCTCCGACGGCATCGCC	StD65
ScResA2	GAATTCGTCACTTCTCCGGCTGGAGGTACGGGGC	StD65
ScResA3	GGATCCACCGGCTCCGACGGCATCGCC	StD65
ScResA4	GAATTCGTCACTTCTCCGGCTGGAGGTACGGGGC	StD65

[a]The reverse primers complement the forward primer, only the forward primer is shown.
[b]pALR9 is a derivative of pUC18 containing the full length resA gene including the ribosome binding site.
[c]pALR33 is a derivative of pUC18 containing full length resA(C74A) including the ribosome binding site.

2.4.3. Ligations

Ligation reaction mixtures were prepared as shown in Table 2.8. The reaction mixture was prepared at room temperature (approximately 20 ^{o}C) in a sterile 1.5 ml tube. The reaction mixture was placed in a water bath and was incubated at 4 ^{o}C overnight and then at room temperature for a further six hours. This method ensured that the reaction mixture would be, for a short time, at all temperature between 4 ^{o}C and 20 ^{o}C. The function of T4 ligase is dependent on the mixture being at optimum temperature, which varies between reactions.

Table 2.8. The components of a typical ligation reaction mixture

Component	Stock concentration	Volume
Plasmid DNA	1 µg /µl	1 µl
DNA fragment	1 µg/µl	4 µl
T4 DNA ligase	10 U/µl	1 µl
5 x T4 ligase buffer	As supplied	3 µl
Water	-	11 µl
	Total volume	15 µl

Table 2.9. Plasmids and cosmids generated and/or used throughout the course of these studies.

Plasmid/ Cosmid	Genotype and/or relevant properties[a]	Origin and/or reference[b]
pUC18	Cloning vector; Ap^R	(105)
pET21a	Expression vector Ap^R	Novagene
pGEX-4T-1	Expression vector Ap^R	GE Healthcare
pALR9	pUC18 with wild type *resA* blunt end cloned at *Sma*I site; Ap^R	This study
pALR12	pVK48 with *Xba*I/*Hind*III fragment containing wild type *resA* under P_{spac}; Ap^R, Cm^R	This study
pALR32	pUC18 with *resA(C77A)* blunt end cloned at *Sma*I site; Ap^R	This study
pALR33	pUC18 with *resA(C74A)* blunt end cloned at *Sma*I site; Ap^R	This study
pALR34	pVK48 with *Xba*I/*Hind*III fragment containing *resA(C74A)* under P_{spac}; Ap^R, Cm^R	This study
pALR35	pVK48 with *Xba*I/*Hind*III fragment containing *resA(C77A)* under P_{spac}; Ap^R, Cm^R	This study
pALR36	pUC18 with *resA(C74A/C77A)* blunt end cloned at SmaI site; Ap^R	This study
pALR37	pUC18 with *resA(E80Q)* blunt end cloned at SmaI site; Ap^R	This study
pALR39	pVK48 with *Xba*I/*Hind*III fragment containing *resA(C74A/C77A)* under P_{spac}; Ap^R, Cm^R	This study
pALR40	pVK48 with *Xba*I/*Hind*III fragment containing *resA(E80Q)* under P_{spac}; Ap^R, Cm^R	This study
pCHN1	pUC18 with *resA(P141S)* blunt end cloned at *Sma*I site; Ap^R	This study
pCHN2	pVK48 with *Xba*I/*Hind*III fragment containing *resA(P141S)* under P_{spac}; Ap^R, Cm^R	This study
pCHN3	pUC18 with *resA(P141T)* blunt end cloned at *Sma*I site; Ap^R	This study
pCHN4	pVK48 with *Xba*I/*Hind*III fragment containing *resA(P141T)* under P_{spac}; Ap^R, Cm^R	This study
pCHN5	pUC18 with *resA(P76H)* blunt end cloned at *Sma*I site; Ap^R	This study
pCHN6	pVK48 with *Xba*I/*Hind*III fragment containing *resA(P76A)* under P_{spac}; Ap^R, Cm^R	This study
pCHN11	Sol ScResA in pUC18 at *Sma*I site	This study
pCHN12	Sol ScResA in pET21a at *Nde*I/*Eco*RI site	This study
pCHN17	Wild type *bdbD* pUC18	This work
pCHN18	Wild type *bdbD* pDG148	This work
pCHN20	pUC18, *bdbD* Q49A	This work
pCHN20.1	pDG148 *bdbD* Q49A	This work[c]
pCHN22	pUC18 *bdbD* E63Q	This work
pCHN22.1	pDG148 *bdbD* E63Q	This work[c]
pCHN23	ScResA in pUC18 at *Sma*I site	This study
pCHN24	ScResA in pGEX-4T-1 at *Bam*HI/*Eco*RI	This study
pCHN26	pUC18 *bdbD* D180A	This work
pCHN26.1	pDG148 *bdbD* D180A	This work[c]
pVK48	pDH32 deriative; P_{spac} *lacI*; Ap^R, Cm^R	V. K. Chary[b]
pDG148	Expression vector, Amp^R Kan^R	(109)
pLUJES1	pHP13Es with *cccA*'-*resA* encoding cyt *c*"-ResA on a 1.1-kb *Eco*RI-*Bam*HI fragment; Cm^R	This study
pIJ790	λ-RED (*gam, bet, exo*), *cat araC, rep101*^{ts}	(110)
pIJ773	P1-FRT-*oriT-neo-aac(3)IV*-FRT-P2	(110)
Supercos 1	*Neo, bla*	Stratagene
StD65	Supercos1 with *S. coelicolor* genome bases 4872741-4911138.	(111)

2.4.4. Preparation of chemically competent *Escherichia coli* cells

5 ml LB were inoculated with *E. coli* and incubated overnight at 37 ^{o}C, 200 rpm. 0.4 ml of overnight culture was used to inoculate 40 ml LB, which was incubated at 37 ^{o}C and 200 rpm until absorbance at 650 nm was between 0.4-0.6. The cells were then harvested by centrifugation at 8000 rpm for 8 min at 4 ^{o}C. The supernatant was discarded and the cells were resuspended in 8 ml of transformation buffer (TF) 1 [7.4 g/l potassium chloride; 0.03 M potassium acetate pH 7.5; 1.5 g/l calcium chloride; 150 g/l glycerol, pH adjusted to 6.4 with 0.2 M acetic acid and sterilised by autoclave before adding 0.05 M manganese chloride (tetrahydrate)]. Resuspended cells were placed on ice for 15 min before the cells were harvested by centrifuge as described above. The supernatant was discarded and the pellet resuspended in 4 ml TF2 [0.74 g/l potassium chloride; 11 g/l calcium chloride (dihydrate); 150 g/l glycerol, sterilised by autoclave then 0.01 M MOPS buffer, pH 6.8 (adjusted with KOH) added]. Competent cells were then used immediately or stored at -80 ^{o}C in 0.2 ml aliquots until needed.

2.4.5. Transformation of chemically competent *E. coli* cells

DNA (50 µl of PCR product or 2 µl of plasmid DNA) was added to 0.2 ml of thawed competent *E. coli* cells. The cells were left on ice for 40 min before being heat shocked at 42 ^{o}C for 2 min. Cells were then placed on ice for a further 5 min. 0.7 ml of warm LB (37 ^{o}C) was added to the cell culture and the cells incubated at 37 ^{o}C for 45 min. Cell cultures were then centrifuged at 10,000 rpm for 5 min. 0.65 ml of the supernatant was removed before the cells were resuspended in remaining supernatant. Successful transformants were screened by plating 200 µl of resuspended cell culture on to LB agar/ampicillin (100

µg/ml) and incubated overnight at 37 °C. Control reactions were set up following the protocol above but without the addition of DNA to the competent cells.

2.4.6. Preparation and natural transformation of competent *B. subtilis* cells

B. subtilis strains were plated on to MG plates with 10 mg/ml tryptophan and incubated overnight at 37 °C. 10 ml MG medium containing 50 µg/ml tryptophan was inoculated from the MG plate and incubated at 37 °C, 200 rpm overnight. The culture was centrifuged at 5000 rpm for 30 min. The supernatant was discarded and the pellet resuspended in 2 ml of sterile water. Absorbance of the resupended cells was measured at 450 nm. An appropriate amount of cell stock (to give a final absorbance of 0.5-0.6) was then used to inoculate 10 ml MG medium (containing 10 mg/ml tryptophan, 10 mg/ml B&W solution and 0.4 mM $MgSO_4$) and incubated at 37 °C, 200 rpm for 3.5 hours. 10 ml MG medium and 1 µM IPTG were then added. The culture was incubated at 30 °C, 200 rpm for 2 hours. 0.5 ml of culture was pipetted into a 10 ml tube and 2 µl of plasmid DNA added and this was incubated at 30 °C, 200 rpm for 30 min. 0.5 ml LB medium was added and the culture incubated at 37 °C for further 30-60 minutes. Successful transformants were screened by plating 200 µl of culture on to TBAB with appropriate antibiotic and incubated overnight at 37 °C. The protocol is based on that previously described by Hock (112).

2.4.7. Transformation of *E. coli* cells by electroporation

10 ml cultures of *E. coli* were inoculated and grown until absorbance at 600 nm reached approximately 0.6. The cultures were harvested and washed five times

in 1 ml ice cold, sterile 10% glycerol before being resuspended in 100 µl ice cold, sterile 10 % glycerol. 50 µl of cell were placed in an ice cold 2 mm width electroporation cuvette (Fisher Scientific) with approximately 100 ng of DNA. Electroporation was carried out in an Eppendorf 2510 Electropotator set to 200 Ω, 25 µF and 2.5 kV. The measured time constant was between 4.5 – 4.9 ms.

2.7.8. Blue/White screening

Blue/white screening is a useful technique to determine whether new DNA has been successfully cloned into the pUC18 (or equivalent) vector. "Blunt end" ligations, such as the introduction of a PCR product into pUC18 at its *Sma*I site are often unsuccessful because it is highly likely that the plasmid will ligate back to circular DNA without including any extra DNA. To screen for *E. coli* cells that have taken up plasmids that have an insert as opposed to those that do not, after transformation the cells are plated on LB agar containing 5-bromo-4-chloro-3-indoyl-β-galactopyranoside (X-gal) and 1 mM IPTG. The multiple cloning site (which includes the *Sma*I site) is positioned within the *lacZ'* gene present on the plasmid. *E. coli* strains such as JM109 do not have a functional *lacZ'* which encodes the α-subunit of β-galactosidase. When DNA is inserted at this site the *lacZ'* gene of the plasmid is interrupted and JM109 will continue to have a non-functional β-galactosidase, if JM109 takes up pUC18 with a non-interrupted *lacZ'* gene then it will have a functional β-galactosidase. X-gal is a colourless, modified galactose sugar which is easily metabolised by β-galactosidase to form an insoluble, bright blue molecule (5-bromo-4-chloroindole). Transformed cells that appear white on X-Gal harbour pUC18 with an interrupted *lacZ'* gene and are selected. The plasmid would then be

further tested for insert by sequencing and restriction digest as it is possible to interrupt the *lacZ'* gene with DNA other than the desired fragment.

Blue/white screening is not normally necessary when cloning using "sticky end" ligation techniques as the plasmid vector will have non-complementary sticky ends so will be unable to re-ligate into circular DNA without the inclusion of DNA with complementary sticky ends.

2.7.9. Isolation of DNA from cell cultures

Genomic DNA was isolated from 2 ml *B. subtilis* cultures using a Wizard genomic purification kit (Promega) as per manufacturer's instructions. Plasmid DNA was isolated from *E. coli* cultures using the QIAGEN mini-prep kit as per manufacturer's instructions.

Cosmid DNA was isolated from *E. coli* cultures using the follow protocol: 1.5 ml of *E. coli* containing cosmid was harvested from an overnight culture at 13000 rpm, 30 sec. Cells were resuspended in 50 mM Tris, 10 mM MOPS, pH 8 by vortexing and 200 µl 200 mM NaOH, 1 % sodium dodecyl sulphate (SDS) was added and mixed by inverting 10 times before adding 150 µl ice cold 3 M potassium acetate, pH 5.5, and mixing further by inverting five times. The mixture was then centrifuged at 13000 rpm for five minutes. The supernatant was carefully transferred to a tube containing 400 µl phenol:chloroform:isoamyl alcohol (25:24:1), and mixed by vortexing for two minutes before centrifuging at 13000 rpm for five minutes. The upper phase was carefully removed and added to 400 µl phenol:chloroform:isoamyl alcohol, again mixed by vortexing and

centrifuged as above. This second phenol:chloroform:isoamyl alcohol extraction to ensure better separation of protein solids. The upper phase was carefully removed and mixed with 600 µl isopropanol by inverting several times. This was incubated on ice for 10 minutes before centrifugation at 13000 rpm for five minutes. The supernatant was discarded and the pellet washed with 70% (v/v) ethanol and centrifuged at 13000 rpm. The supernatant was discarded and the pellet allowed to dry before resuspension in 50 µl 20 mM Tris, pH 8.

2.4.10. DNA quantification

Determination of DNA concentrations was achieved by measuring the absorbance of DNA solutions at 260 nm in a 1 cm pathlength cuvette and using the conversion factor in Equation 2.1.

1 absorbance unit at 260 nm ≡ DNA concentration of 50 µg/ml (Equation 2.1)

DNA purity was determined by also measuring the sample at 280 nm to establish an A260/A280 ratio. Pure double stranded DNA has a ratio of approximately 1.8. A lower value indicates contamination with protein and a higher value indicates contamination with RNA.

2.4.11. Agarose gel electrophoresis

1% w/v agarose gels were prepared by dissolving molecular biology grade agarose in TAE buffer (40 mM Tris acetate, 1 mM EDTA, pH 8) in a microwave (300 W) for approximately 5 minutes. The solution was allowed to cool to approximately 50 ^{o}C before the addition of ethidium bromide at a final

concentration of 1 µg/ml. The gel was then poured into the casting unit and allowed to set. DNA samples were prepared in loading buffer (0.25% w/v bromophenol blue, 0.25% w/v xylene cyanole, 15% w/v Ficoll 400, 50 mM Tris, 5 mM EDTA, 20% w/v glycerol, pH 8) so that the final concentration of DNA was between 0.5-1 µg/µl. Typically, 18 µl of sample was loaded on to the gel. Gels were run at 80 V for approximately 45 minutes, for a 40 ml gel; larger gels required more time. DNA bands were visualised over a 312 nm UV light source. If necessary DNA was purified from the gel using the QIAGEN Agarose Gel Clean Up Kit, as per manufacturer's instructions.

2.4.12. DNA sequencing

The cloned inserts of expression plasmids were verified by DNA sequencing by Eurofins MWG Operon, 318 Worple Road, Raynes Park, London, SW20 8QU.

2.4.13. LUGOL staining for amylase activity

Plasmid pVK48 allows the introduction of a gene, by way of a double crossover event, into the chromosome of *B. subtilis* at the *amyE* locus, which has the affect of disrupting the *amyE* gene and therefore knocking out amylase activity (Figure 2.1). This has two major advantages. First it ensures only one copy of the *resA* gene is introduced to *B. subtilis*; and secondly, it means that successful transformants can be easily detected by their inability to utilize starch as a carbon source. This is done simply by restreaking chloramphenicol resistant transformed colonies on to TBAB containing starch and staining them with LUGOL solution.

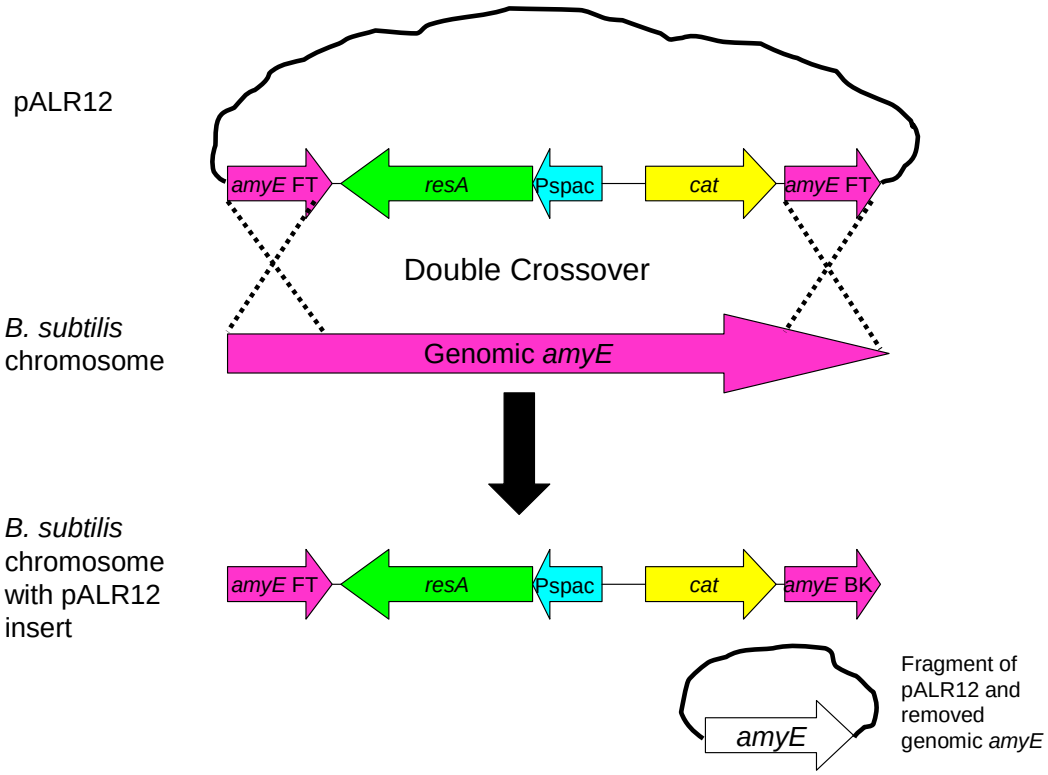

Figure 2.1. Insertion of pALR12 into the *amyE* gene in the *B. subtilis* genome. The 5' and 3' ends of the *amyE* gene (*amyE* ft and *amyE* bk, respectively) on the pALR12 plasmid base pair match with the front and back ends of the genomic *amyE* gene causing a double cross over event in which the middle section of the genomic *amyE* is substituted with the region between *amyE* ft and *amyE* bk from the plasmid, in this case the *resA* gene, the P_{spac} promoter and a chloramphenicol resistance gene (*cat*). The removed section of the genomic *amyE* and the non-inserted fragment of pALR12 cannot replicate and does not propagate within the cell. Note that pVK48 (and therefore pALR12) also contains *lacZ*, *lacI* and ampicillin resistance genes on the plasmid, which are not involved in the insertion event and so have been left out of the figure for simplicity.

In order to determine successful plasmid insertion into the *amyE* gene of *B. subtilis*, single colonies were re-streaked onto starch TBAB plates, see Table 2.1. The plates were incubated at 37 ^{o}C overnight and then at room temperature for a further 24 hours. To stain for amylase activity LUGOL solution (98.98% H_2O:0.34% iodine:0.68% potassium iodine solution) which stains starch dark blue was poured on to the starch TBAB plates. If the area around the colony was

not stained by the LUGOL solution this indicated that starch was not present and the *amyE* gene was therefore still active, showing that correct insertion of DNA had not occurred. Staining around the colonies indicated inactivation of the *amyE* gene, consistent with a successful transformation and mutation, see Figure 2.2.

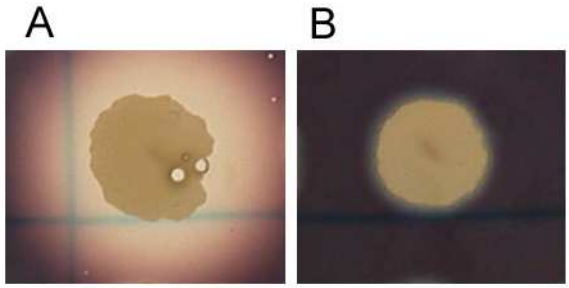

Figure 2.2. Confirmation of gene insertion at *amyE* locus by LUGOL staining. Transformed *B. subtilis* strains were grown on starch TBAB over night at 37 ^{o}C and then left at room temperature for a further day before staining with LUGOL solution. Colonies with a halo (A) were able to utilize starch (and removed it from the surrounding medium) showing that the *amyE* gene of the strain had not been interrupted and the chromosomal integration had not been completely successful. Those colonies without a halo (B) contained a defective *amyE* gene, indicating that the *resA* gene had been correctly inserted in to this region. This conclusion was further confirmed by PCR amplification.

2.5. Sample preparation

2.5.1. *B. subtilis* membrane preparations

B. subtilis strains were plated on to TBAB and incubated overnight at 37 ^{o}C. Cells on plates were resuspended in 5 ml NSMP medium and absorbance measured at 600 nm. 500 ml NSMP was inoculated with resuspended cells to give a starting absorbance of 0.05 at 600 nm. Growth of cells was monitored via absorbance at 600 nm. Cells were harvested by centrifugation at 7000 rpm for 15 min one hour after they reached stationary phase. The pellet was resuspended in 50 mM potassium phosphate pH 8, 35 ml/g. Cell weight was estimated using the following equation: Cell weight (g) = final OD_{600} x 1.4 x culture volume (L). The following quantities are all per g of cells. Cells were resuspended in 35 ml 50 mM potassium phosphate pH 8 at 37 ^{o}C. 18 mg lysozyme, 0.2 mg RNase, 0.2 mg DNase and 0.35 ml 1 M $MgSO_4$ was added to the resuspended cells and incubated at 37 ^{o}C for 30 min with occasional mixing. 2.1 ml 0.25 M EDTA pH 7.4 was added and the mixture incubated for further 2 min. 1.05 ml 1 M $MgSO_4$ was added and the mixture centrifuged for 30 min at 7300 rpm to remove all unbroken cells. The supernatant was then centrifuged at 20,000 rpm for 40 min and the pellet resuspended in 1.5 ml 0.1 M potassium phosphate pH 6.6 and centrifuged at 30,000 rpm for 30 min in a Beckman Coulter Optima Max Ultracentrifuge with a MLN-80 rotor. The pellet was then resuspended in 1.0 ml 20 mM MOPS pH 7.4. Membrane preparations were stored at -80 ^{o}C until needed. This protocol is based on that previously described by Hederstedt (113).

2.5.2. *S. coelicolor* membrane preparations

Membranes were prepared from 40 ml LB cultures, grown for 2-3 days, 250 rpm, 30 ^{o}C. Cells were harvested at 4000 rpm, 5 min, 4 ^{o}C, resuspended in 1 ml TCB (100 mM Tris, 50 mM NaCl, pH 8) and lysed on ice by sonication. Cell debris was removed by centrifugation at 8000 rpm, 30 min, 4 ^{o}C. The soluble fraction was collected and centrifuged at 30,000 rpm for 50 min, 4 ^{o}C in a Beckman Coulter Optima Max Ultracentrifuge with a MLN-80 rotor. The supernatant was discarded and the pellet resuspended in 200 µl 20 mM MOPS, pH 8, used immediately or stored at -20 °C until required.

2.5.3. Determination of protein concentrations

For a sample of pure protein with a known extinction coefficient, absorbance spectroscopy was used to determine the concentration of a protein sample using the Beer-Lambert law, Equation 2.4, where A is absorbance, ε is the extinction coefficient (M^{-1} cm^{-1}), c is concentration (M) and l is pathlength (cm).

$$A = \varepsilon c l \qquad \text{(Equation 2.4)}$$

For mixed proteins samples, such as membrane preparations, the bicinchoninic acid (BCA) assay was used (114). Membrane samples were diluted 20 fold and mixed with a BCA/copper solution (20 ml BCA solution (Sigma-Aldrich), 0.4 ml 4% (w/v) copper (II) sulphate pentahydarate), this dilution typically gave good absorbance at 562 nm within the range of the standard curve. Samples were incubated at 37 ^{o}C for 30 minutes before absorption at 562 nm was recorded. Each sample was repeated in triplicate so a mean A_{562} could be calculated. A

standard curve was generated using known concentrations of bovine serum albumin (BSA) from 0-1 mg/ml in increments of 0.2 mg/ml; this was used to estimate the concentrations of the membrane sample by comparing absorption at 562 nm.

2.5.4. Gel filtration chromatography

Gel filtration chromatography allows the separation of proteins based on their size. It utilises a column matrix that consists of a resin made up of porous beads. The pores are of a specific size (the exclusion limit) allowing proteins below that size to become trapped within the matrix and causing them to flow through the column at a lesser rate than that of larger proteins. The exclusion limit is specific to the type of resin selected for use in the column matrix. There are many different resins available for use in gel filtration chromatography. This project required two different resins for two different purposes, desalting and purification. Desalting was done using PD-10 columns (GE Healthcare). These contain Sephadex G-25 (Dextran), which has a fractionation range for globular proteins between 1-5 kDa. Since the proteins studied here were significantly larger than 5 kDa, the column allowed the separation of low molecular weight species (e.g. buffers) from the protein, facilitating, for example, buffer exchange. Purification required Superdex 75 (Dextran covalently bound to highly crosslinked agarose), which has a fractionation range for globular proteins between 3-75 kDa.

2.5.5. Anion exchange chromatography

Anion exchange chromatography allows the separation of proteins based on differences between their isoelectric point (pI) values. A pre-packed 5 ml HiTrap Q column (GE Healthcare) containing positively charged Sepharose media was used. Negatively charged proteins became bound to the column and were then eluted with buffer containing NaCl according to the strength of their interaction with the positively charged matrix. The more negatively charged the protein, the more tightly it will bind to the column matrix and the higher the NaCl concentration will have to be to elute it. Details of the buffers and conditions used are discussed in the results chapters where relevant.

2.6. Analytical techniques

Upon the generation of variant strains, membrane samples and pure protein samples several analytical procedures were employed to assess their biophysical and phenotypic properties.

2.6.1. SDS PAGE

Two SDS PAGE gel systems were employed during the course of this study. The first system, described by Laemmli *et al* (115), was used for analysis of whole cell protein content and for analysis during protein purification steps. This system provided good resolution when multiple proteins of variable masses were to be visualised using Coomassie staining. The second system, described by Schäggar and von Jagow (116), was used for haem staining and Western Blotting as it allowed better resolution when visualising single proteins.

2.6.1.1. SDS PAGE – Laemmli

The Laemmli gel system consisted of a resolving gel (3.5 ml acrylamide [70% acrylamide /30% bis-acrylamide]; 2.62 ml 1 M Tris pH 8.8; 70 µl 10% SDS; 0.84 ml H_2O; 4.6 µl 1,2-bis(dimethylamino)-ethane [TEMED]; 46 µl 10% w/v ammonium persulphate [AMPS]) and a stacking gel (1.1 ml acrylamide; 0.83 ml 1 M Tris pH 6.8; 66 µl 10% SDS; 4.64 ml H_2O; 6.6 µl TEMED; 33 µl AMPS) set in mini gel kit (Hoefer Mighty Small II for 8 x 9 cm Gels). The gel kit was filled with running buffer (made up in H_2O; 3 g/L Tris; 14.4 g/L glycine; 1 g/L SDS). 15 µl protein samples with 5 µl SDS loading dye (1 ml 1 M Tris pH 6.8; 200 mM DTT; SDS 4 %; 1 grain bromophenol blue; 2 ml glycerol, made up to 10 ml with H_2O) were boiled for 10 min before loading on to the gel. Gels were run at 180 V until the loading buffer had reached the bottom of the gel.

2.6.1.2. SDS PAGE - Shäggar and von Jagow (SVJ)

This consisted of a resolving gel (1.5 ml acrylamide; 2 ml gel buffer [3 M Tris pH 8.45, 0.3% SDS]; 1.6 ml 50% glycerol; 0.85 ml H_2O; 5 µl TEMED and 30 µl 10% AMPS) and a stacking gel (0.31 ml acrylamide; 0.78 ml gel buffer; 2.5 ml H_2O; 2.5 µl TEMED and 25 µl AMPS). The upper buffer consisted of 0.1 M Tris; 0.1 M tricine; 0.1% SDS; pH 8.25. The lower buffer was 0.2 M Tris pH 8.9. Membrane samples were mixed with an equal volume of loading buffer (as above but with 15% SDS) and incubated at 20 ^{o}C for 30 minutes prior to loading. SVJ gels were run at 100 V until the sample dye approached the bottom of the gel.

2.7.2. Haem staining

100 µg of prepared membrane sample was run on an SVJ SDS-PAGE gel. The gel was first soaked in 10% TCA for 10 minutes, washed twice for 10 minutes in distilled water to remove TCA and then stained for haem by incubation in 20 ml staining solution (1 mg/ml *o*-dianisidine-HCl; 0.1 M tri-sodium-citrate, pH 4.4; 0.7% w/v H_2O_2) at room temperature for 30 minutes. The reaction was stopped by washing the gel several times in water. Haem containing proteins were visible as the *o*-dianisidine turns green when oxidised by heam/H_2O_2. This protocol is based on that previously described by Schulz *et al* (73).

2.6.3. Western blots

25 µg of membrane preparation was loaded on to an SVJ SDS-PAGE gel and run as described above. The gel was then soaked for one hour in Towbin buffer (25 mM Tris, 192 mM glycine, 20% methanol) (117). The protein samples were then transferred on to polyvinylidenefluoride (PVDF) membrane (Hybond-P, GE Healthcare) in a tank blotting device (MiniVE, Hoefer) for 1.5 hours at 25 V. The membrane was blocked in 20 ml PBS (8 g/L NaCl; 0.2 g/L KCl; 0.2 g/L KH_2PO_4; 1.15 g/L Na_2HPO_4) and 10 % w/v milk for 10 min. The membrane was then placed in 5% w/v milk/PBS with the primary antibody (anti-ResA, from rabbit) at 1000 fold dilution from stock for one hour. The membrane was washed three times in 20 ml PBS and placed in 20 ml 5% w/v milk/PBS with secondary antibody (anti-rabbit, horseradish peroxidase linked, from donkey, Sigma) at 5000 fold dilution from stock for one hour. The membrane was then washed three times with 20 ml PBS. Western blots were visualised by soaking membrane in peroxidase reactive fluorescing reagent (GE Healthcare) as per

manufacturer's instructions. Excess reagent was drained from the membrane and the membrane was wrapped in cling film. The membrane was then exposed to Kodak scientific imaging film for between 30 seconds and 30 minutes (depending on the signal strength) in the dark. The film was then developed with an X-ograph according to the manufacturer's instructions.

2.6.4. Fluorescence spectroscopy

Fluorescence spectroscopy was used in two ways during the project. Firstly, tryptophan fluorescence was used to determine the folded/unfolded states of protein; secondly, badan fluorescence was used to determine the pK_a values of cysteines at the active site of proteins. The principle behind the techniques is the same in both cases: UV-visible light is used to excite protein molecules from their ground state into an excited electronic state (the process of absorbance). The relaxation of these molecules back down to their ground state can, under some conditions, result in the release of a photon. This phenomenon is called luminescence. Where the excited state, from which the photon is released, and the ground state share the same spin multiplicity, the luminescence is termed fluorescence.

Mechanisms of relaxation exist that do not result in the release of a photon, in which case the excess energy is dissipated in a non-radiative process as heat. Mechanisms which prevent or reduce fluorescence intensity are said to be quenching. Whether radiative or non-radiative relaxation mechanisms dominate can reveal information about the environment of the protein or more specifically about the environment of the fluorescent species. For example, in proteins

tryptophan residues are often fluorescent, but only within a fully folded protein. Upon unfolding, the fluorescence is efficiently quenched as the tryptophan side chain becomes exposed to the solvent.

Properties other than the folding state can also affect the protein tryptophan fluorescence. In thioredoxin-like proteins, for example, in which at least one tryptophan residue is located close to the CXXC active site, the oxidation state of the proteins significantly affect the fluorescence intensity, becoming quenched upon oxidation to the disulphide. This has enabled the use of fluorescence spectroscopy for the determination of reduction potentials of thioredoxin-like proteins (15).

To measure tryptophan fluorescence samples were excited at 290 nm and fluorescence recorded between 300-500 nm in a PerkinElmer Life Sciences LS55 fluorescence spectrometer, excitation slit set to 3 nm and the emission slit set to 7 nm and the scan speed was 1000 nm/min.

Fluorescence spectroscopy was also used to monitor the covalent binding of the fluorescent probe ***6-Bromoacetyl-2-dimethylaminonaphthalene*** (badan, Figure 2.3) to cysteine thiols to determine the pK_a values of the reactive thiol groups. This again relied on the fact that fluorescence properties of the probe were very different in solvent compared to when it was attached to the protein. Badan is a fluorescent probe that reacts specifically with thiols and has been used to determine the pK_a of the active site cysteine thiols in TDORs (15). When badan

reacts with a thiol a covalent bond is formed with the sulphur and HBr is released.

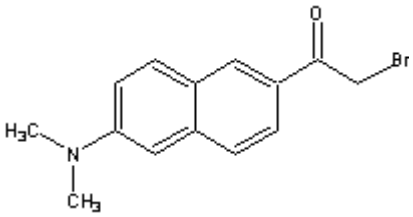

Figure 2.3. Badan (6-Bromoacetyl-2–dimethylaminonaphthalene).

Protein samples were reduced by the addition of 1 mM DTT overnight at 4 °C. The DTT was then removed by gel filtration using a (PD-10 desalting column, GE healthcare) equilibrated in 20 mM Tris pH 8 under aerobic conditions. Badan was prepared in a mixed buffer and allowed to equilibrate for at least one hour in the dark at room temperature. The badan was used in excess amounts compared to ScResA (i.e. under pseudo-first order conditions) in order to calculate a pseudo first order rate constant for the reaction at each pH value.

For badan experiments, samples were excited at 391 nm in a PerkinElmer Life Sciences LS55 fluorescence spectrometer and fluorescence was recorded between 400 and 600 nm, with emission and excitation slits both set to 5 nm, the scan speed was 1000 nm/min and the samples were scanned once a minute until the reaction appeared to be complete. In all cases the fluorescence of the 7 µM badan alone was observed before adding 0.25 µM (final concentration) reduced protein to act as a reference to show the spectrum of free badan.

2.6.5. Cytochrome *c* oxidase assay

6.9 mg of cytochrome *c* from horse heart was dissolved in 20 mM Tris pH 8 and reduced with 1 mM sodium dithionite. Excess dithionite was removed using a desalting column (PD-10, GE Healthcare) from which cytochrome *c* was eluted as a 160 µM solution in 3.5 ml of 20 mM MOPS pH 7.4. This was then further diluted to 80 µM with 20 mM MOPS pH 7.4. Membrane preparations were diluted to 80 µg/ml in 20 mM MOPS pH 7.4. The cytochrome *c* concentration ([cyt c] mM) was determined using Equation 2.3 and a $\Delta\varepsilon_{550nm}$ of 19.6 $mM^{-1}cm^{-1}$ (118).

$$\frac{A_{550(red)} - A_{550(ox)}}{19.6} = [\text{cyt c}]\text{mM} \qquad \text{(Equation 2.3)}$$

A Perkin Elmer Lambda 800 spectrophotometer was used to measure absorbance at 540 and 550 nm every 15 seconds. 1 ml of reduced cytochrome *c* was added to a 3 ml quartz cuvette containing a stirrer bar. 1 ml of the membrane preparation was added to the cuvette and the absorbance at 540 and 550 nm was recorded every 15 seconds for 6 minutes. Oxidation of cytochrome *c* results in a decrease in absorbance at 550 nm. The wavelengh 540 nm is an isosbestic point and does not change as cytochrome *c* changes from the reduced to the oxidised states. Therefore, deducting the absorbance at 540 nm from the absorbance at 550 nm compensates for any additional absorbance at these wavelength caused by the addition of the membrane protein. The difference in absorbance (A_{550nm}-A_{540nm}) was plotted against time and the initial rate of change in absorbance (dA/dt) was determined by drawing tangents to the initial data to represent the maximum and

minimum rates. An example is shown in Figure 2.4. Equation 2.3 was used to calculate these rates of cytochrome *c* oxidation (mM min^{-1}).

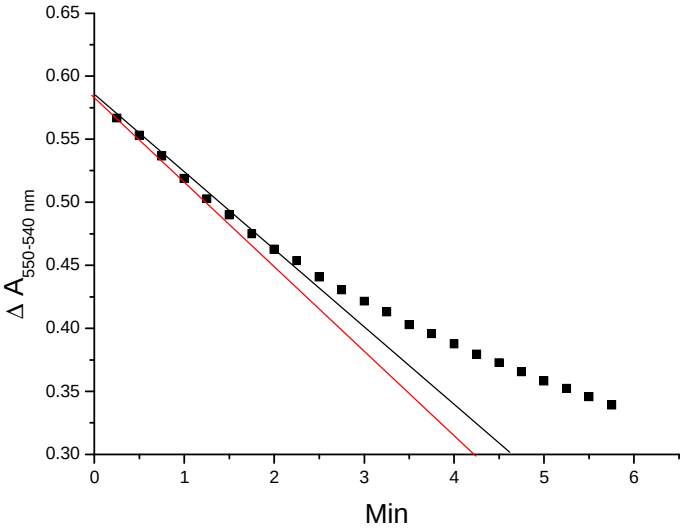

Figure 2.4. A typical cytochrome *c* oxidation assay plot. $A_{550\text{-}540nm}$ is plotted against time with maximum (red) and minimum (black) tangent lines drawn to determine the initial rate of oxidation.

The rate in absorbance per minute was converted to mM cytochrome *c* oxidised per minute ($d[cyt]_{ox}/dt$) using Equation 2.4 below, where [cyt] is the concentration of cytochrome *c* used and ΔA_t is the total absorbance change in going from fully reduced to fully oxidised cytochrome *c*. This protocol was adapted from van der Oost *et al* (119).

$$\frac{d[cyt]_{ox}}{dt} = \frac{dA}{dt} \text{ x } \frac{[cyt]}{\Delta A_t} \qquad \text{(Equation 2.4.)}$$

2.6.6. TMPD staining for cytochrome *c* oxidase activity

Cytochrome caa_3 oxidase activity is required for the rapid oxidation of N,N,N',N'-tetramethyl-p-phenylenediamine (TMPD). TMPD is an easily

oxidised compound that serves as a reducing co-substrate for haem-containing enzymes, including cytochrome *c* oxidase, which in *B. subtilis* is the principle TMPD-oxidising enzyme. Therefore, TMPD can be used as a probe for the presence of active cytochrome *c* oxidase. Because the enzyme contains a *c*-type haem it can be used to probe for the presence of functional CCM. TMPD undergoes one-electron oxidation producing a highly coloured product that absorbs at 611 nm, giving a blue colour easily observable to the naked eye (120). Colonies were stained for caa_3 oxidase activity directly on agar plates, as described by Le Brun *et al* (54). Single colony transformants were plated on to TBAB, incubated at 37 ^{o}C overnight, then incubated at room temperature for 24 hours to ensure colonies were tightly bound to the plate. The plates to be stained were then incubated at -20 ^{o}C for 12 min before pouring on TMPD stain (1.6 ml 10% Triton X-100 in 0.1 M potassium phosphate pH 7; 0.4 ml 10% sodium deoxycholate; 2.0 ml EtOH; 4.0 ml 1.5% w/v agar). The agar was heated to 55 ^{o}C before mixing. 2.0 ml 1% w/v TMPD was added to the mix immediately before the stain was poured on to the plate. Colonies that turned blue/purple demonstrated cytochrome *c* oxidase activity.

Chapter 3: *In vivo* studies of the active site residues of *B. subtilis* ResA

3.1. Introduction

ResA is an extracytoplasmic membrane-bound thiol-disulfide oxidoreductase required for cytochrome *c* maturation in the Gram positive bacterium *Bacillus subtilis*. Previous biochemical and structural studies have identified several potential key residues required for the function of ResA, including the active site cysteinyls. Various site directed mutations were made in the full length *resA* gene to study the effects of alterations of these key residues on ResA activity. The mutant genes were then inserted into the genome of a ResA deficient strain of *B. subtilis*. Gene expression was induced with IPTG but protein production was regulated by the natural *resA* ribosomal binding site located in the flanking DNA at the 5' end of the *resA* gene. In this way it was possible to show the importance of these residues for function *in vivo*.

As discussed in detail in Chapter 1, cytochromes *c* have many and diverse functions within cells and differ from other cytochromes as they have haem covalently bound to a highly conserver CXXCH haem binding motif, (45,70). Although many cytochromes *c* have been studied in detail, less is known about how they acquire their covalently bound haem, a post translational process referred to as cytochrome *c* maturation (CCM). *B. subtilis* possesses a CCM system II that has three dedicated proteins ResA, ResB and ResC (54). ResA is a thiol-disulfide oxidoreductase (TDOR) and contains a CXXC active site motif.

The midpoint reduction potential varies greatly among TDORs. Thioredoxin from *E. coli* is highly reducing with a midpoint potential of -270 mV at pH 7 (121,122), whereas DsbA from *E. coli* has a much higher potential of -89 to -110 mV at pH 7 (7,8). ResA has a very low redox midpoint potential (-256 mV) at pH 7 which means it has strong reducing capabilities (19) and, consistent with this ResA is more stable in its oxidised form (14). *In vitro* studies have demonstrated that the glutamate and the proline that lie between the two cysteines of the ResA active site (Glu75 and Pro76, respectively) are important to maintain the low reduction midpoint potential of ResA by maintaining the pK_a values of the active site cysteines. Crystal structures of the active site variants, solved from the soluble forms of the proteins, are shown in Figure 3.1.

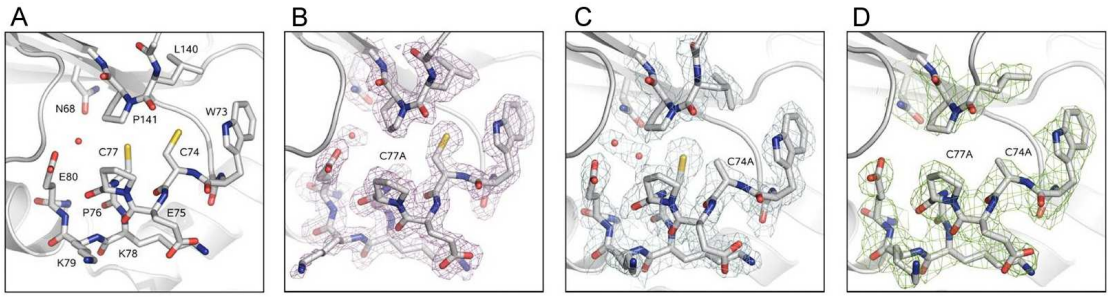

Figure 3.1. Crystal structures of wild type ResA and active site cysteine variants. Panels correspond to: A, wild type ResA; B, C77A ResA; C, C74A ResA; and D, C74A/C77A ResA. Carbon, nitrogen, oxygen and sulphur are shown in white, blue, red and yellow respectively. The red spheres represent water molecules. Figure prepared from PDB files 1SU9, 2H1A, 2H19 and 2H1G for wild type, C74A, C77A and C74a/C77A respectively using pymol (www.pymol.org).

The roles of the active site cysteines and Pro76 were investigated *in vivo* by the expression of genes coding the ResA variants C74A, C77A, C74A/C77A and P76H in a ResA deficient strain. Using several methods of determining cytochrome *c* content and activity, it was shown that both of the active site cysteinyls are essential for function. Furthermore, Pro76, which lies between the

two cysteines of the active site, has little effect on *in vivo* function even though *in vitro* results demonstrated it has a role in maintaining the pK_a value of the active site cysteines.

3.2. Materials and Methods

All the methods used in this work are described in Chapter 2. The bacterial strains, oligonucleotide primers and plasmids used and/or generated during the course of this study are listed in Chapter 2, Tables 2.1, 2.7 and 2.9, respectively.

3.3. Results

3.3.1. Construction of vectors and strains

In order to ascertain the importance of the residues found in the active site of ResA in the cell, site directed mutagenesis was employed to introduce nucleotide changes to the *resA* gene by PCR that would result in single amino acid residue changes in the ResA protein. First the *resA* gene, including its natural ribosome binding site, was amplified by PCR and blunt end cloned into pUC18 at the *Sma*I site. This plasmid, pALR9, was then used as a template for the PCR mutagenesis. Primers were designed to introduce mutations in the amplified DNA and used as described in Chapter 2. Mutagenised plasmid DNA was sequenced to ensure the correct mutation had been introduced before the *resA* gene was excised from the pUC18-derivative and cloned into plasmid pVK48 between the *Hin*dIII and *Xba*I sites generating plasmids pALR12 (wild type *resA*), pALR34 (C74A *resA*), pARLR35 (C77A *resA*), pALR39 (C74A/C77A *resA*) and pCHN6 (E75Q *resA*). These plasmids were used to transform LUL9, a ResA deficient derivative of the 1A1 wild type strain (12).

Once a successful transformation had been confirmed by LUGOL staining for starch, genomic DNA was prepared from 5 ml cultures of these transformed strains as described in Chapter 2. Primers were designed to amplify the region of DNA between the 5' and 3' *amyE* regions of pVK48. These primers were used to amplify the genomic DNA from the *resA* variant *B. subtilis* strains. Successful plasmid insertion into the LUL9 chromosome resulted in a fragment of 948 bps, see Figure 3.2.

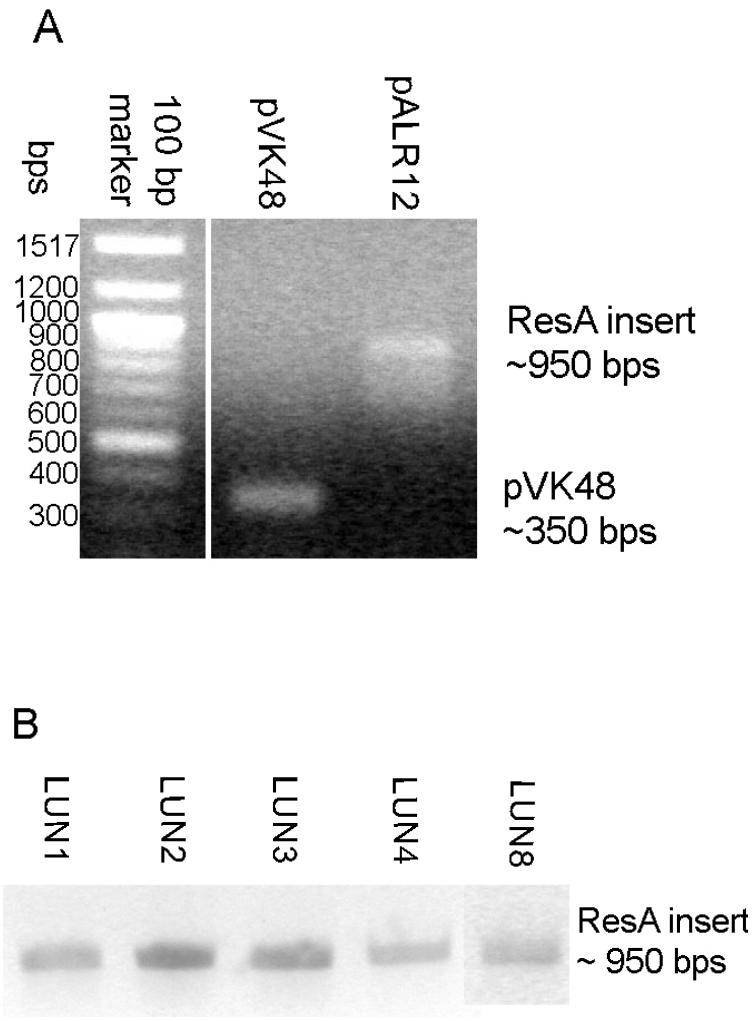

Figure 3.2. PCR amplification of *amyE* region of the LUL9 chormosome. A, control amplification of pVK48 plasmid DNA resulted in a ~ 350 bps fragment while a ~ 950 bps fragment is amplified from plasmid pALR12. B, *amyE* region was amplified from genomic DNA extracted from *B. subtilis* strains LUN1 (wild type), LUN2 (C74A), LUN3 (C77A), LUN4 (C74A/C77A) and LUN8 (P76H). PCR products were run on a 1% agarose gel. This demonstrated that the replacement of *amyE* by *resA* was successful.

As with the wild type gene, the gene is in single copy and the transcribed mRNA contains the natural ribosome binding site but is not transcribed from its natural promoter as it is under the control of the IPTG inducible P_{spac} promoter. Western blot analysis was used to confirm that variant ResA protein was produced at levels comparable to that of wild type, Figure 3.3.

3.3.2. Analysis of protein production by Western blotting

Western blotting was employed to determine the level of production of the variants of ResA in LUL9-based strains. Membranes were prepared from *B. subtilis* strains grown in NSMP as described in Chapter 2. 25 µg of membrane protein samples were run on SDS PAGE and transferred to PVDF membrane and the blot developed, as described in Chapter 2, using ResA antibodies raised in rabbits that were available from previous studies (12). The blot (Figure 3.5) confirmed that the variant proteins (C74A, C77A and C74A/C77A) were produced to levels comparable to that of wild type protein in 1A1 and wild type ResA generated from wild type *resA* integrated at *amyE* in LUL9. As expected, LUL9 did not give rise to band as it is defective in ResA (12).

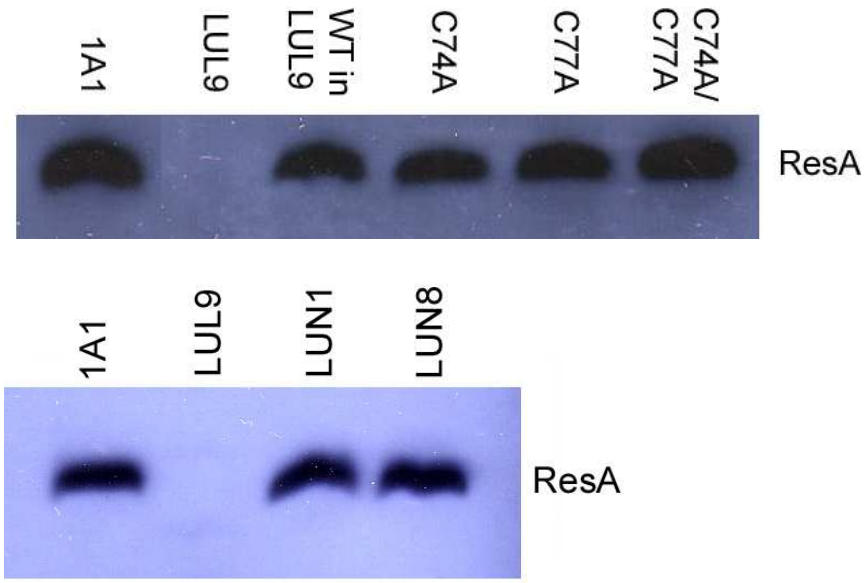

Figure 3.3. Western blot analysis of ResA production in LUL9-derivative strains. 25 µg of membranes sample, prepared from the resA variant expressing *B. subtilis* strains, were tested for the presence of ResA by Western blotting. In the 1A1 wild type strain and the ResA variants in LUL9 based strains LUN1 (WT ResA), LUN2 (C74A), LUN3 (C77A), LUN4 (C74A/C77A) and LUN8 (P76H) there is good signal from the peroxidase labelled secondary antibody, which demonstrates that the proteins are present at similar levels as in the wild type strain. As expected, LUL9, the ResA deficient strain, shows no expression.

3.3.3. Investigation of ResA activities by TMPD staining

Once it had been confirmed that the ResA variants were being produced in the LUL9 based strains, preliminary tests were carried out to see if these proteins were functional using TMPD staining. The active site variants were restreaked on to NSMP/agar medium and stained with TMPD as described in Chapter 2. 1A1, LUN1 (wild type ResA) and LUN8 (P76H ResA) all demonstrated good levels of staining and therefore an active cytochrome *c* oxidase (Figure 3.4). All three cysteine variants show a similar phenotype to LUL9, which has no visible staining and therefore no functioning cytochrome *c* oxidase (Figure 3.4). TMPD staining is an effective way of quickly showing whether or is not there is any

cytochrome *c* oxidase activity, but is not quantitative and it does not offer information about the other cytochromes *c* present in *B. subtilis*.

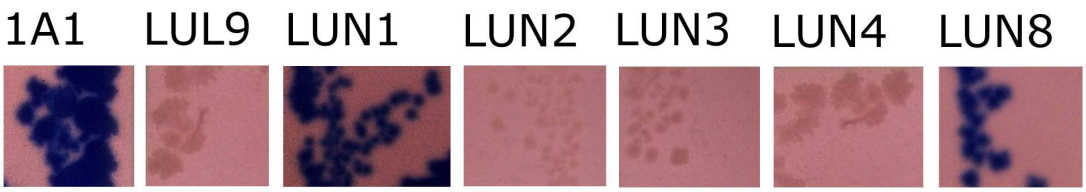

Figure 3.4. TMPD stains of *B. subtilis* wild type, ResA deficient and ResA active site variant strains. *B. subtilis* strains expressing variant resA genes were re-streaked on to TBAB medium and stained with TMPD as described in Chapter 2. *B. subtilis* colonies made up of cells with an active cytochrome *c* oxidase are stain blue as the TMPD reacts. The active site cysteine variant strains (LUN2, LUN3 and LUN4) have a similar phenotype to the ResA deficient strain (LUL9). The ResA P76H variant (LUN8) appears to have a similar phenotype to the wild type ResA strains (1A1 and LUN1).

The staining data showed that LUL9 was complemented by the presence of wild-type ResA, and that some activity was present for LUL9 complimented with P76H ResA. The other strains, in which C74A, C77A and C74A/C77A ResA proteins were present, did not contain obvious cytochrome *c* oxidase activity.

3.3.4. Cytochrome *c* oxidase assays.

TMPD staining, shown above, demonstrated that the P76H variant of ResA gave rise to a functioning cytochrome *c* oxidase but the active site cysteine ResA variants did not. In order to more precisely quantify the level of cytochrome *c* oxidase activity, a spectroscopic cytochrome *c* oxidase assay was employed. 40 µg of membrane protein (final concentration) was added to 40 µM reduced horse heart cytochrome *c* in a cuvette and the absorbance was recorded at 550 and 540 nm every 15 seconds to monitor the oxidation of cytochrome *c*. The absorbance at 540 nm was subtracted from that at 550 nm and plotted against time in order to calculate the oxidation rates of cytochrome *c* (Figure 3.5; see Chapter 2, for more

detail). Initial rates (ΔA/dt) were obtained by drawing a tangent to the initial, linear part of the kinetic traces and calculating the gradient. A mean value was obtained by estimating the extremities of the initial gradient.

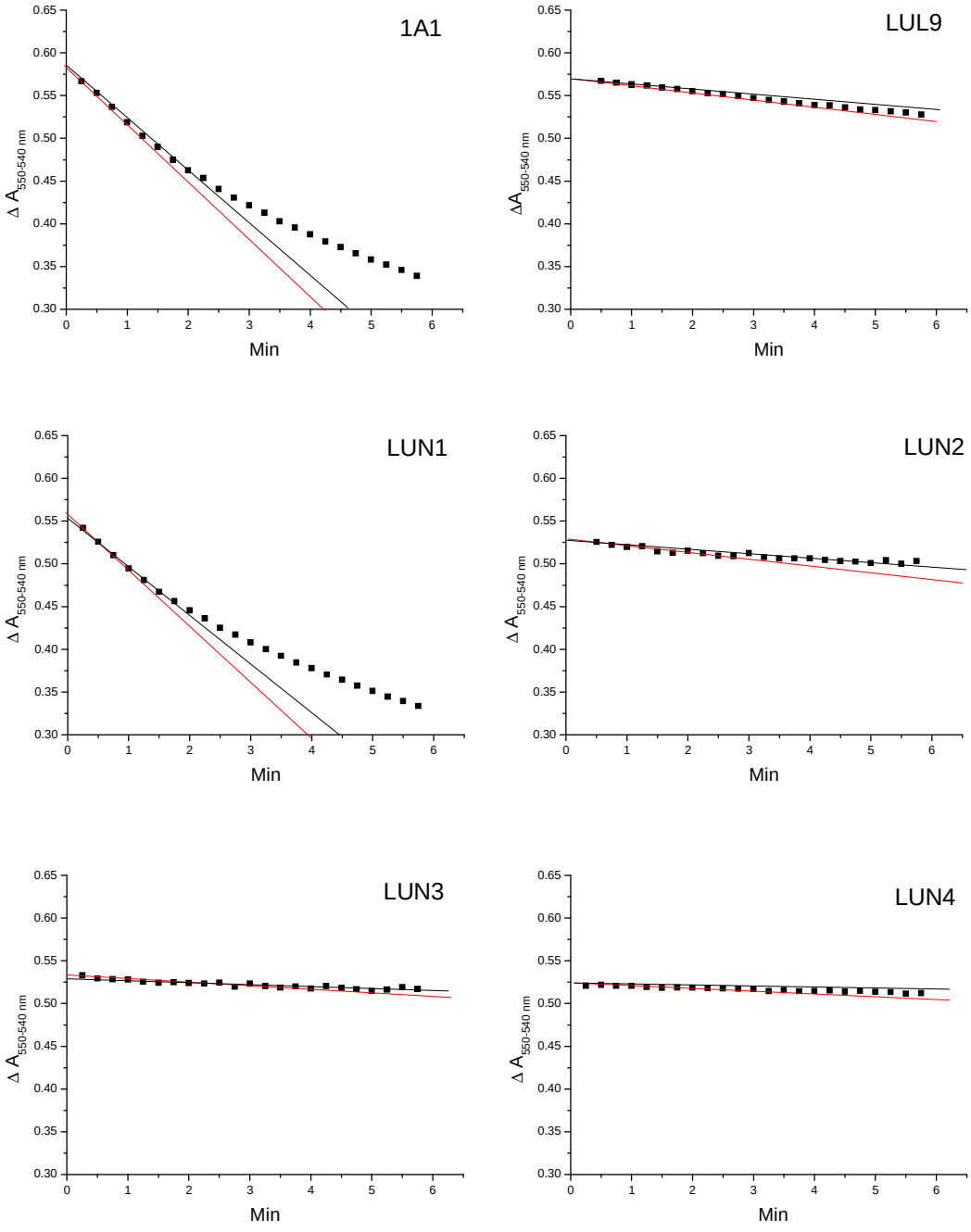

Figure 3.5. Cytochrome *c* oxidase assays. Representative plots of Δ $A_{550\text{-}540\ nm}$ as a function of time following mixing of *B. subtilis* membranes with reduced horse heart cytochrome *c*. Two lines were fitted to each plot to represent the maximum (red) and minimum (black) rates of reaction. The gradients of these lines were used to calculate a mean rate of reaction.

Experiments were carried out in triplicate using at least two independently prepared membrane batches. The rate, in absorbance per minute, was converted to nM cytochrome *c* oxidised per minute as described in Chapter 2. Rates were normalised by dividing by the mass of membrane protein present in each sample.

Table 3.1. Cytochrome *c* oxidation activities of ResA and ResA active site variants

Strain	ResA variant	Oxidation activity (nM min^{-1} mg $protein^{-1}$)[a]
1A1	Wild type	83 ± 4
LUL9		5 ± 4
LUN1	Wild type	82 ± 6
LUN2	C74A	13 ± 1
LUN3	C77A	4 ± 2
LUN4	C74A/C77A	4 ± 1
LUN8	P76H	35 ± 4

[a] The data are the means ± standard errors of several measurements ($n \geq 3$) obtained using at least two different membrane preparations.

Analysed results from cytochrome *c* oxidase assays are shown in Table 3.1. The cytochrome *c* oxidase assay demonstrated that the complementation of LUL9 with wild-type *resA* at the *amyE* locus gives a wild-type phenotype. The background rate of cytochrome *c* oxidation (in the absence of ResA) was calculated to be about 6% of that of the wild-type. Similar rates were also measured for LUN3 (C77A) and LUN4 (C74A/C77A). LUN2 (C74A) gave a rate somewhat higher, indicating that some activity was present even in the absence of the N-terminal cysteine. LUN8, which exhibited clears levels of TMPD staining, exhibited about 40% cytochrome *c* oxidase activity compared to wild type strains, suggesting that although P76 is not essential, the decreased pK_a values and increased reduction potential associated with the active site cysteines in P76H ResA *in vitro* has an effect on the activity of ResA *in vivo*.

3.3.5. Haem staining of the active site variants.

Neither TMPD staining nor the cytochrome *c* oxidase assay report any information about the presence of cytochromes *c* other than CtaC of cytochrome *c* oxidase. In order to obtain a broader view of cytochrome *c* content of membranes a haem staining method was employed. 100 µg of membrane samples were run on an SDS-PAGE gel and stained for haem as described in Chapter 2, see Figure 3.6. All three of the cysteine variant strains appeared to be unable to synthesise any cytochromes *c*. The only band visibly stained in these samples was QcrB, which is a cytochrome *b* with an unusual covalently bound haem, which is attached to the protein via a pathway (which is currently unknown) distinct from that of CCM system II. This demonstrates that the active site cysteines of ResA are required for the correct maturation of all CCM system II-dependent cytochromes *c*. The P76H variant (LUN8) was found to be capable of maturing all the cytochromes *c* but to seemingly lesser levels than the wild type strains. This is in agreement with the cytochrome *c* oxidase assays above, where it was shown that P76H ResA only has about 40% activity compared to that of the wild type protein. This further demonstrates the importance of P76 in maintaining the high pK_a values of the active site cysteines and the low redox potential of the active site.

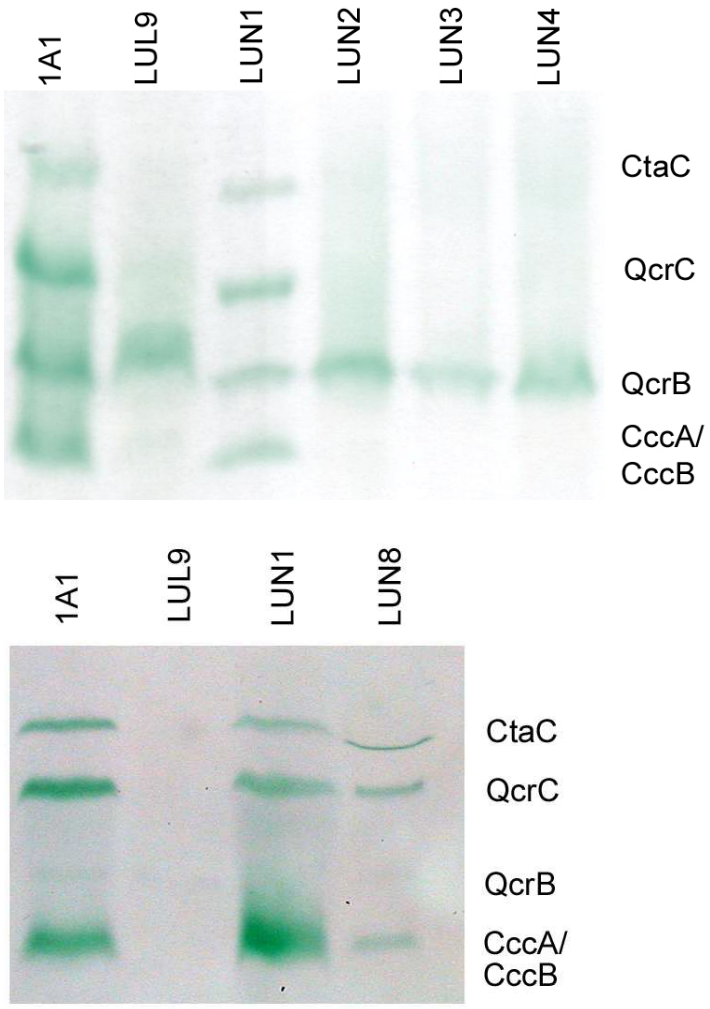

Figure 3.6. Haem stain of cytochromes *c* present in the membranes of active site cysteine variant ResA strains. 100 µg of membrane protein from *B. subtilis* strains 1A1 (wild type), LUL9 (ResA$^-$), LUN1 (wild type insertion), LUN2 (C74A), LUN3 (C77A), LUN4 (C74A/C77A) and LUN8 (P76H) were run on SDS-PAGE and stained for haem. Bands due to cytochromes *c* are as indicated on the right. QcrB is a cytochrome *b* that unusually has a covalently bound haem that is attached by an unknown means outside of the Res system. The staining of QcrB is variable from sample to sample, it is not known why this is.

3.3.6. The wild type CCM phenotype is restored with addition of dithiothreitol (DTT) to the growth medium.

It was previously demonstrated that the wild type CCM phenotype can be restored in the ResA deficient strain LUL9 by the addition of 15 mM DTT to the growth medium when the strain was grown on NSMP/agar and stained for

TMPD oxidase activity (12). As discussed above, TMPD staining only provides information about CtaC. To determine whether the addition of DTT facilitates the maturation of all the cytochromes *c* of *B. subtilis*, membranes were prepared from cultures of LUL9, LUN2, LUN3 and LUN4 that had been grown in the presence of 1 mM DTT from halfway through the exponential growth phase. Adding DTT before the culture had reached this point proved to be toxic, as did adding any more than 1 mM DTT in liquid culture. 100 µg of membrane protein samples were run on SDS-PAGE and stained for haem as previously described, see Figure 3.7. The maturation of all *c*-type cytochromes, to wild-type levels, was observed for LUN2-4. Lower but detectable levels of cytochrome *c* were observed for LUL9 grown with DTT.

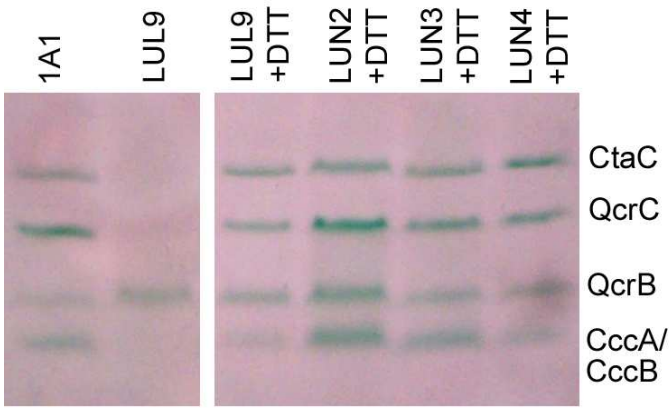

Figure 3.7. Haem stain of cytochromes *c* found in membranes of cysteine variant ResA strains and LUL9 grown in the presence of 1 mM DTT. 100 µg of membrane protein samples from *B. subtilis* strains 1A1 (wild type), LUL9 (ResA$^-$), LUN1 (wild type insertion), LUN2 (C74A), LUN3 (C77A) and LUN4 (C74A/C77A) run on SDS-PAGE and stained for haem. Bands due to QcrB and cytochromes *c* are indicated as on the right.

3.4. Discussion.

Variations in the active site of *B. subtilis* ResA have revealed information about the mechanism of disulfide exchange in this protein. Substitution of the active site cysteines resulted in a complete loss of activity with respect to cytochrome *c* maturation in LUN3 (C77A ResA) and LUN4 (C74A/C77A ResA) and close to no activity in LUN2 (C74A ResA). This is consistent with the accepted mechanism of disulphide exchange discussed in Chapter 1, which would be interrupted if either cysteine were removed.

Similarly to the *resA* inactivation in *B. subtilis*, a deletion of *ccmG* in *E. coli* also resulted in a complete loss of CCM (123). Complementation of the Δ*ccmG E. coli* strain with genes encoding active site cysteine variants of CcmG resulted in low but detectable level of heterologously expressed *Bradyrhizobium japonicum* cytochrome c_{550}, suggesting that, in addition to the TDOR activity of CcmG, it may also have a chaperone function in CCM (75) . The findings with the ResA active site variants suggest that its principle role lies with disulfide exchange and it plays no other essential part in CCM. This is consistent with the observation that CCM can be restored to a ResA deficient strain by the introduction of the reducing agent DTT to the growth medium or the inactivation of BdbD (12). This showed that ResA is not essential to CCM unless the substrate proteins are in the oxidised state or there is an alternative source of electrons available. DTT can clearly access the outer side of the cytoplasmic membrane to fulfil this role. Interestingly, LUL9 not complemented with a variant *resA* gene did not demonstrate as much CCM activity as LUL9 with a complementing *resA* gene. This suggests that ResA may have another role in CCM in addition to the

reduction of the proposed apo-cytochrome *c* substrate proteins, possibly as a chaperone, directing the apo-cytochromes *c* to the other Res proteins.

The *in vivo* effect of the P76H variant can be explained by the *in vitro* findings. The crystal structure of the soluble version of this variant demonstrated that the overall structure of ResA was largely unaffected by the substitution of Pro76, although changes were observed in the vicinity of the active site. The P76H variant exhibited significant flexibility compared to that of the wild type protein or the P76H/E75P (DsbA-type) variant. A proline at either position 75 or 76 is likely to be important for imparting structural rigidity on to the active site and subsequent loss of this rigidity found in the P76H ResA variant could have a detrimental effect on the function of the protein. The lowered pK_a values of the active site cysteines of the P76H variant and the related increase in reduction potential is likely to make it less energetically favourable for ResA to pass reducing equivalents to its substrate protein, presumed to be apo-cytochrome *c*. The decrease in pK_a values of the active site cyteines could also lead to ResA being more active toward non-natural substrate proteins, introducing a competition between ResA substrates and other proteins that would not exist for the wild type protein. Finally, the side chain of the histidine in position 76 has the ability to fold back into the hydrophobic cavity and interact with Glu80. Glu80 is believed to play an important part in substrate recognition (discussed in Chapter 4); therefore this interaction may inhibit the recognition of ResA with its natural substrates.

Chapter 4: *In vivo* studies of the functional importance of the hydrophobic cavity and the membrane anchor of *B. subtilis* ResA

4.1 Inroduction.

Previous studies have identified several functionally important amino acid residues in the *B. subtilis* ResA polypeptide. These include the two active site cysteine residues, discussed in Chapter 3, and a glutamate, Glu80, within the near-active site hydrophobic cavity. Also identified was Pro141 which is located in the hydrophobic cavity region of the protein and adopts a *cis* configuration. The *cis*-proline is a highly conserved residue amongst TDORs, and appears to play a key role in, for example, TDOR-substrate interactions and stability (16,18). *In vitro* studies have shown Glu80 of ResA to be important in controlling the acid/base properties of the active site. It is also thought to be involved in substrate recognition. In order to investigate the importance of these residues in the living cell the following variants were constructed and expressed in a ResA deficient strain, LUL9: P141S, P141T and E80Q. Glu80 and Pro141 are both located within this hydrophobic cavity. A stick representation of the high resolution structure of this region of ResA is shown in Figure 4.1.

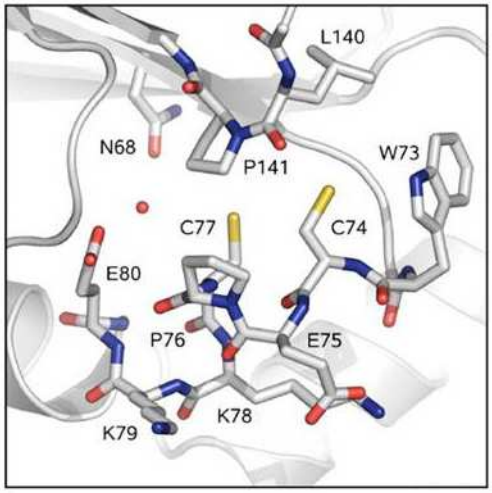

Figure 4.1. Crystal structure of the active site and hydrophobic cavity region of wild type *B. subtilis* ResA obtained at pH 9.25. Carbon, nitrogen, oxygen and sulphur molecules shown in white, blue, red and yellow, respectively. A water molecule, depicted in red, fills the space between N68, C77 and E80. Figure adapted from Lewin *et al*, 2006 (15)

ResA is attached to the membrane by an N-terminal membrane anchor. *In vitro* studies of the ResA protein were performed using a form of the protein lacking the hydrophobic anchor region. Therefore, little is known about the importance or role (if any) of the membrane anchor outside of its primary function of keeping the protein attached to the membrane. To study the role of this region a fusion protein was constructed containing the N-terminal anchor region of the *B. subtilis* cytochrome *c* CccA and the C-terminal, solvent exposed domain of ResA. CccA is a small cytochrome *c* with, as yet, no known function.

```
ResA          MKKKRRLFIRTGILLVLICALGYTIYNAVFAGKESISEGS 40
CccA          MKWNP--LIP--FLLIAVLGIGLTFFLSVKGLDDSREIAS 36
```

Figure 4.2. Comparison of the N-terminal amino acid sequences from *B. subtilis* ResA and *B. subtilis* CccA. Residues highlighted in yellow are conserved, residues highlighted in green represent a conservative substitution and the numbers represent the position the final residue shown here is found in the full length amino sequence of the protein.

A comparison of the N-terminal regions of CccA and ResA revealed several conserved residues (Figure 4.2.), but they are sufficiently different to test the importance of the specific sequence of the N-terminal membrane anchor for ResA function. The importance of the transmembrane domain of ResA was also investigated by the generation of a CccA:ResA fusion protein, containing the transmembrane domain of CccA and the solvent exposed, active domain of ResA.

4.2. Materials and Methods.

All the methods used in this work are described in Chapter 2. The bacterial strains, oligonucleotide primers and plasmids used and/or generated during the course of this study are listed in Chapter 2, Tables 2.1, 2.7 and 2.9, respectively.

4.3. Results.

4.3.1. *In vivo* studies of the key residues found in the hydrophobic cavity.

Site directed PCR mutagenesis was employed in order to generate genes encoding P141S, P141T and E80Q ResA as described in Chapter 2, Materials and methods. Plasmid pALR9, which contains a 0.73 kb DNA fragment containing *resA* and its natural promoter, was used as a template for mutagenesis, and successful PCR mutagenesis was confirmed by sequencing (MWG Biotech). The variant *resA* genes were cut from the pUC18 vector and ligated into plasmid pVK48 between the *Xba*I and *Hin*dIII restriction sites. Plasmid pVK48 allows insertion at the *amyE* locus (described in Chapter 2). Correct gene insertion was further confirmed by PCR amplification, see Figure 4.3. Primers were designed to amplify the region between the *Xba*I and *Hin*dIII restriction sites of the

pVK48 plasmid, which is now inserted at the *amyE* locus and contains the *resA* gene. These primers were used to amplify this region from genomic DNA. Correct gene insertion gave rise to a ~950 bp fragment of DNA.

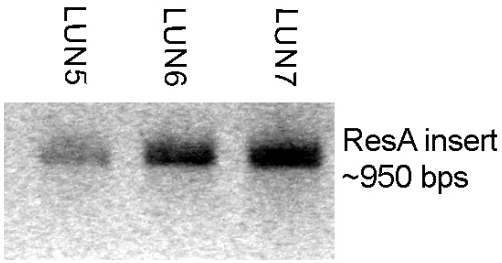

Figure 4.3. PCR amplification of *resA* insertion in the genome of *B. subtilis* LUL9 at the *amyE* locus. Genomic DNA was prepared from the *B. subtilis* strains LUN5 (E80Q), LUN6 (P141S) and LUN7 (P141T) and the *amyE* region was amplified by PCR. The *amyE* gene is 1980 bps in length but if it has been interrupted with *resA* from a pVK48 vector the region between the *amyE* 5' and 3' ends will only be ~950 bps. Each of the variants demonstrated a band at ~950 bps. Although LUN5 appears to have a weaker band than LUN6 and LUN7, the presence of the band demonstrates correct gene insertion.

4.3.2. Confirmation of expression of variant ResA proteins by Western Blotting.

Once the correct insertion of the variant *resA* genes in the *amyE* position had been confirmed for each strain it was important to confirm the gene was being expressed and that the protein was being produced. Although the variant *resA* genes are expressed from an IPTG inducible P_{spac} promoter, the transcribed RNA contains the natural ribosome binding site, which should encourage the protein to be expressed at levels similar to that of the wild type strain 1A1, although this will also depend on the rate of transcription. Antibodies raised in rabbits against ResA (12) were employed to develop a Western blot to detect levels of ResA production in the variant strains. Western blotting showed that, like the cysteine

variants described in Chapter 3, the E80Q variant was produced to similar levels to that of the wild type protein in 1A1 (Figure 4.4). Initial attempts to detect the P141 variants in this manner failed, with no ResA detected. Attempts by Dr Allison Lewin to purify the soluble versions of these proline variants had also failed, despite good levels of expression in *E. coli*. It was hypothesised that variations in the *cis*-proline could lead to a rapid degradation of ResA due to an instability of the protein fold. To try to counter this, fresh membranes from LUN5 and LUN6 were prepared and immediately run on SDS PAGE and transferred to PVDF membrane. On developing the blot low levels of ResA were detected at approximately 25% of wild type level, Figure 4.5. When these substitutions were introduced to the equivalent *cis*-proline in DsbA, P151, it was possible to trap the protein in a complex with substrate proteins as the kinetics of the resolution reaction were slowed (16). Attempts were made to perform similar experiments with the proline variant ResA proteins but it was not possible to detect ResA-substrate complexes.

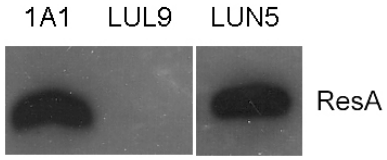

Figure 4.4. Western blot of ResA E80Q variant. 25 µg of membrane sample was run on SDS-PAGE. This was then transferred to PVDF before being exposed to the ResA antibody and visualised using a peroxidase tagged anti-rabbit antibody. LUN5, which produces E80Q ResA, appears to have similar levels of ResA production to the wild type, 1A1. As expected, LUL9, the ResA deficient strain, produce no ResA.

The experiment described by Kadokura *et al* had several steps to trap protein complexes that could not be recreated here. In addition to this, we now know

that P141 is important for the stability of ResA, so if P141 is also important for substrate release, and it was possible to trap ResA in complexes with substrates, then it is likely that the P141 variants would have decayed before it was possible to detect them by Western blotting.

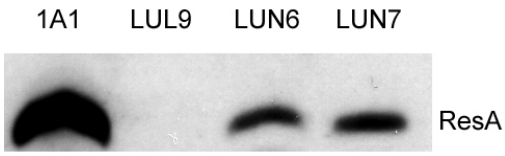

Figure 4.5. Western blot of proline 141 variants. 25 µg of membrane sample was run on SDS-PAGE then transferred to PVDF before being exposed to the ResA antibody and visualised using a peroxidase tagged anti-rabbit antibody. LUN6 and LUN7, which produce P141S and P141T ResA respectively, have significantly less detectable ResA present in the membrane than the wild type, 1A1. As expected, LUL9, the ResA deficient strain, produce no ResA.

4.3.3. TMPD staining of ResA variant strains P141S, P141T and E80Q.

To assess activities of the P141S, P141T and E80Q variants of ResA they were examined by restreaking colonies on to NSMP agar and staining for cytochrome *c* oxidase activity using TMPD, as described in Chapter 2 (Figure 4.6).

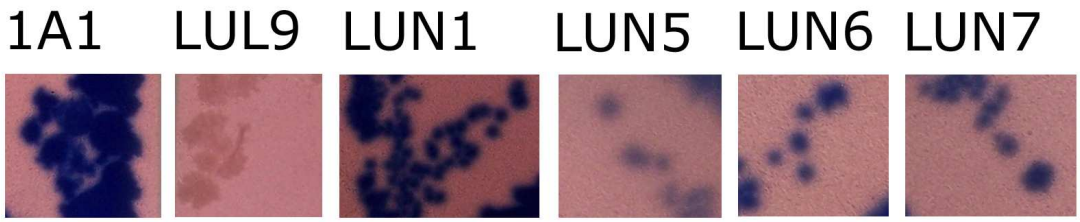

Figure 4.6. TMPD staining of the hydrophobic cavity variants. ResA variant strains were restreaked onto NSMP-agar and stained with TMPD. 1A1 and LUN1 both produce wild type ResA and demonstrate intense staining; LUL9, a ResA deficient strain, has no visible staining; LUN5 (E80Q), LUN6 (P141S) and LUN7 (P141T) each exhibit staining, although not at wild type levels suggesting that B. subtilis expressing these ResA variants are less affective at producing CtaC than the wild-type protein.

The TMPD staining demonstrated that all three of the hydrophobic cavity variants have some level of cytochrome *c* oxidase activity. However, they do not appear to be stained to the wild type levels of 1A1 or LUN1 (Figure 4.6). As shown above in the Western blots, both of the proline variants are unstable so activity would be expected to be less than that of the wild type strains. TMPD staining is not a quantitative measure of caa_3 activity so a cytochrome *c* oxidase activity assay was employed to ascertain a more precise level of caa_3 activity of the *B. subtilis* strains expressing variant ResA proteins.

4.3.4. Cytochrome *c* oxidase assays of strains producing ResA hydrophobic cavity variants.

To quantitatively assess the activity of the variant ResA homologues in relation to the maturation of CtaC a cytochrome *c* oxidase assay was employed as described in Chapter 2. Δ550-540 nm was plotted against time and straight lines were fitted to calculate the initial rates of cytochrome *c* oxidation (Figure 4.7). The calculated rates are shown in Table 4.1.

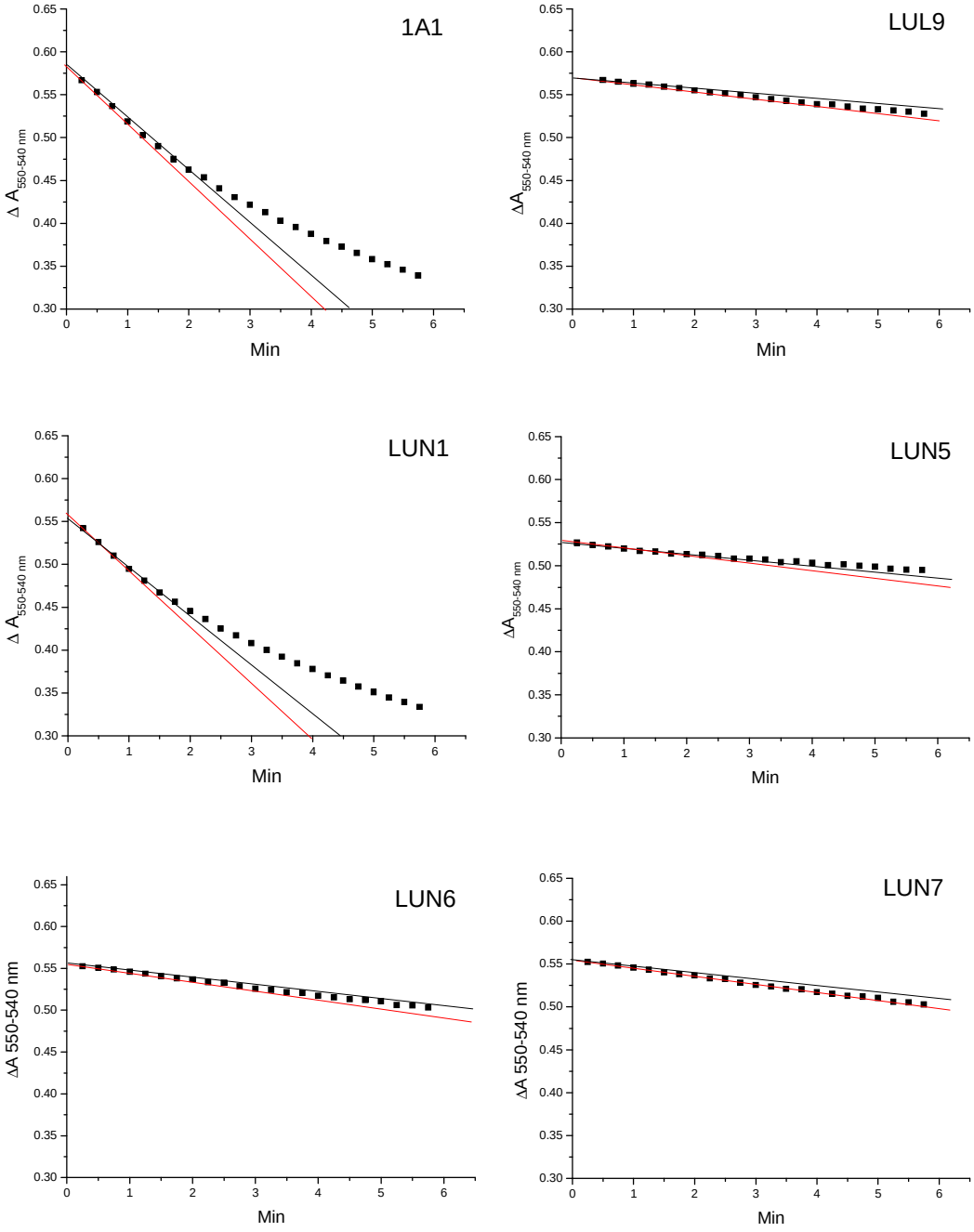

Figure 4.7. Cytochrome *c* oxidase assays of ResA hydrophobic cavity variants. Representative plots of $\Delta A_{550\text{-}540\ nm}$ as a function of time following the mixing of *B. subtilis* membranes with reduced horse heart cytochrome *c*. Two lines were fitted to represent the maximum (red) and minimum (black) rate of reaction. The gradients of these lines were used to calculate a mean rate of reaction. The LUN strains are LUL9 complimented with *resA*, LUN1 (wild type), LUN5 (E80Q), LUN6 (P141S) and LUN7 (P141T). All of the *resA* variant expressing strains have visibly less caa_3 activity than the wild-type *resA* expressing strains. The calculated rates are shown in Table 4.1.

Table 4.1. Cytochrome *c* oxidase activity of hydrophobic variants

Strain	ResA variant	Oxidation activity (nM min^{-1} mg $protein^{-1}$)[a]
1A1	Wild type	83 ± 4
LUL9		5 ± 4
LUN1	Wild type	82 ± 6
LUN5	E80Q	12 ± 3
LUN6	P141S	15 ± 2
LUN7	P141T	28 ± 4

[a] The data are the means ± standard errors of several measurements ($n \geq 3$) obtained using at least two different membrane preparations.

Each of the three hydrophobic cavity variants demonstrated significantly reduced cytochrome *c* oxidase activity compared to the wild type strains; the P141S variant had less than 20% activity, the P141T variant had approximately 35% activity and E80Q had only about 15% of wild type ResA activity.

4.3.5. Haem staining of strains producing hydrophobic cavity variants.

As neither the TMPD stain nor the cytochrome *c* oxidase assay offer any information about the cytochromes *c* in *B. subtilis* other than CtaC, a haem stain system was employed. 100 µg of membrane sample was run on SDS-PAGE and stained for haem, as described in Chapter 2. As expected from the data provided by the TMPD staining and caa_3 assays, CtaC is present in all hydrophobic cavity variants but to lower levels to that of the wild type ResA-producing strains, 1A1 and LUN1. It appears that no other cytochromes *c* are present at detectable levels. The hydrophobic cavity has been predicted to be important for substrate recognition. The data demonstrate that the *cis*-proline, as well as being important for structural stability, is also important for substrate recognition. Glu80 appears to be important for substrate recognition as well controlling the acid/base properties of the active site (15).

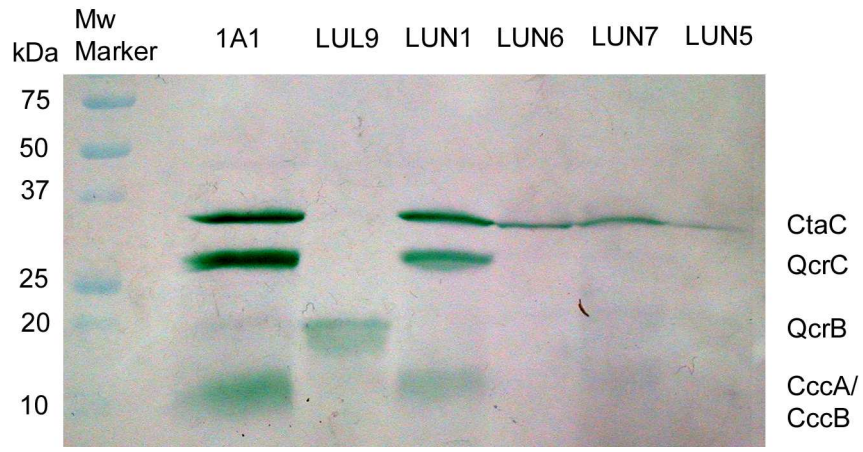

Figure 4.8. Haem stain of cytochromes *c* present in the membranes of *B. subtilis* strains containing hydrophobic cavity variants of ResA. 100 µg of membrane sample was run on SDS-PAGE and stained for haem. Only CtaC is detectable in the hydrophobic cavity variant strains LUN6 (P141S), LUN7 (P141T) and LUN5 (E80Q) and at seemingly lesser levels to that of the wild type ResA strains 1A1 and LUN1. As expected the ResA deficient strain, LUL9, has no cytochromes *c* present.

4.3.6. Generation, expression and production of CccA:ResA fusion protein in LUL9.

B. subtilis ResA is located on the outside of the cytoplasmic membrane, where it is tethered by an N-terminal transmembrane segment. A soluble form of ResA has been structurally characterised (in both oxidised and reduced states) and the pK_a and redox properties of the protein have been determined (14,15,124). While it is unlikely that the membrane anchor significantly affects the physiochemical properties of the soluble domain, it is not clear whether the transmembrane domain serves only to localize ResA to the correct cellular compartment. To investigate the importance of the specific sequence of the transmembrane segment of ResA, a fusion protein was created featuring the transmembrane segment of CccA and the solvent exposed domain of ResA. Analysis of the transmembrane segments of these two proteins showed a high

degree of similarity (Figure 4.2). Plasmid pLUJEs1, which is a derivative of pHP13Es containing the *cccA'-resA' Eco*RI-*Bam*HI gene fragment, was provided by Professor Lars Hederstedt (Lund University, Sweden). The gene is expressed from the IPTG inducible P_{spac} promoter and the transcribed mRNA contains the natural ribosome binding site found upstream of *cccA*. The ResA deficient strain LUL9 was transformed with pLUJEs1 as described in Chapter 2.

4.3.7. Western blot of a *B. subtilis* strain producing the CccA:ResA fusion.

The CccA:ResA fusion protein is transcribed from the multi-copy plasmid pHP13Es with the mRNA being translated from the natural ribosomal binding site of CccA. This means that it is unlikely that expression of this fusion protein will be the same as that from a single genomic copy of wild type ResA with its own natural ribsome binding site.

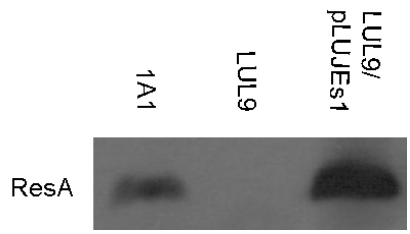

Figure 4.9. Western blot analysis of CccA:ResA production in the ResA deficient strain, LUL9. 25 µg of membrane sample from the *cccA:resA* expressing LUL9 strain were examined by Western blotting. There is significantly more CccA:ResA present in LUL9 expressing the pLUJEs1 plasmid than wild type ResA produced in 1A1. As expected no ResA is produced in LUL9.

In order to ascertain how much CccA:ResA was produced, Western blots using anti-ResA antibodies were carried out. 25 µg of membrane sample prepared from LUL9 producing the CccA:ResA fusion protein was run on an SDS-PAGE gel and transferred on to PVDF membrane and developed as described in

Chapter 2. The Western blot shows that the fusion protein was produced at a significantly higher level than that of the wild type protein, see Figure 4.9.

4.3.8. Investigation of CccA:ResA fusion activity by haem staining.

To investigate the activity of the CccA:ResA fusion protein in cytochrome *c* maturation, 100 µg of membrane sample from LUL9/pLUJEs1 was run on SDS-PAGE and stained for covalently bound haem (Figure 4.10). The CccA:ResA fusion protein is capable of maturing all of the *B. subtilis* cytochromes but to lower levels compared to that of the wild type.

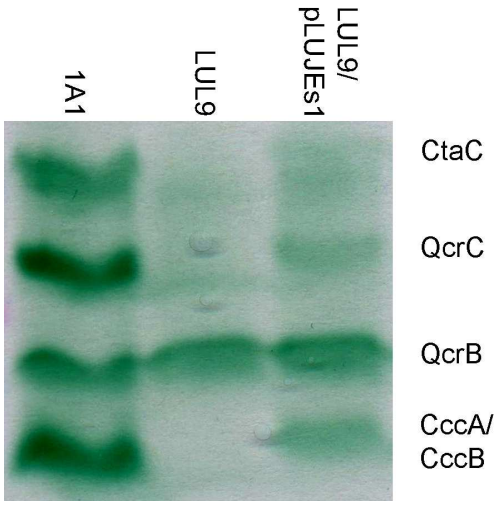

Figure 4.10. Haem stain of *B. subtilis* cytochromes *c* in LUL9/CccA:ResA membranes. 100 µg of membrane sample run on SDS PAGE and stained for haem. LUL9 harbouring the pLUJEs1 plasmid and producing the CccA:ResA fusion protein is capable of maturing all of the *B. subtilis* cytochromes *c* but at noticeably lower levels than the wild type 1A1. As expected, no significant level of cytochrome *c* can be detected in the ResA deficient strain, LUL9.

The Western blot (Figure 4.9) demonstrated that there is about four times more CccA:ResA present in membranes from LUL9 harbouring pLUJEs1 than wild type ResA in 1A1. If it is estimated that there is only 50% CCM activity provided by the CccA:ResA fusion, then because it is present at higher levels,

this suggests that it has only 10-15% activity of the wild type ResA protein. It is also possible that the excess amounts of CccA:ResA could be affecting the function of the protein, as with the case of the over-production of BdbD in a *bdbD* deletion strain of *B. subtilis*, discussed in Chapter 5.

4.3.9. Cytochrome *c* oxidase assays of membranes from a strain producing the CccA:ResA fusion protein.

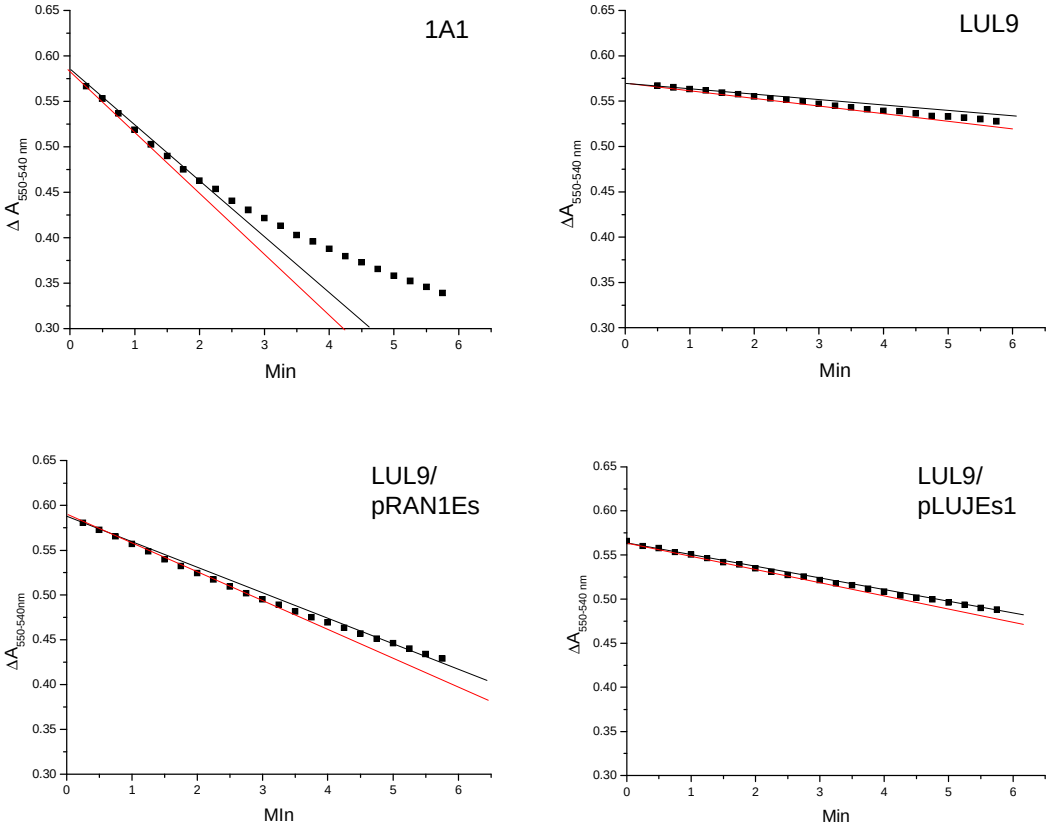

Figure 4.11. Cytochrome *c* oxidase assays of CccA:ResA fusion. Representative plots of $\Delta A_{550\text{-}540\ nm}$ as a function of time following the mixing of *B. subtilis* membranes with reduced horse heart cytochrome *c*. Two lines were fitted to represent the maximum (red) and minimum (black) rates of reaction. The gradients of these lines were used to calculate mean rates of reaction which are shown in Table 4.2.

Although the haem stain (above) suggests that the ability of the CccA:ResA fusion protein to mature cytochromes *c* is less than that of wild type ResA it is

important to quantify levels of activity more accurately. For this cytochrome *c* oxidase activity assays were employed. Membranes prepared from LUL9/pRAN1Es (wild type *resA* expressed from the pHP13Es) and LUL9/pLUJEs1 were mixed in a cuvette with reduced horse heart cytochrome *c* and the absorbance at 550 nm and 540 nm was recorded as described in Chapter 2. ΔA550-540 nm was plotted as a function against time, Figure 4.11. Straight lines were fitted to these plots to represent the maximum and minimum rates in order to calculate a mean initial rate, see Table 4.2.

Table 4.2. Cytochrome *c* oxidase assays of CccA:ResA fusion protein. Horse heart cytochrome *c* oxidation was plotted against time and used to calculate the initial rate of (nM min^{-1} mg $protein^{-1}$)

Strain	**ResA Variant**	**Oxidation activity (nM min^{-1} mg $protein^{-1}$)[a]**
1A1	Wild type	83 ± 4
LUL9		5 ± 4
LUL9/pRAN1Es	Wild type	50 ± 2
LUL9/pLUJEs1	CccA:ResA	20 ± 6

[a] The data are the means ± standard errors of several measurements ($n \geq 3$) obtained using at least two different membrane preparations.

It is clear from the cytochrome *c* oxidase assays that the CccA:ResA fusion is capable of maturing CtaC to only about 25% to that of the wild type 1A1. This is consistent with the fainter cytochrome *c* bands for the CccA:ResA fusion observed on the haem stain, above. What is less clear is that why the LUL9/pLRAN1Es (wild type ResA expressed from the pHP13Es plasmid) has less activity than the 1A1. Wild type ResA was produced to similar high levels as the CccA:ResA protein from the pHP13Es plasmid when compared to the wild type 1A1 (12). A possible reason for this could be that the excess of ResA is interfering with its function, possibly because there is not enough CcdA present

to keep the ResA in the reduced form. This was not apparent from previous analysis of the entire cytochrome *c* contents of 1A1 and LUL9/pRAN1Es (12).

4.4. Discussion

The replacement of the N-terminal transmembrane anchor region of ResA with the equivalent membrane anchor of CccA resulted in a decrease of cytochrome *c* maturation activity. As both ResA and CccA have similar N-terminal sequences to direct them to and through the cytoplasmic membrane it is expected that the protein is positioned on the outer side of the cytoplasmic membrane. This conclusion is supported by the presence of cytochrome *c* maturation activity and the fact the protein was detected in membrane preparations. However the activity is significantly lower than that of the wild type (1A1) or the wild type *resA* being expressed from the pHP13Es plasmid in LUL9 (LUL9/pRAN1Es), expressed from the same promoter as the fusion protein. This could be explained by an imbalance between the levels of ResA compared to levels of ResB and ResC and/or CcdA. The membrane anchor of the fusion protein originates from a cytochrome *c*, and a possible complication in the interpretation of the data is that the membrane anchor of CccA may be involved in the interaction of apo-CccA with the Res proteins during haem attachment and so it cannot be ruled out that the CccA anchor blocks the interactions of apo-cytochromes *c* with the Res system, leading to the reduced level of cytochrome *c* maturation observed. However, it is unlikely that the membrane anchors of apo-cytochromes *c* are important for Res interactions because they have highly variable sequences and the N-termini of CccB and CtaC are processed to generate lipoproteins (51,52). In the case of CtaC it is known that the lipid modification and cleavage are not required for haem attachment (52). Only the region around the haem binding

motif has significant sequence similarity amongst all the *B. subtilis* cytochromes with CtaC having a short sequence after the haem binding site that is not present in the other cytochromes *c*, see Figure 4.12. It is possible that this region allows the interaction of apo-CtaC with the P141 and E80 variant ResA proteins and reduction of the haem binding site to occur. Therefore, CccA, CccB and QcrC are more sensitive to recognition by the hydrophobic cavity region as they lack this motif.

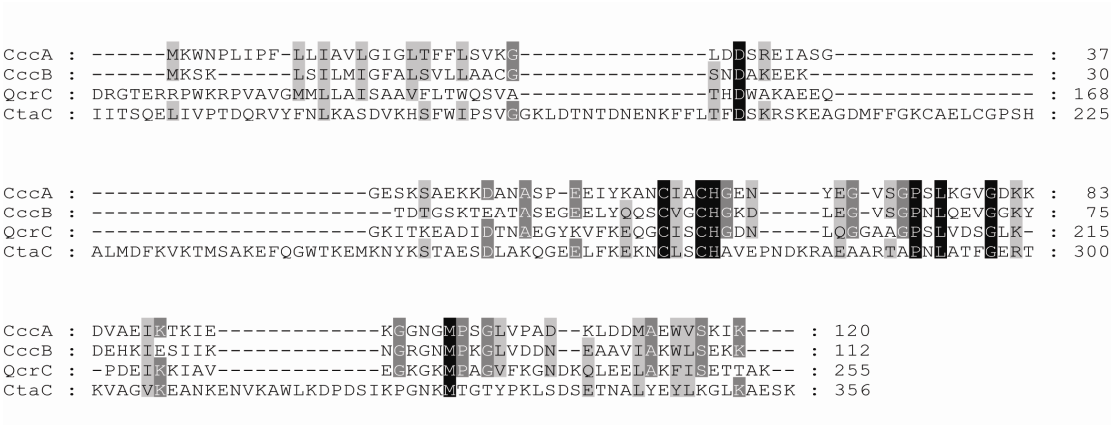

Figure 4.12. Alignment of haem binding domain of *B. subtilis* cytochromes *c*. Residues highlighted black are conserved, residues highlighted grey with white lettering represent a conservative substitution and residues highlighted grey with black lettering represent residues that are conserved across three out of the four proteins.

It is therefore likely that this region determines the specificity of the interactions of the Res proteins with the apo-cytochromes *c*. Nevertheless, the specific sequence of the membrane anchor of ResA does have an effect on cytochrome *c* maturation in *B. subtilis*. The precise extent of the effect is difficult to be sure about: an approximately 50% reduction in CCM activity was detected but the concentration of the protein was about four-fold higher than in the wild type strain. However, as discussed above, CCM activity is likely to be limited by

ResB and ResC and these proteins were not overproduced in these experiments. Therefore, CCM activity is not linearly related to the levels of ResA present. Nevertheless, CCM activity was significantly lower than in wild type cell, and it is concluded that although the principle function of the transmembrane segment is to tether the protein to the membrane, it also plays a role in modulating CCM activity. One possibility is that this occurs through interactions with the integral membrane proteins ResB and ResC. This conclusion is supported by studies of the membrane anchor of CcmG, a homologue of ResA involved in cytochrome *c* maturation in *E. coli*. CcmG also has an influence on function as when the membrane anchor of CcmG was replaced with the anchor of CcmE the levels of cytochrome *c* maturation were reduced by approximately 50% (125).

Pro141 lies close to the active site of ResA forming part of the hydrophobic cavity (See Fig 4.1). Replacement of this residue with a serine or threonine was found to destabilize the structure of the protein; significant amounts of P141S or P141T ResA could be detected only in freshly prepared *B. subtilis* membranes, and levels depleted quickly following a freeze/thaw cycle. These observations are consistent with the instability of the soluble forms of these variants, which proved too unstable to purify. This suggests that Pro141 is important for the stability of the protein fold. This contrasts with a report for *E. coli* CcmG, in which replacement of the *cis*-pro144 by an alanine resulted in a stable protein with a structure very similar to that of the wild type protein but with altered redox properties (18). The presence of small amounts of the Pro141 variants in *B. subtilis* membrane samples correlated well with low CtaC activity. Therefore, for CtaC, the normalized activity would be similar to that of wild type protein,

indicating that Pro141 does not appear to be important for CtaC maturation. It should be noted that the levels of the Pro141 ResA variants might be different in the living cell and the degradation of the protein might only occur after the cells have been harvested and lysed. None of the other cytochromes *c* (CccA, CccB and QcrC) were matured to detectable levels in the ResA Pro141 variants. This demonstrates that in addition to the structural importance of Pro141, this residue also plays a crucial role in the recognition of substrate apo-cytochromes *c* other than CtaC, as previously suggested by structural studies (14). Selective maturation of CtaC was also observed in the ResA E80Q variant *B. subtilis* membranes. CtaC contains a short sequence (residues 77-81) that is not present in the other cytochromes *c*, which could be responsible for this selective maturation.

Structural data previously indicated that residue Glu80, which lies at the base of the hydrophobic cavity juxtaposed to the active site cysteine motif, may be potentially important for substrate recognition (14). The E80Q variant was present at wild type levels in terms of abundance and stability, but only small amounts of CtaC were observed. This demonstrates that Glu80 is important for the maturation of all cytochromes *c*; it exhibits some activity toward CtaC but essentially none towards CccA, CccB and QcrC. Although it has been previously demonstrated that the active site cysteine pK_a values are different in a soluble E80Q ResA variant (15), it seems unlikely that this alone would account for the loss in mature cytochromes *c* other than CtaC, particularly as this is not an issue for the P76H variant, see Chapter 3.

While it is clear that ResA is essential for the reduction of apo-cytochromes *c* prior to covalent haem attachment and a model for substrate activation of ResA reductase has been proposed (15), a direct interaction between ResA and its substrates has yet to be observed.

Chapter 5: *In vivo* studies of the TDOR BdbD from *B. subtilis*.

5.1. Introduction

BdbD is a membrane associated, oxidising thiol:disulphide oxidoreductase (TDOR) found in *Bacillus subtilis*. It functions to oxidise cysteine thiols of proteins and peptides to disulphide bonds on the outside of the cytoplasmic membrane, playing a key role in disulphide bond management. The *in vivo* regulation of disulphide bond formation is essential for many cell processes. They are formed upon the oxidation of two cysteine side chain thiols and are essential for function, stability and assembly of many membrane bound and secreted proteins and peptides (26,126-128). Intricate systems have evolved to regulate the redox state of cysteines on the outside of the cytoplasmic membrane involving enzymatic proteins known as thiol-disulphide oxidoreductases (TDORs) (129). Proteins of the thioredoxin-like TDOR family contain several conserved features; a cysteine containing active site, usually arranged in a CXXC motif; the thioredoxin fold; and a near active site *cis*-configuration proline (42,129).

TDORs can be characterised by their redox properties, BdbD is an example of an oxidising TDOR: it will oxidise two cysteine thiol (-SH) groups in a substrate protein to form a disulphide bond (S-S). Previous *in vivo* studies has shown it to be capable of introducing disulphide bonds to apo-cytochrome *c* and is essential for the natural uptake of DNA, due to the fact that several competence (Com) proteins contain disulphide bonds, see Chapter 1 for more details (9,25,26).

BdbD is homologous to *E. coli* DsbA, a soluble periplasmic protein, which contains the thioredoxin fold with an additional helical domain (130). The DsbA/DsbB system of *E. coli* has been characterised in great detail with DsbA being capable of oxidising several known redox partners and DsbB re-oxidising DsbA (16,29,42). *B. subtilis* also contains two DsbB homologues, BdbB and BdbC, with BdbC being the most likely natural redox partner of BdbD, as both BdbC and BdbD are required for competence development (25). The crystal structure of BdbD showed that it is clearly related to DsbA, having both the thioredoxin domain and the α-helical domain, shown in Chapter 1 (27).

Recent *in vitro* studies have confirmed the oxidising power of BdbD, demonstrating it has a reduction mid point potential of -75 mV versus SHE (27), making it one of the most highly oxidising TDORs known. Surprisingly, the crystal structure of BdbD revealed a metal binding site, fully occupied by calcium, which was suggested to boost the oxidising power of the protein. This site is located 14 Å from its closest active site cysteine and is coordinated by three residues, Gln49, Glu115 and Asp180, Figure 5.1 (27). The oxidising power of BdbD is thought to be derived from the instability introduced by the addition of a disulphide bond in the oxidised form and, although calcium depleted BdbD exhibited no major structural changes, it was significantly less stable in the reduced form than the calcium containing protein. The calcium depleted BdbD also demonstrated a shift in the midpoint reduction potential of about -20 mV, leading to the proposal that the calcium ion functions to enhance the oxidising power of the protein (27).

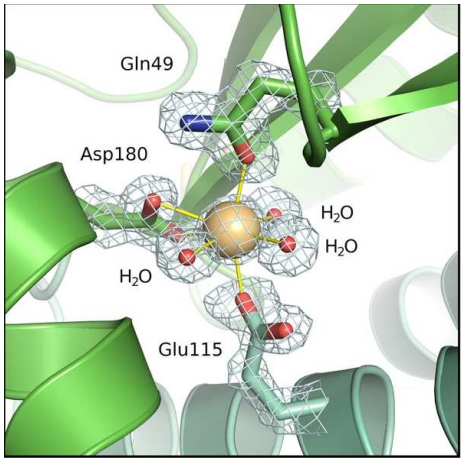

Figure 5.1. Calcium binding site of BdbD. Monodendate ligands of Gln49, Glu115 and bidendate ligands of Asp180 position the Ca^{2+} ion, large orange sphere. The smaller red spheres are water molecules. Figure adapted from Crow *et al*, 2009 (27).

Because BdbD was expressed heterologously in *E. coli*, it is not certain that Ca^{2+} is the natural metal ion. However, it is reasonable to propose this because the concentration of Ca^{2+} ions is very low in the cytoplasm of bacteria and the protein was not exposed to Ca^{2+} at any stage during the purification or crystallization. However, *in vivo* data on the importance of this novel metal site is required.

To investigate the importance of the calcium within BdbD *in vivo*, PCR mutagenesis was employed to substitute the key residues involved in calcium binding. These variant genes were cloned into a multicopy plasmid which was then used to transform a BdbD/CcdA deficient strain of *B. subtilis* in order to complement the BdbD deficiency and cause the strain to regain a CcdA-only deficient phenotype in terms of cytochrome *c* maturation (CCM) ability. Also explored here was the role of a near active site glutamate, Glu63. A near active site glutamate residue is a feature of many TDORs. This residue can have varying functions throughout the TDOR family, including substrate recognition and maintaining the pK_a of the active site cysteines in ResA (13,15).

5.2. Experimental Procedures

The majority of the procedures used in this study are outlined in Chapter 2 and only methods that are exclusive to the work in this chapter are outlined here. Bacterial strains, plasmids and oligonucleotide primers are described in Chapter 2. The first step in introducing variant *bdbD* genes in to the CcdA/BdbD deficient strain of *B. subtilis* was to amplify the *bdbD* gene along with its predicted ribosome binding in the 5' flanking region. This could then be ligated into pUC18 and used as a template for the PCR mutagenesis.

5.2.1. PCR amplification of *bdbD* gene and upstream ribosome binding site.

1A1 genomic DNA was used as template for the PCR reaction. The amplification reaction mix was as described in Chapter 2. The reaction was performed in a Techne thermocycler using the Expand Hi-Fidelity PCR system (Roche) under the following reaction conditions described in Table 5.1. The reaction was analysed by agarose gel electrophoresis, Figure 5.2. The band of amplified *bdbD* was excised from the gel and cleaned from the agarose using a QIAGEN DNA agarose clean up kit.

Table 5.1. PCR reaction condition used to amplify the bdbD gene including the upstream ribosome binding site.

Process	Temp ^{o}C	Time	Repeat
Initial denaturation	94	2 min	1
Cycle 1			
Denaturation	94	30 s	
Primer annealing	55	30 s	10
Extension	62	45 s	
Cycle 2			
Denaturation	94	15 s	
Primer annealing	55	30 s	20
Extension	62	45 s – 2 min	
Final Extension	62	10 min	1

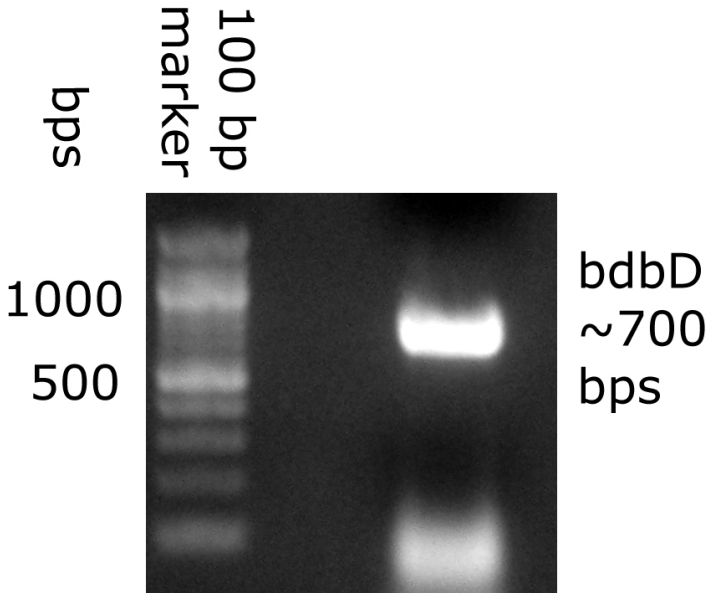

Figure 5.2. PCR amplification of the *bdbD* gene from *B. subtilis* 1A1 genomic DNA. 15 µl sample of the *bdbD* PCR reaction was run on a 1% w/v agarose gel as described in Chapter 2. A band can be observed at 700 bps, the expected size of the bdbD gene with the additional 5' ribosome binding sequence.

5.2.2. Cloning *bdbD* into pUC18

The cleaned *bdbD* fragment was ligated into pUC18 at the *Sma*I site as described in Chapter 2. The ligation reaction was used to transform *E. coli* JM109;

successful transformants were screened by plating on to LBA containing 100 µg/L ampicillin. Successful ligation of *bdbD* gene into pUC18 was determined using X-gal blue/white screening, as described in Chapter 2. Six white colonies were picked and used to inoculate 5 ml LB, 100 mg/L ampicillin, incubated overnight at 37 ^{o}C, 200 rpm. Plasmids were purified from these cultures using QIAGEN miniprep kit, as per manufacturer's instructions. Restriction digestion with *Hin*dIII and *Sph*I and subsequent analysis by agarose gel electrophoresis was used to confirm correct *bdbD* insertion into the pUC18 plasmid, Figure 5.3. Correct insertion of the wild type *bdbD* gene was further confirmed by DNA sequencing (MWG Biotech). pUC18 plasmid containing the *bdbD* insert was designated pCHN17.

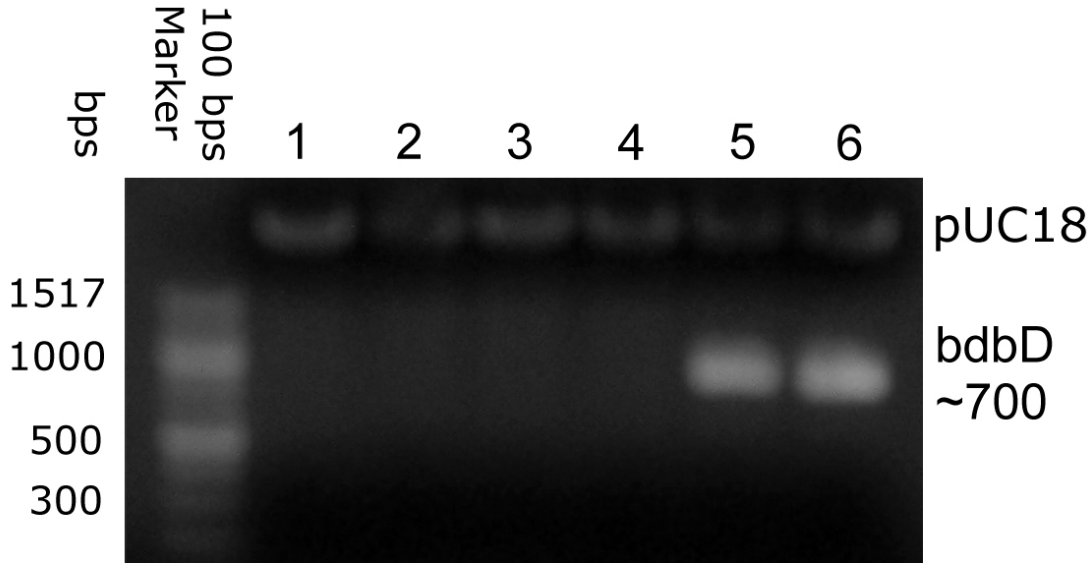

Figure 5.3. Restriction digest confirmation of *bdbD* insertion into pUC18. Six transformed colonies were picked, cultured and plasmid purified from them. These were cut with *Hin*dIII and *Sph*I and run on a 1% agarose gel, lanes 1-6. Of these plasmids retrieved only 5 and 6 contained the correct sized insert.

5.2.3. Cloning *bdbD* into pDG148

Once *bdbD* had been successfully cloned into pUC18 it needed to be transferred into a plasmid compatible for replication and gene expression in *B. subtilis*. The *bdbD* insert was cut from pCHN17 using *Hin*dIII and *Sph*I and separated by agarose gel electrophoresis, and the *bdbD* fragment was cleaned from the agarose using the QIAGEN DNA agarose clean up kit, as per manufacturer's instructions. This fragment was then cloned into pDG148 at the *Sph*I/*Hin*dIII site and used to transform *E. coli* JM109 as described in Chapter 2.

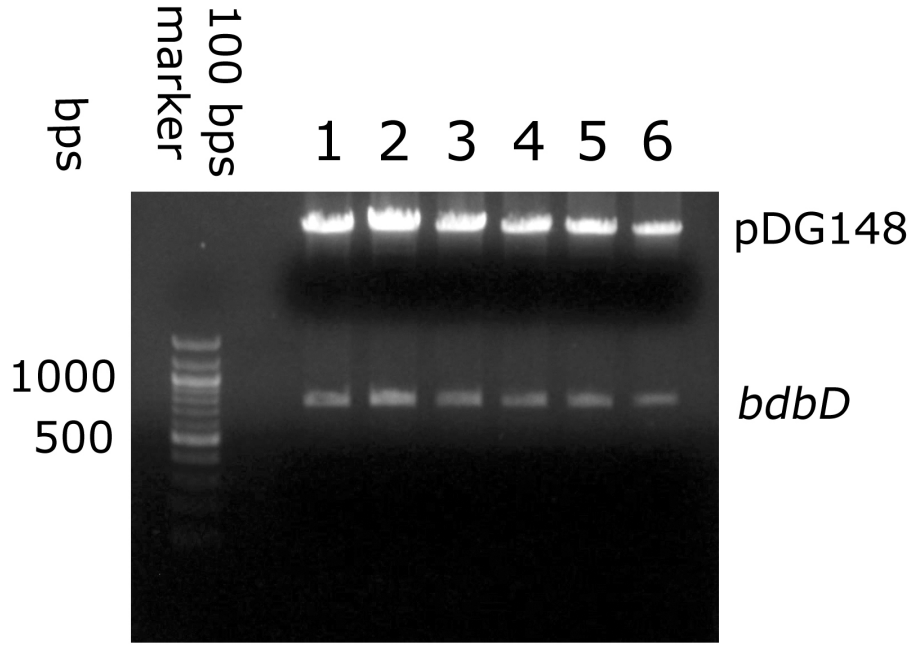

Figure 5.4. Confirmation of successful ligation of *bdbD* into pDG148. Plasmids were digested using *Hin*dIII/*Sph*I and separated by agarose gel electrophoresis. Of the six plasmids tested, all six had the correctly sized *bdbD* insert.

Successful transformants were screened on LBA containing 100 mg/L ampicillin. Successful transformants were picked and used to inoculate 5 ml LB culture containing 100 mg/L ampicillin. The plasmid DNA was purified from cultures using a QIAGEN miniprep kit. Successful gene insertion into pDG148 was confirmed by restriction digest with *Sph*I and *Hin*dIII, Figure 7.4.

5.2.4. Targeted PCR mutagenesis of *bdbD*

Site directed mutagenesis was used to explore the importance of the predicted key amino acid residues within BdbD. Using pCHN17 as template DNA, PCR was used to generate mutant *bdbD* genes encoding D180A, Q49A and E63Q BdbD variants. The PCR mutagenesis procedure was performed as described in Chapter 2, using the primers described in Table 5.2. Successful transformants were screened by plating on to LBA containing 100 µg/ml ampicillin. Single colonies were picked and used to inoculate 5 ml LB cultures, 100 µg/ml ampicillin, 37 ^{o}C, 200 rpm overnight. Plasmid DNA was purified from cell culture (as described above) and sequenced (MWG biotech) to confirm the correct mutation and that no other mutations had been introduced; *bdbD* variant plasmids are listed in Table 5.1. The variant *bdbD* genes were cut from the pUC18 vector and ligated into pDG148 as described above. This and the ligation steps was performed by the Lars Hederstedt laboratory, Department of Cell and Organism Biology, Lund University, Lund, Sweden, SE 223 62.

5.2.5. Transformation of *B. subtilis* LUL7 protoplasts with variant *bdbD* genes

As discussed above, *B. subtilis* without a functional *bdbD* gene is not capable of natural DNA uptake as described in Chapter 2. It was therefore necessary to transform the cells by other means. After several unsuccessful attempts to transform cells by electroporation using protocols based on techniques described for several *Bacillus* species (131-133), Lars Hederstedt's laboratory was able to introduce the variant BdbD encoding plasmid to LUL7 protoplasts.

5.3. Results

The premise on which this experimental system was based was that wild type *bdbD* expressed from a plasmid should be able to retrieve the CCM negative phenotype of a CcdA/BdbD deficient mutant strain of *B. subtilis*. Once this was achieved, variant BdbD proteins could then be introduced in a similar fashion and their functionality compared to that of the wild type protein. *B. subtilis* LUL7 is deficient in both CcdA and BdbD and so is able to mature cytochromes *c*. BdbD oxidises the thiols of apo-cytochrome *c* which mean they are unable to covalently bind haem. CcdA is thought to maintain the reducing nature of ResA, which, in turn, reduces the disulphide bond between the cysteines of apo-cytochrome *c*, allowing the covalent binding of haem. A CcdA deficient *B. subtilis* is unable to produce mature cytochrome *c* because the apo-cytochrome *c* remains in the oxidised form. If the strain is also deficient in BdbD, as with LUL7, mature cytochromes *c* will be present as there will be no need to re-reduce the apo-cytochrome *c* as it has not been oxidised in the first place. On complementing a BdbD/CcdA deficient strain with a wild type *bdbD* gene it would be expected that the CCM positive phenotype would be replaced with a CCM negative one. By introducing genes expressing variant BdbD proteins it should be possible to judge the impact of the variation on the function of BdbD by assessing the ability of the protein to recover a CCM deficient phenotype in LUL7. A fully functional BdbD protein will be CCM negative; a non-functional BdbD will be CCM positive.

5.3.1. TMPD staining of variant BdbD producing LUL7 strains.

Initially the LUL7 strains harbouring plasmids expressing variant BdbD proteins were restreaked on to NSMP containing appropriate antibiotics and 1 mM IPTG, to induce expression of the *bdbD* genes from the P_{spac} promoter and stained with TMPD as described in Chapter 2. All strains, including LUL7 expressing wild type *bdbD*, had high levels of staining, indicating CCM activity. To ensure that BdbD was being produced, Western blotting was employed (discussed below). This showed that BdbD was being produced to much higher levels when the gene was expressed from the plasmid than under wild type conditions in 1A1, in which there is only one copy of the gene, Figure 5.6. It seemed possible that the excessive level of BdbD present in the cell membrane was disrupting the redox balance. To try to counter this, the strains were re-streaked on to NSMP agar containing appropriate antibiotics but with only 10 or 50 µM IPTG. The Western blot, shown below (Figure 5.6), demonstrated that BdbD production was similar to that of wild type levels in 1A1 in liquid media at these concentrations of the inducer. Plates were stained with TMPD as before and again all strains demonstrated a high level of staining, see Figure 5.5. It is possible that the concentrations of inducer suitable for liquid do not match those of cells grown on plates. Unfortunately, due to time constraints, it was not possible to 'fine tune' IPTG concentration in NSMP agar to a degree where it would be possible to obtain any useable data from TMPD staining.

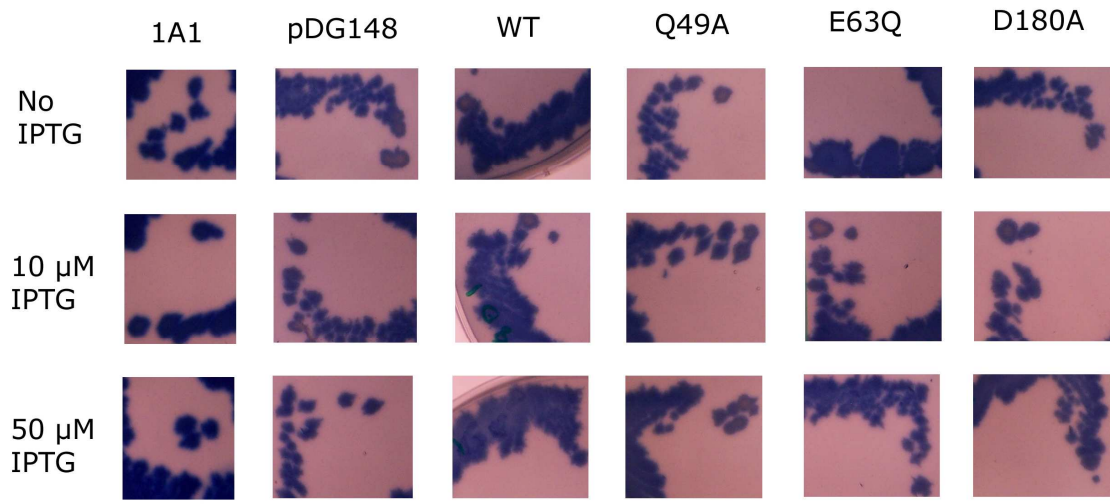

Figure 5.5. TMPD staining of LUL7 expressing variant *bdbD* induced by different concentrations of IPTG. All concentrations of IPTG appear to give similar high levels of staining (CCM positive phenotype) for all BdbD variant and the wild type. 1A1 is shown to demonstrate a true wild type CCM positive phenotype.

5.3.2. Western Blotting

To confirm production levels of BdbD and BdbD variants Western blotting was employed. Although protein production is driven from the natural ribosome binding of *bdbD*, gene expression is driven from an IPTG inducible P_{spac} promoter. As well as this, pDG148, although a low copy number plasmid, is still present in multiple copies in *B. subtilis*. It is very important to have consistent levels of protein production across the variants in order to make reasonable conclusions as to what effect each variation has.

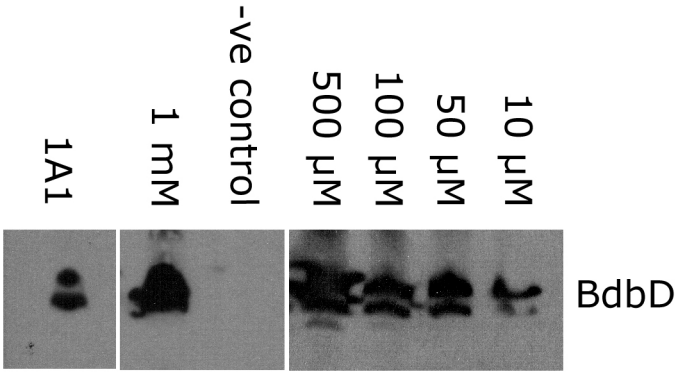

Figure 5.6. Western blot showing wild type BdbD production from pCHN18 in *B. subtilis* LUL7. Gene expression was induced with varying levels of IPTG, indicated above the lanes. 1A1 is the wild type strain and '-ve control' is LUL7 harbouring the pCHN18 plasmid but grown in the absence of IPTG. BdbD production in LUL7 from pCHN18 clearly remains significantly greater than wild type expression from 1A1 until IPTG concentration is as low as 10 µM. It is not known why these blots contain two bands for BdbD, it was not a feature of previous blots using these antibodies published previously (27).

An initial Western blot was developed with anti-BdbD antiserum on membranes prepared from each LUL7 based BdbD variant expressing strain, as well as 1A1 (wild type), LUL7 (CcdA and BdbD deficient) LUL7/pCHN18 (LUL7 expressing wild type *bdbD* from pDG148) as controls. This blot demonstrated that in the presence of 1 mM IPTG significantly more BdbD was produced when the gene was expressed from the pDG148 plasmid under P_{spac} control than under natural, wild type regulation of the single chromosomal copy of *bdbD* in the strain 1A1.

To determine whether protein production could be controlled by tighter regulation of gene expression by lowering the concentration of IPTG in the growth medium, 0.5 L cultures were grown in the presence of 10 µM to 1 mM IPTG with the relevant antibiotics and membranes were prepared. 0.25 µg of each membrane sample was run on a 12% SDS-PAGE gel before transferring to

PVDF membrane. BdbD was visualised by first introducing the anti-BdbD antibody (1/1000 dilution, from rabbit (27)) then with peroxidase labelled anti-rabbit (1/5000 dilution, GE Healthcare); this was developed using the Xograph. This demonstrated that the amount of protein produced could be controlled by altering the concentration of IPTG in the growth medium and to accomplish a level of BdbD production comparable to 1A1, only 10 µM IPTG was needed in liquid medium (Figure 5.6).

5.3.3. Haem staining of membranes from BdbD variant strains

As experiments relating to transcriptional control of *bdbD* with varying IPTG concentrations were only conducted in liquid media it was not realistic to relate these to agar based solid media, so TMPD staining was not pursued further. Haem staining of membranes prepared from liquid cultures was employed to analyse the effectiveness of BdbD production control by altering IPTG concentration to control *bdbD* transcription. Initially, a haem stain using the same membrane samples that were analysed by Western Blotting (Figure 5.6, above) demonstrated that all IPTG concentrations between 1 mM – 10 µM appeared to have the CCM positive phenotype. As discussed above, one possibility was that production of too much BdbD in these cell membranes had a negative impact on BdbD activity. To investigate this further, fresh membranes were prepared from LUL7/pCHN18 (the CcdA/BdbD deficient strain expressing *bdbD* from pDG148) cultures grown in the presence of 0.1 – 10 µM IPTG. 100 µg of membrane samples were run on a 12% SDS-PAGE gel and stained for haem as described in Chapter 2, see Figure 5.7. This suggested that it was possible to generate a CcdA-deficient CCM negative phenotype when the

LUL7/pCHN18 was grown in the presence of between 1 and 5 µM IPTG. Unfortunately it was not possible to obtain a good quality conclusive Western blot from these samples to demonstrate the levels of BdbD in the membrane samples. It is presumed that, as with previous Western blots, that higher than normal levels of BdbD were present in the membrane when the culture was grown with 10 µM IPTG and it is likely that when IPTG concentration was less than 1 µM then there was not enough IPTG present to induce transcription of *bdbD* at levels sufficient to generate enough BdbD to influence the phenotype. Unfortunately, it proved to be extremely difficult to reproducibly achieve the levels of CCM, seen in Figure 5.7, by BdbD production control.

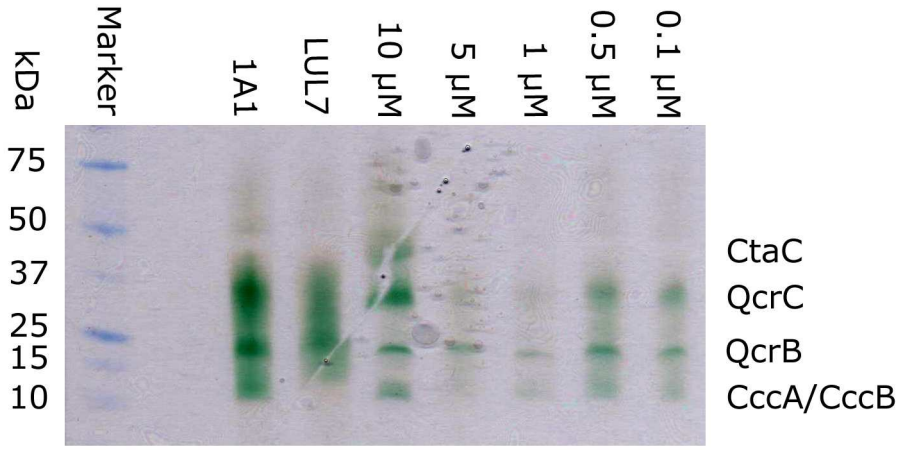

Figure 5.7. Haem stain of membrane samples prepared from LUL7/pCHN18 grown in the presence of 10–0.1 µM IPTG. Both 1A1, LUL7 and LUL7/pCHN18 (grown with 10µM IPTG) all demonstrated a CCM positive phenotype. When IPTG concentration was reduced to 5 and 1 µM the CCM negative phenotype of a CcdA-only deficient strain of *B. subtilis* was apparent. When IPTG concentration was reduced to 0.5 or 0.1 µM, the CCM positive phenotype returned, presumably because there is not enough IPTG present to induce the P_{spac} promoter and *bdbD* transcription.

5.4. Discussion

Here, an experimental system was constructed to test the *in vivo* functional importance of residues identified as being important from sequence alignment and/or structural data.

Wild type *bdbD* expressed from a multicopy plasmid (pDG148) was used to complement the BdbD deficiency of a strain (LUL7) lacking both CcdA and BdbD. LUL7 lacks both the oxidatative and reductive branches of disulphide bond management that operate in CCM resulting in a CCM positive phenotype. Complementation with *bdbD* was expected to rescue the oxidative pathway, resulting in the inability of the cell to produce cytochromes *c*.

In practice, the system was more complicated than expected. The production of large quantities of BdbD in LUL7 failed to rescue the BdbD deficient phenotype. It was proposed that this could have been a consequence of there being too much BdbD present. BdbD is an oxidising TDOR, but in order to function as such, must be maintained in its oxidised state in the *B. subtilis* membrane. This is believed to occur via the activity of BdbC, an integral membrane protein. Since BdbC was not overproduced in the *bdbD*-complemented strain, it is likely that the proportion of oxidised BdbD relative to reduced BdbD was abnormally low, leading to an effect on the net activity of BdbD. An excess of reduced BdbD may well have rendered the cell unable to effectively oxidise apo-cytochromes *c*, resulting in the *bdbD*-complemented strain retaining its CCM positive phenotype.

To test this, lower levels of BdbD were produced by reducing the concentration of IPTG, the inducer of the P_{spac} promoter from which *bdbD* expression was controlled. Western blot analysis revealed that this was successful and a concentration of ~ 10 µM IPTG in liquid culture generated levels of BdbD similar to that in 1A1 wild type cultures. As perhaps might have been anticipated, this concentration of IPTG was not appropriate for cells grown on solid media.

In Chapter 3, it was shown that to complement the CCM negative phenotype of a ResA deficient strain of *B. subtilis*, only 1 mM of the reductant DTT was needed in liquid medium. However, previous studies had determined that 100 mM DTT was required to achieve the same result for cells grown on agar based, solid medium. This concentration proved to be toxic for cultures grown in liquid medium. It should be possible to use Western blotting to determine levels of BdbD present in strains grown on solid media by preparing membranes from cells grown as lawns on NSMP agar, but time restraints prevented this.

Haem staining of membranes prepared from liquid culture was used to investigate CCM activity in the LUL7 complemented strain. Initial experiments showed that 10 µM IPTG did not generate a CCM-deficient phenotype and so a series of dilutions in the range 0.1 – 10 µM IPTG were investigated. These data generated were consistent with the proposal that the amount of BdbD produced was key to obtaining complementation. At 10 µM IPTG, too much BdbD was presumably present and so the oxidative branch was not functioning sufficiently well and CCM was observed at wild type levels. At 0.1 and 0.5 µM IPTG

significantly reduced CCM activity was detected. This suggests that at these concentrations of inducer, the level of BdbD was sufficient to restore the oxidative branch, but insufficient to disrupt the redox balance, resulting in oxidised apo-cytochrome *c* and reduced CCM activity. Clearly, Western blot analysis of these membrane samples would be required to verify these conclusions about BdbD levels.

At this point, the system appeared to be promising in that if the appropriate concentration of inducer was used, complementation of BdbD was observed. However, attempts to reproduce the data were not always successful, indicating that it was difficult to reproducibly obtain the necessary levels of BdbD production. It is not clear why this was the case and this would require further investigation. As a means to test the activity of BdbD variants, this system proved to be too unreliable. However, the data generated here provide new insight into redox processes outside of the membrane. The data suggest that the balance between oxidised and reduced forms of BdbD is crucial for the activity of the oxidative branch and that this can be readily disrupted by the overproduction of BdbD. Further experiments to verify BdbD levels and also to probe the redox state of BdbD are now necessary to demonstrate this. Given the above, it is likely that a different experimental system will be needed to investigate the *in vivo* properties of key residues within BdbD. An approach similar to that employed to investigate the *in vivo* properties of ResA in Chapters 3 and 4 may be more appropriate, where a single copy of the *resA* gene was inserted at the *amyE* locus. This should avoid overproduction of BdbD.

Chapter 6: Studies of the Res system in *Streptomyces coelicolor*

6.1. Intoduction

Genetic analysis identified a clear homologue of the *B. subtilis res* operon in *S. coelicolor*. As well as genes encoding for the three Res proteins required to produce a CCM system II, the operon also contains a gene encoding a homologue of another TDOR, CcdA. Using the recombination genetic engineering method, two knock out mutations were introduced to remove either the *res* operon or the single *resA* gene from *S. coelicolor* M145 to examine the importance of the products encoded by these genes for cytochrome *c* maturation in *S. coelicolor*. The cytochrome *c*, QcrC, was found to be absent from membranes prepared from *S. coelicolor* strains which were lacking either the entire *res* operon or the single *resA* gene. In addition to the study of phenotypes of the *S. coelicolor resA* and *res* operon knock-out strains, the *S. coelicolor* ResA protein (ScResA) was over-expressed and purified from *E. coli*. This allowed the study of the biophysical properties of the protein.

6.2. Experimental Procedures

The majority of the general experimental procedures used in the work presented in this chapter can be found in Chapter 2 and procedures exclusive to the work presented here are described below.

6.2.1. Generation of the *resA* and *res* operon *S. coelicolor* mutants

Mutational analysis has proved a very powerful tool to characterise the function of genes. In-frame deletions of genes in *S. coelicolor* can be generated using a

specific PCR-targeting approach, developed for use in *Saccharomyces cerevisiae* by Baudin *et al* in 1993 (134) and adapted for use in *S. coelicolor* as described by Gust *et al*, 2003 (110). This powerful technique, commonly referred to as recombineering (recombination-mediated genetic engineering), allows the disruption of a specific gene by generating a non-polar in-frame deletion, thus avoiding effects on downstream genes. Knock-out mutations in the *S. coelicolor* chromosome are commonly engineered by first introducing the desired mutation to a copy of the gene carried on a cosmid, from an ordered cosmid library (111). This is done by interrupting or replacing the gene with an antibiotic marker. The mutated cosmid is then conjugated into *S. coelicolor* and a cross over event is selected for, whereby the interrupted gene from the cosmid replaces the chromosomal wild type copy. The *S. coelicolor res* operon can be found on cosmid StD65. The cosmids, plasmids and strains used in this study are all described in Chapter 2. Antibiotics were used at the following final concentrations, unless otherwise stated: Apramycin (50 µg/ml), kanamycin (40 µg/ml), chloramphenicol (25 µg/ml), carbenicillin (100 µg/ml) and nalidixic acid (25 µg/ml). Experimental procedures specific to the work presented in this chapter are described below and are based on the recombineering protocol described by Gust *et al* (110).

6.2.1.1. Verification of cosmid StD65 by restriction digestion

The 8.6 Mb genome of *S. coelicolor* has been fragmented and cloned into Supercos1 to create an accessible and ordered genomic library of 319 cosmids (111). The cosmid which contains the part of the *S. coelicolor* genome that encodes the *res* operon is designated StD65. As cosmids are large circular DNA

molecules, they are prone to mutation when they are replicated in *E. coli* cells, and the cosmid can be re-ordered, by random recombination events. To ensure that the cosmid StD65 was correctly ordered it was analysed by cutting it with restriction enzymes. Using the cosmid restriction cut tool on the redirect website (http://streptomyces.org.uk/redirect/res_cosmid2.html) it was possible to predict the band sizes that would be observed when StD65 was cut with *Hin*dIII and *Xba*I, see Table 6.1. StD65 was incubated with *Hin*dIII and *Bam*HI for one hour at 37 ^{o}C before separating the fragments by agarose gel electrophoresis (Figure 6.1), as described in Chapter 2.

Table 6.1. Expected bands generated by the restriction digest of StD65 with *Eco*RI and *Hin*dIII. Prediction generated using the restriction cut tool found at http://streptomyces.org.uk/redirect/res_cosmid2.html

***Eco*RI, *Hin*dIII digestion of StD65 (bp)**					
25837	12062	4565	2227	539	20

All of the predicted bands were present and fully detectable on the agarose gel, with the exception of the 20 bp fragment, which only appeared as a faint blur, which could be expected due to the very small amount of DNA present. Verification of the cosmid in this way was repeated throughout the gene disruption procedure.

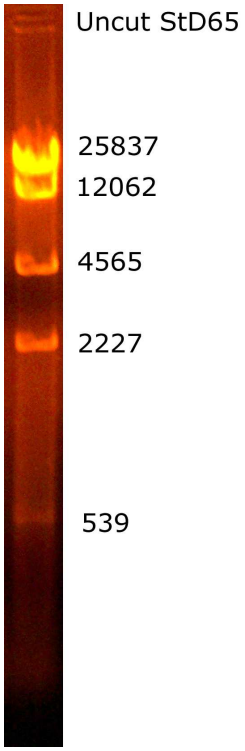

Figure 6.1. Verification of StD65 by restriction digest. StD65 was incubated with *Hind*III and *Eco*RI for one hour at 37 ^{o}C before separating the generated fragments by agarose gel electrophoresis. The cut pattern matches prediction made in Table 6.1, which demonstrates the cosmid is highly unlikely to have become mutated during replication. It was not possible to clearly visualise the predicted 20 bp fragment. This is likely to be because there was not enough DNA was present and the poor resolving ability of a 1% agarose gel for small size DNA fragment.

6.2.1.2. PCR amplification of the *resA* and *res* operon disruption cassettes

Primers were designed to amplify the apramycin resistance cassette (Apra^{R}), *oriT* and the FRT sites found on plasmid pIJ773. Before use as template DNA this region was excised from the plasmid using *Eco*RI and *Hin*dIII. The 20 and 19 nt priming sequences (at the 5' and 3' ends, respectively) of this cassette are always the same. The primers also have a 39 nt sequence ending at the start codon (plus the 36 upstream bases) or the stop codon (plus the 36 downstream bases of the complementary strand) for the upstream and downstream primers, respectively, see Table 6.2 for primer details. A schematic of the primer design process is shown in Figure 6.2. The PCR reaction required to amplify this DNA fragment in unique to work presented in this chapter and so is described below, not in Chapter 2.

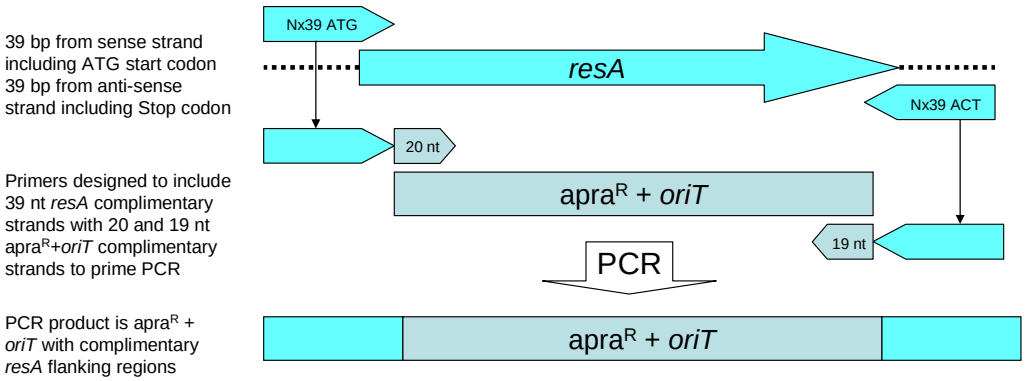

Figure 6.2. Schematic of primer design process to design primers to PCR amplify apra^R+oriT cassette with *ScresA* flanking regions. Primers with 39 nt flanking regions of *resA* and 20 nt and 19 nt complementary regions from the apra^R+*oriT* cassette are used to generate a version of the apra^R+*oriT* cassette with *resA* flanking regions using PCR. This can be used to transform *E. coli* BW25113 harbouring StD65 and pIJ790 for λ-Red mediated double crossover to knockout the StD65 *ScresA* gene, replacing it with apra^R+*oriT.* For clarity, the FRT sites are not shown in this figure.

These primers allow the amplification of a DNA fragment that contains Apra^R, *oriT*, the FRT sites and the flanking regions of the gene or genes to be knocked out, in this case *resA* or the *res* operon. The 50 µl PCR reaction mix contained 50 pmol of each primer, 50 ng template DNA (the Apra^R cassette), DNA polymerase (Roche, Expand High Fidelity PCR System), 50 µM dNTP mix, 5% DMSO, 5 µl 10 x reaction buffer and was made up to 50 µl with sterile dH_2O. The reaction was carried out in a Techne thermocycler under the conditions shown in Table 6.3. 5 µl of the PCR reaction mix was used to confirm that the reaction had been successful (see Figure 6.3) and the remaining 45 µl was cleaned using the QIAGEN PCR purification kit according to the manufacturer's instruction.

Table 6.2. Primers used to generate *resA* and the *res* operon knock-out cassettes by PCR. The *resA* forward primer was used in conjunction with the *resA* reverse or the *resA-C* reverse to generate and amplify the disruption cassettes for *resA* or the *res* operon, respectively. The PCR reaction conditions are described in Table 6.3 and the reaction mixture is described in the text. The FRT sites are highlighted yellow. The test primers were designed to amplify the region between the flanking regions of *resA* or the *res* operon to confirm that the gene or the operon had been replaced by the disruption cassette. Again *resA* test forward was used in conjunction with *resA* reverse test or *resA-C* reverse test for disruption of the *resA* gene or the *res* operon, respectively.

Primer	**Sequence**
resA forward	gcaagatcctcggaacggacatgcgaaactttcacatgattccggggatccgtcgacc
resA reverse	agccctcggccgcgagggtggtcactgcggacacgtcatgtaggctggagctgcttc
resA-C reverse	tgggtcacgggaaccggcctttggccgtgccttgatcatgtaggctggagctgcttc
resA forward test	Gcaagatcctcggaacggac
resA reverse test	Agccctcggccgcgagggtg
resA-C reverse test	Tgggtcacgggaaccggcct

Table 6.3. PCR reaction conditions required to amplify the AprR cassette with the 5' and 3' flanking regions of the gene of interest.

Process	**Temp ^{o}C**	**Time**	**Repeat**
Initial denaturation	90	2 min	1
Cycle 1 Denaturation Primer annealing Extension	 94 50 72	 45 s 45 s 90 s	 10
Cycle 2 Denaturation Primer annealing Extension	 94 55 72	 15 s 45 s 90 s	 15
Final Extension	72	5 min	1

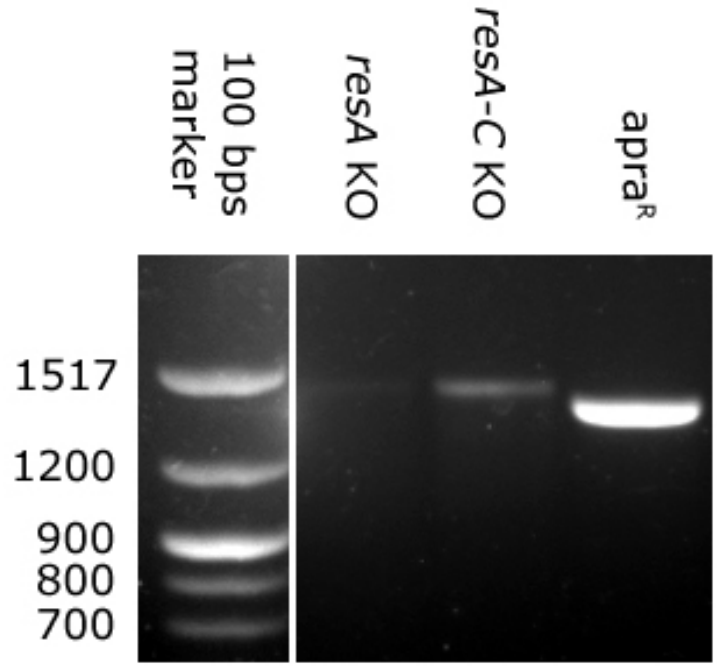

Figure 6.3. PCR amplification of the *resA* and *resA-C* disruption cassettes. The apra^R was used as the template DNA to amplify the cassettes. This 1382 bp fragment, which was cut from plasmid pIJ773 using *Eco*RI and *Hin*dIII, contains the apramycin resistance gene as well as FLP recognition target sites. The amplified *resA* and *resA-C* disruption cassettes are 78 bp larger than the apra^R cassette due to the two 39 bp flanking regions which are specific for the *resA* or the *resA-C* regions on StD65. Although the band showing for *resA* KO appears to be very weak, enough DNA was present to enable the transformation of BW25113/pIJ790/StD65, see below.

6.2.1.3. Transformation of BW25113/pIJ790 with StD65

Upon confirmation that StD65 was correct it was necessary to introduce it, by electroporation to *E. coli* BW25113 harbouring the λ Red recombination plasmid (pIJ790). pIJ790 contains a chloramphenicol resistance marker and has a temperature sensitive origin of replication that requires it to be grown at 30 ^oC in the presence of chloramphenicol to maintain the plasmid. 10 ml cultures of *E. coli* BW25113/pIJ790 were grown overnight at 30 ^oC, 200 rpm in LB containing chloramphenicol. 100 µl of this overnight culture was used to inoculate 10 ml cultures in LB containing chloramphenicol, which were grown at 30 ^oC, 200 rpm. These cells were harvested and prepared for electroporation, then

transformed with ~ 100 ng of StD65 DNA as described in Chapter 2. One ml of ice cold LB was immediately added to the shocked cells and they were incubated at 30 ^{o}C, 200 rpm for one hour. This transformation reaction was plated on to LBA containing carbenicillin and kanamycin to select for StD65 and chloramphenicol to select for pIJ790, and incubated at 30 ^{o}C overnight.

6.2.1.4. Disruption of the *resA* gene and the *res* operon on StD65 by recombineering

In order to introduce the required mutations to the StD65 cosmid the PCR product disruption cassette must be introduced to BW25113/pIJ790/StD65. The induction of the λ Red genes (located on the pIJ790 plasmid) can then be induced by the addition of 10 mM L-arabinose (final concentration) to the growth medium, to initiate the disruption of the *resA* gene or the *res* operon by the disruption cassette via λ-Red mediated double crossover, Figure 6.4.

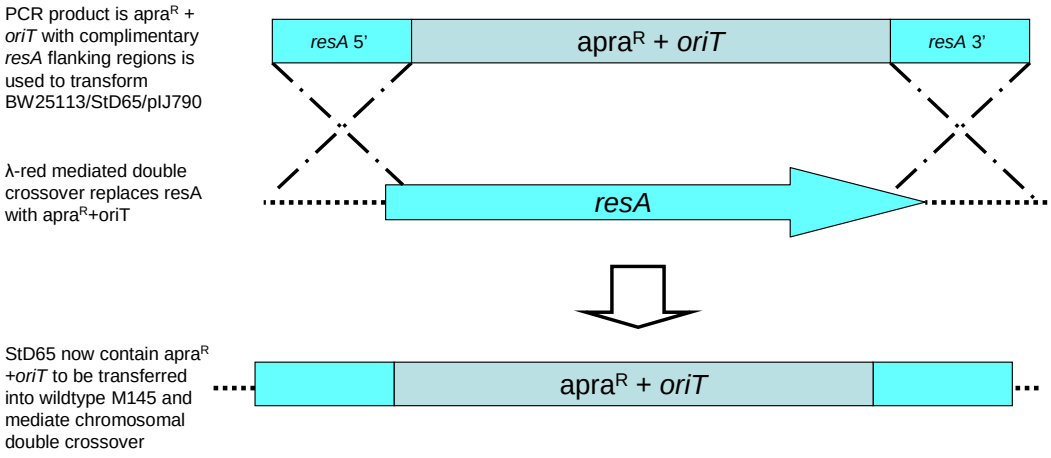

Figure 6.4. Schematic of λ-Red mediated double crossover. PCR generated knockout cassette is used to transform *E. coli* BW25113 harbouring pIJ790 and wild type StD65. The λ-Red (located on pIJ790) are induced at 37 ^{o}C, initiating the double crossover event.

A single colony of BW25113/pIJ790 successfully transformed with the StD65 cosmid was used to inoculate 5 ml of LB containing carbenicillin, kanamycin and chloramphenicol in the quantities described above. This culture was grown overnight at 30 ^{o}C, 200 rpm. 250 µl of the overnight culture was used to inoculate 10 ml of SOB (without $MgSO_4$) containing carbenicillin, kanamycin and chloramphenicol in the quantities described above. 100 µl of 1 M L-arabinose was added to the culture (final concentration 10 mM) to induce the λ Red genes, and the cells grown at 30 ^{o}C, 200 rpm until OD_{600} reached about 0.5. This culture was harvested and prepared for electroporation as described in Chapter 2. Cells were transformed with 1 µl of the resistance cassette by electroporation as described in Chapter 2, plated on to LBA containing apramycin and kanamycin to select for the mutated StD65 cosmid and incubated overnight at 37 ^{o}C. Incubation at 37 ^{o}C and the lack of chloramphenicol in the growth medium discourages the procreation of plasmid pIJ790. Transformed colonies were picked and used to inoculate 5 ml cultures in LB containing apramycin and kanamycin, grown at 37 ^{o}C, 200 rpm.

Table 6.4. Predicted *Sac*I restriction digest pattern of wild type StD65 and the StD65 *resA* and *resA-C* knock out mutants. Digest pattern generated using webcutter2 (http://rna.lundberg.gu.se/cutter2/)

Wild Type	***resA* KO**	***resA-C* KO**
21693	16925	13125
12550	12550	12550
2927	4690	4690
1228	2927	2927
	1228	1228
	751	751

The mutated StD65 cosmid was purified from the cell culture as described in Chapter 2, and compared to wild type StD65 by analysing restriction cut patterns and PCR, see Figures 6.5 and 6.6, respectively. When cosmid StD65 is cut with *Sac*I it is predicted to have a specific pattern when run on an agarose gel; when certain areas have been interrupted, removed or replaced that restriction digest pattern will change. A comparison of the predicted restriction digest pattern of wild type StD65 and the *resA* and *res* operon deletion strain is shown in Table 6.4.

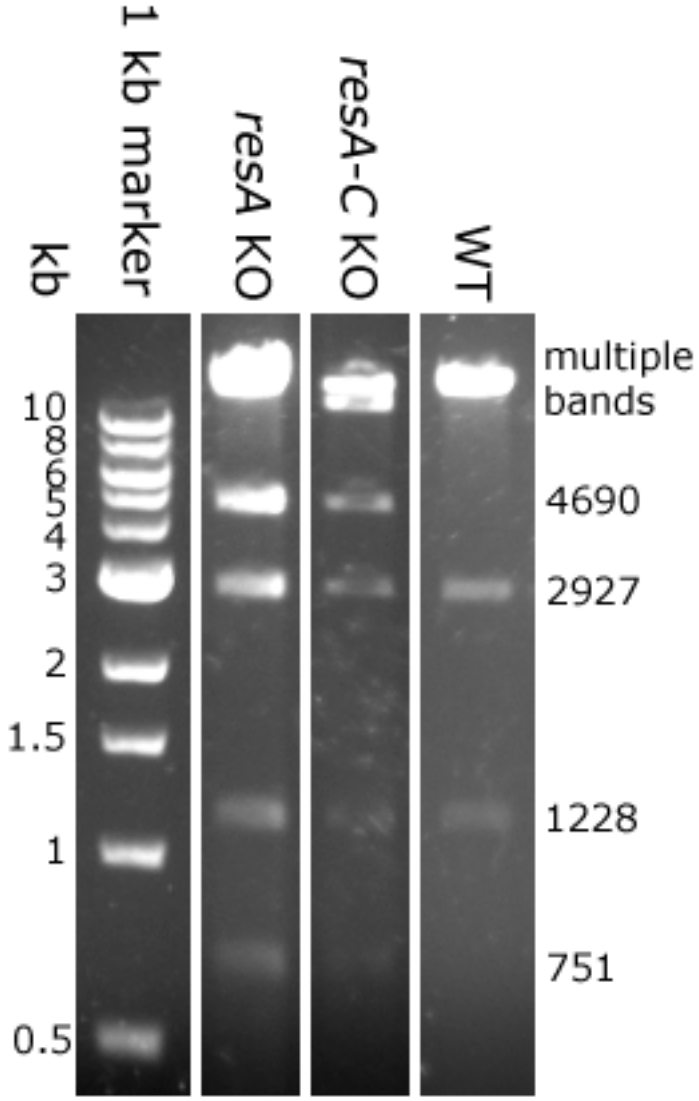

Figure 6.5. *Sac*I restriction digest of wild type StD65 and the *resA* and *resA-C* knock out (KO) mutants. The StD65 cosmids containing the resA and res operon knock-out mutations demonstrate a different pattern to the wild-type StD65 cosmid when cut with SacI and the resulting fragments separated by agarose gel electrophoresis. The expected fragment sizes were predicted using Webcutter2 (shown in Table 6.4). It was not possible to fully resolve the larger fragments (over 10 kb) on this gel so they appear as one large band, labelled 'multiple bands'. Importantly, the extra bands generated by the apra^{R} insertion into the *resA* and *resA-C* knockouts at 4690 and 751 bp are clearly visible.

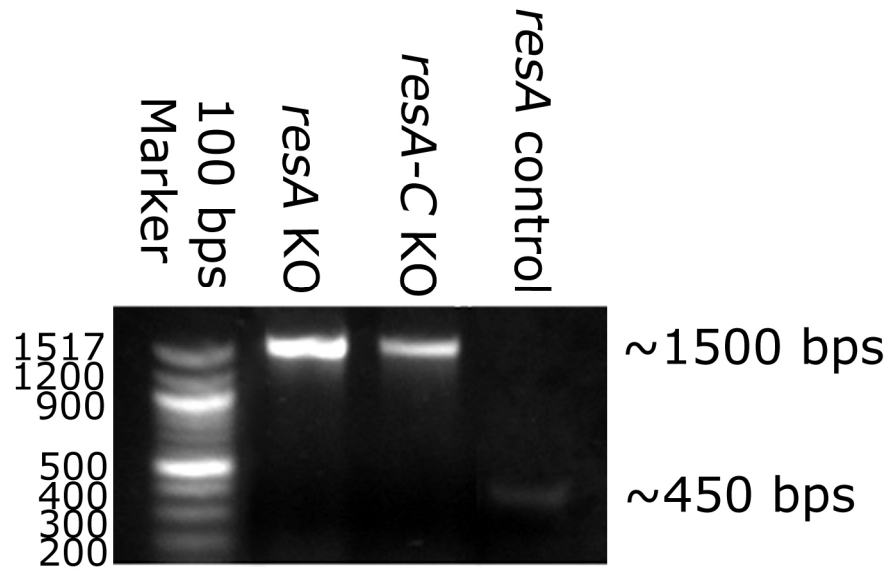

Figure 6.6. PCR confirmation of *resA* and *resA-C* disruption with apra^R resistance cassette. After transformation with the disruption cassette, disrupted StD65 cosmids were purified from the transformed cells as described in Chapter 2. The *resA* or *resA-C* regions of these cosmids were amplified using the test primers (Table 5.3). The *resA* gene is only ~450 bps in length, whereas the disruption cassette is closer to 1500 bps. The *resA* control shows the *resA* gene amplified from wild type StD65 cosmid template using the same primers as used to amplify the region in the *resA* KO. Although it was not possible to amplify the wild type *resA-C* region (~5500 bps) from wild type StD65, it was possible to amplify the disruption cassette using primers specific for the *resA-C* region, demonstrating that the disruption of the *resA* and *resA-C* regions were successful.

On confirmation that the appropriate mutations had been introduced to StD65 to create StD65Δ*resA* and StD65Δ*resA-C* (for the *resA* and *res* operon knockout mutations, respectively) these were used to transform the methylation-deficient *E. coli* strain, ET12567/pUZ8002 by electroporation as described in Chapter 2. The resulting transformants were selected on LBA containing kanamycin and apramycin for selection of mutated StD65 cosmid DNA and chloramphenicol for selection of the pUZ8002 plasmid.

6.2.1.5. Conjugative transfer of StD65Δ*resA* and StD65Δ*resA-C* to *S. coelicolor* from *E. coli*.

The mutated cosmids were transferred from *E. coli* ET12567/pUZ8002 to *S. coelicolor* M145 by conjugation. ET12567 is a methylation deficient strain of *E. coli*, and this was employed here because *S. coelicolor* will digest methylated DNA. The pUZ8002 plasmid contains the genes necessary for conjugative transfer. Single colonies of ET12567/pUZ8002 harbouring either StD65Δ*resA* or StD65Δ*resA-C* were cultured overnight in LB containing kanamycin, apramycin and chloramphenicol at 37 ^{o}C, 200 rpm. These cells were harvested and resuspended twice in LB to wash and remove any remaining antibiotic that may inhibit the growth of *S. coelicolor*. 10 µl (~10^{8} per ml) of *S. coelicolor* M145 spores was added to 500 µl 2 x YT broth and this was incubated at 50 ^{o}C for 10 minutes to heat shock the spores. These were then cooled to room temperature and 0.5 ml was mixed with 0.5 ml of the resuspended *E. coli* preparation. This mixture was briefly centrifuged and the majority of the supernatant removed. The pellet was resuspended in the residual supernatant (~50 µl). The resuspended cell/spore mixture was diluted in series (10^{-1} to 10^{-4}) in 100 µl sterile dH_2O. 100 µl of the diluted suspensions was plated on to MS agar with 10 mM $MgCl_2$, without antibiotics and incubated at 30^{o}C for 20 hours. The plates were overlaid with 1 ml H_2O containing 0.5 mg nalidixic acid (which selectively kills *E. coli*) and 1.25 mg apramycin (to select for the resistance cassette in the disrupted gene). The plates were then incubated at 30^{o}C for a further two days, when single *S. coelicolor* colonies were easily visible. Any plates with single colonies were replica-plated on to DNA (a growth medium that gives fast, non-sporulating growth of *S. coelicolor*) containing nalidixic acid and apramycin and

either with or without kanamycin. The replica plates were compared to identify apramycin resistant, kanamycin sensitive colonies. Double crossover ex-conjugants are apramymycin resistant (due to the $Apra^R$ in the disruption cassette) and kanamycin sensitive because the kanamycin resistance gene is located on the Supercos1 backbone, which is no longer present. Kanamycin sensitive colonies were picked and re-streaked onto MS containing apramycin and nalidixic acid and incubated at 30 ^oC for 2-3 days. The plates were replica plated again on to DNA with and without kanamycin to confirm that all colonies were sensitive. Kanamycin sensitve strains were verified for disruption to the *resA* gene or *res* operon by PCR, using the test primers (Table 5.3) and *S. coelicolor* M145Δ*resA* and M145Δ*resA-C* genomic DNA as template. Upon confirmation that the *resA* and the *res* operon had been disrupted, spores were collected and used to inoculate cultures for membrane preparations, as described in Chapter 2.

6.2.2. Purification of a soluble form of *S. coelicolor* ResA

In order to study reactivity and structural properties of ScResA *in vitro* a purified soluble form of the protein was required.

6.2.2.1. Purification of a soluble native form of ScResA

Initially primers were designed to amplify the part of the *ScresA* gene predicted to encode the soluble domain of ScResA from the cosmid StD65. The PCR amplification reaction was carried out as described in Chapter 2 using primers ScResA1 and ScResA2 as the forward and reverse primers respectively. These primers introduced an *Nde*I site and an ATG 'start codon' at the 5' end of the

gene and a *Hin*dIII restriction site at the 3' end. This amplified fragment of DNA was blunt end cloned into pUC18 at the *Sma*I site, generating plasmid pCHN11. After confirmation of successful PCR amplification and ligation by sequence analysis, the gene was excised from pUC18 and ligated into pET21a at the *Nde*I/*Hin*dIII site (generating plasmid pCHN12) for expression in *E. coli* BL21 strains. pCHN12 was used to transform BL21 DE3 as described in Chapter 2.

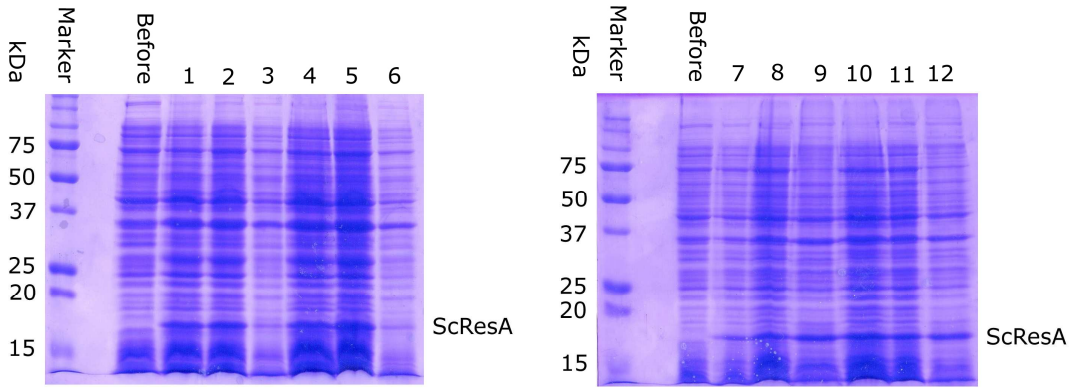

Figure 6.7. Test expressions of the pCHN12 plasmid in BL21 DE3. Whole cell samples were taken from cultures grown in LB containing 100 µg/ml ampicillin. The cell were suspended in loading buffer and analysed by SDS-PAGE stained with Coomassie. All cultures were grown at 37 ℃ until induction with 1 mM IPTG. The lanes labelled 'Before' corresponds to a cell sample taken before induction. Samples in lanes are as follows: 1, 2 and 3 were induced with 1 mM IPTG when OD_{600} reached 0.8, they were then grown for a further 3 hours, 5 hours or overnight, respectively, at 30 ℃; 4, 5 and 6 were induced when OD_{600} reached 0.6 they were then grown for a further 3 hours, 5 hours or overnight, respectively, at 30 ℃; 7, 8 and 9 were induced when OD_{600} reached 0.6 they were then grown for a further 3 hours, 5 hours or overnight, respectively, at 37 ℃; 10, 11 and 12 were induced when OD_{600} reached 0.8 they were then grown for a further 3 hours, 5 hours or overnight, respectively, at 37℃. Over-produced ScResA protein can been observed at ~17 kDa.

The ability of *E. coli* to express ScResA from plasmid pCHN12 was tested. 40 ml cultures (LB containing 100 µg/ml ampicillin) were inoculated and grown at 37 °C, 200 rpm until the optical density at 600 nm (OD_{600}) reached 0.6 or 0.8,

where gene expressed was induced by the addition of 1 mM IPTG and the cultures were then grown for a further 3 hours, 5 hours or overnight at either 30 °C or 37 °C , 200 rpm. These tests demonstrated that ScResA was produced by inducing gene expression with 1 mM IPTG when the culture reached 0.8 at OD_{600}. Allowing the culture to continue growing overnight at 37 °C before harvesting yielded the most amount of ScResA in respect to other proteins, see Figure 6.7. But when this was scaled up protein production appeared to be very inconsistent, with several attempts yielding no detectable ScResA at all.

One early attempt demonstrated that it was possible to partially purify ScResA by ammonium sulphate precipitation, in accordance with the BsResA purification protocol developed by Erlendsson *et al* (12). The prepared cytoplasm was treated by the addition of 50% w/v ammonium sulphate. This caused many proteins, not including ScResA, to precipitate. Ammonium sulphate concentration was then increased to 80% w/v causing remaining protein, including ScResA, to precipitate. The ammonium sulphate was removed by dialysis, and a sample of this was analysed by SDS-PAGE. A large amount of ScResA was detected but the sample was not completely pure (Figure 6.8). In an attempt to remove any remaining impurities the sample was loaded on to an anion exchange column (Hi-Trap Q, GE Healthcare) and was eluted with a gradient of 0-1 M NaCl over 60 ml, but very little ScResA was found in any of the elution fractions (Figure 6.8). Furthermore, it was not possible to reproducibly obtain a high level of purification by ammonium sulphate precipitation. Using the small amount of ScResA that was retrieved from the anion exchange column it was possible to demonstrate that the protein was stable up to 60 °C for 30 minutes. 50 µl samples of impure ScResA were incubated at

30, 40, 50, 60, 70 and 80 °C for 15 minutes. These samples were centrifuged at 14000 rpm for 15 minutes to separate any denatured, insoluble protein from the soluble protein that remained in the supernatant, which was carefully removed. The supernatant and the pellet were analysed by SDS PAGE (Figure 6.9).

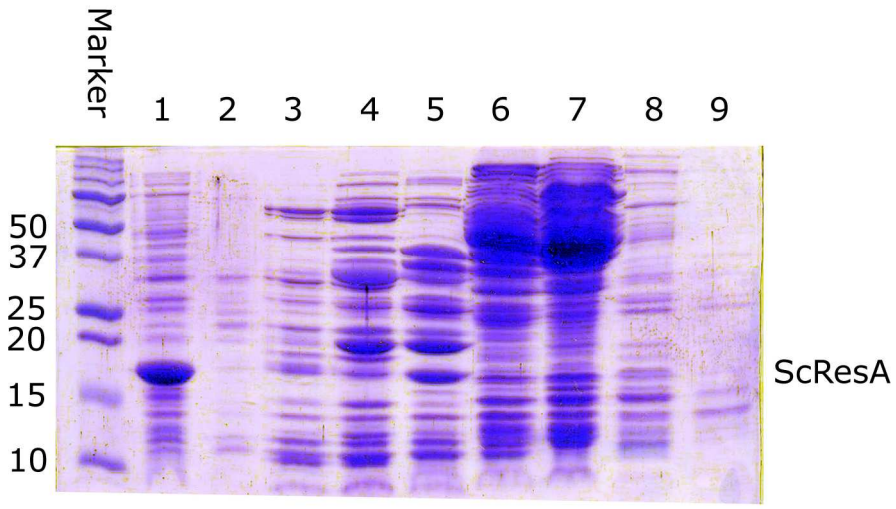

Figure 6.8. Ammonium sulphate precipitation and anion exchange of ScResA. Samples of protein were taken form various stages during the purification and analysed by SDS-PAGE stained with Coomassie. Lane 1 shows a sample of the *E. coli* cytoplasm containing ScResA (after 80% w/v ammonium sulphate has been removed by dialysis) which was loaded on to the anion exchange column. Lanes 2-9 represent various fractions eluted from the anion exchange column as the concentration of NaCl increases. Approximate maximum NaCl concentrations in the fractions are as follows: lane 2 (0 M, column flow though); lane 3 (0.2 M); lane 4 (0.25 M); lane 5 (0.3 M); lane 6 (0.45 M); lane 7 (0.5 M); lane 8 (0.7 M); lane 9 (0.95 M). ScResA can be be observed at ~17 kDa. This gel demonstrates that it was not possible to further purify ScResA from the *E. coli* cytoplasm using anion exchange chromatography.

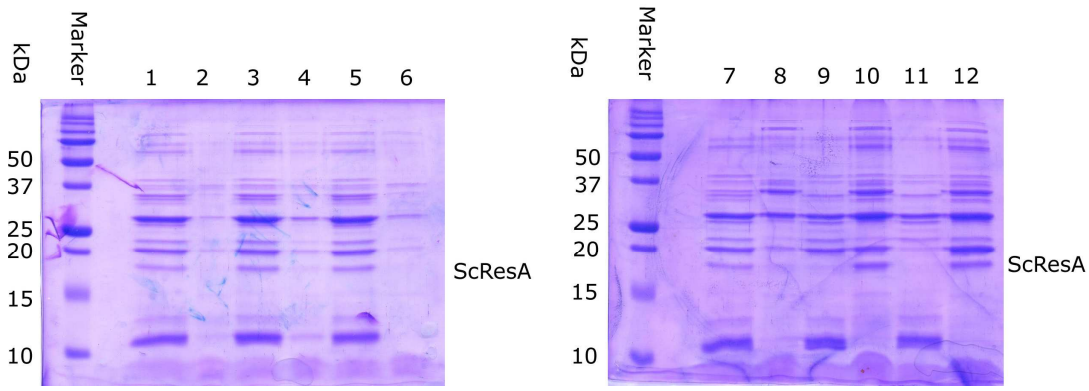

Figure 6.9. Heat stability of ScResA. Impure ScResA samples were heated to temperatures between 30-80 ℃ for 15 minutes and th en separated in to soluble and insoluble fractions before analysing the samples by SDS PAGE stained with Coomassie. Lanes: 1, 30 ℃, soluble; 2, 30 ℃, insoluble; 3, 4 0 ℃, soluble; 4, 40 ℃ insoluble; 5, 50 ℃, soluble; 6, 50 ℃, insoluble; 7, 60 ℃ soluble; 8, 60 ℃ insoluble; 9, 70 ℃, soluble; 10, 70 ℃, insoluble; 11, 80 ℃, soluble; 12, 80 ℃ , insoluble. ScResA can be observed at ~ 17 kDa. ScResA is visible in the soluble fractions up to and including 60 ℃ but was denatured and insoluble from 70 ℃.

Unfortunately, despite repeated efforts, expression of ScResA from this construct proved very inconsistent and attempts to purify the protein in this way were abandoned in favour of creating a GST fusion construct using the pGEX system (GE Life Sciences).

A second set of primers were designed to amplify the same part of the gene as described above but to introduce a *Bam*HI restriction site at the 5' end and a *Eco*RI restriction site a the 3' end of the gene to allow ligation in the pGEX-4T-1 plasmid (GE Healthcare) to create a ScResA:GST fusion protein.

The part of the gene predicted to encode the soluble domain of ScResA was amplified by PCR using the Roche Expand High Fidelity PCR system. The reaction was carried out as described in Chapter 2 using primers ScResA3 and ScResA4 as the forward and reverse primers, respectively, in a Techne

thermocycler. Correct amplification of the gene was confirmed by agarose gel electrophoresis (Figure 6.10). The amplified gene was then excised from the gel and cleaned from the agarose using a QIAGEN DNA agarose clean up kit. The gene was then ligated into the pUC18 plasmid which had been cut with *Sma*I to allow "blunt end" ligation of the *ScresA* gene into the vector. The pUC18/*ScresA* ligation reaction mix was used to transform *E. coli* JM109 cells, which were plated on to LBA (containing 1% X-GAL, 1 µM IPTG, 100 µg/ml ampicillin) in order that successfully transformed cells containing pUC18 with the *ScresA* gene insert could be identified by "blue/white" screening. Successfully transformed colonies were used to inoculate 5 ml LB overnight cultures from which the plasmid could be extracted using the QIAGEN plasmid extraction kit. Extracted plasmids were further checked for correct gene insertion by cutting the gene out with *Bam*HI and *Eco*RI. On confirmation of a correctly sized gene insert by gel electrophoresis (Figure 6.11) the plasmids were sequenced to confirm the insertion of the *ScresA* gene (MWG biotech) and the plasmid was designated pCHN23. The gene could then be ligated into pGEX-4T-1 using the *Bam*HI and *Eco*RI restriction sites. Successful pGEX:ScResA ligations were confirmed by restriction cutting and gel electrophoresis (Figure 6.12). The pGEX-4T-1:*ScresA* plasmid was designated pCHN24.

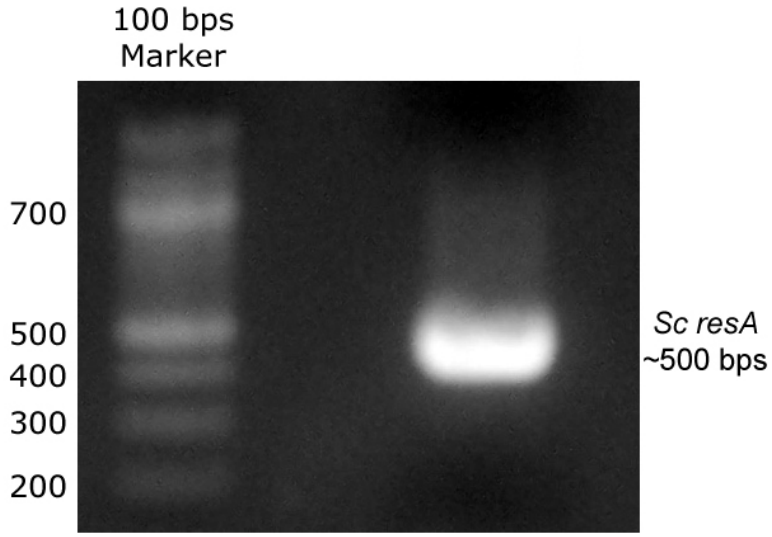

Figure 6.10. PCR amplification of part of *ScresA* gene predicted to encode soluble domain. The *resA* gene was amplified from cosmid StD65 by PCR using primers ScResA3 and ScResA4 as described in Chapter 2. A 15 µl sample of PCR reaction was run on a 1% agarose gel containing ethidium bromide and visualised under UV light. The amplified *ScresA* gene can be seen at ~500 bps, no other non-specific bands can be observed, demonstrating the PCR reaction was successful.

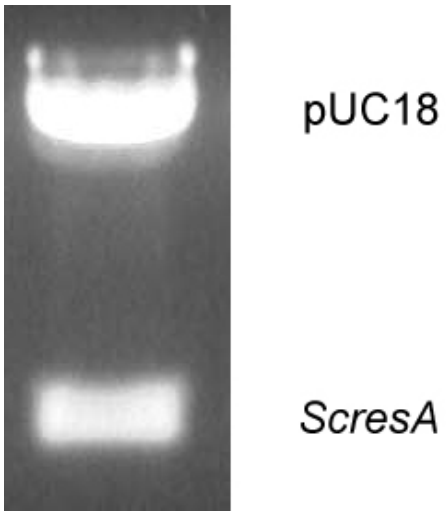

Figure 6.11. Confirmation of correct insertion of the gene encoding *ScresA* into pUC18. The *ScresA* fragment generated by PCR was cleaned from the agarose gel (Figure 6.10) and was blunt end cloned into pUC18 at the *Sma*I site. The amplified *ScresA* fragment was amplified to include a *Bam*HI and an *Eco*RI site, these were used to liberate the insert from pUC18. 15 µl sample of restriction reaction was run on a 1% agarose gel containing ethidium bromide and visualised under UV light to demonstrate the ligation was successful. This was further confirmed by DNA sequencing.

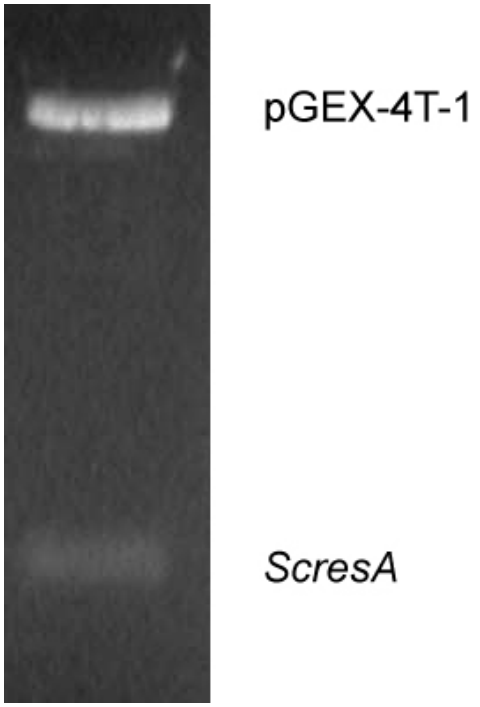

Figure 6.12. Confirmation of correct ScResA encoding gene insertion into pGEX-4T-1. *ScresA* was cloned into pGEX-4T-1 at the *Eco*RI/*Bam*HI site and these enzymes were used to liberate the fragment to confirm the successful ligation. 15 µl sample of restriction reaction was run on a 1% agarose gel containing ethidium bromide and visualised under UV light to demonstrate the correct ligation of the *ScresA* gene into pDG148.

6.2.2.2. Expression of GST:ScResA in *E. coli* BL21 CodonPlus(DE3)-RP

Plasmid pCHN24 was used to transform chemically competent *E. coli* BL21 CodonPlus(DE3)-RP as described in Chapter 2, materials and methods. The *E. coli* BL21 CodonPlus(DE3)-RP strain offered the best yield of protein production compared to *E. coli* BL21 (star), BL21 (pLysS) and BL21 (Rossetta R2), (Figure 6.13). Both the *E. coli* BL21 CodonPlus(DE3)-RP and Rosetta strains have been specifically engineered to allow the expression of genes with codons which would be rarely found in normal strains of *E. coli*. 0.5 L cultures were inoculated with 5 ml of an overnight culture and the 0.5 L culture would be grown at 37 °C, 200 rpm until the OD_{600} reached approximately 0.8. Expression of the of the GST:ResA fusion was induced with the addition of 1 mM IPTG. 100 µg/ml

ampicillin was present during all growth stages. The temperature was reduced to 30 °C and the cells were grown for a further three hours before harvesting by centrifugation, 7000 rpm, 15 minutes, 4 °C. Cells were resuspended in 50 mM Tris, 100 mM NaCl, 1 mM phenylmethanesulphonylfluoride (PMSF), pH 8. 35 ml of buffer was used to resuspend cells harvested from one litre of cell culture.

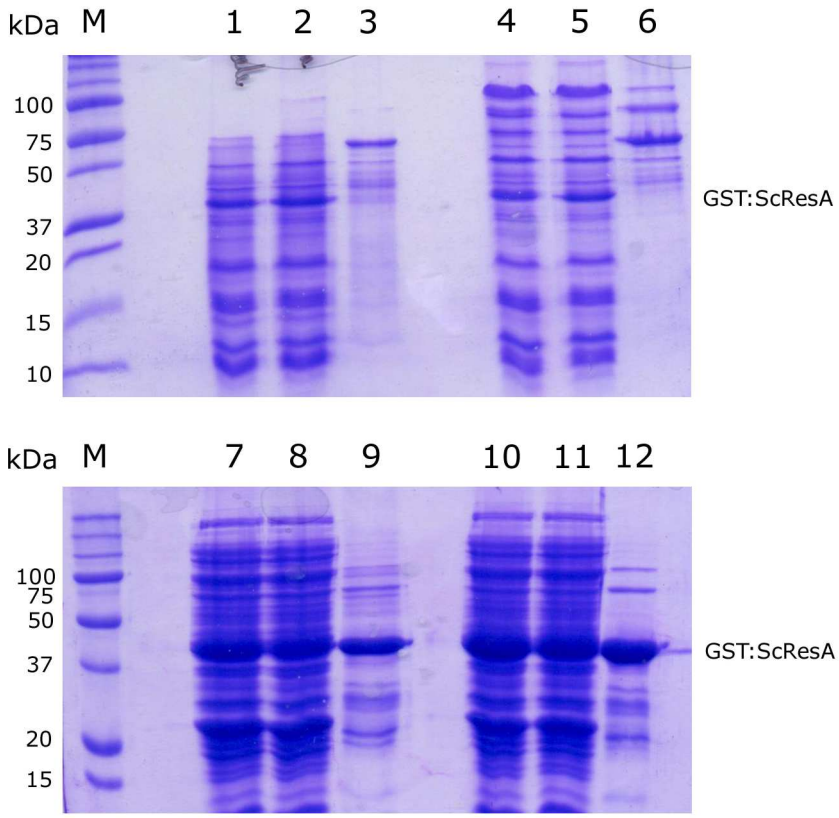

Figure 6.13. Test expression/test purification of GST:ScResA from different *E. coli* strains: Plasmid pCHN24 was introduced to four different strains of *E. coli,* BL21 (star), BL21 (pLysS), BL21 (Rossetta R2) and BL21 CodonPlus (DE3)-RP. The ability of these transformed to strains to produce soluble ScResA from plasmid pCHN24 was explored, by analysing whole-cell sample by SDS-PAGE, the growth and gene induction conditions are discussed in the text. BL21 (Star), lanes 1-3; BL21 (pLysS) lanes 4-6; BL21 (Rossetta R2) lanes 7-9; BL21 CodonPlus (DE3)-RP 10-12. Lanes 1, 4, 7 and 10 are the soluble fraction of the cell lysate; lanes 2, 5, 8 and 11 are the flow through from the GST column; lanes 3, 6, 9 and 12 are the reduced glutathione elution.

6.2.2.3. Purification of GST:ScResA

Resuspended cells were lysed by sonication on ice. The soluble cell lysate was separated from the insoluble cell debris by centrifugation at 20,000 rpm for 45 minutes. The soluble cell lysate was applied to a 2 ml glutathione sepharose column (GE Healthcare) equilibrated with buffer (50 mM Tris, 100 mM NaCl, pH 8), note that this buffer was used throughout the purification unless otherwise stated. The GST:ResA protein was bound to the matrix which was washed with 5 volumes of buffer to remove non- and loosely bound protein. 40 units of thrombin (GE Healthcare) in 5 ml buffer was then applied and the column sealed and mixed well by inverting several times and left at room temperature overnight to cleave the ResA from the GST tag. The flow through was then collected and the column washed with a further 2 ml of buffer to elute any remaining cleaved ResA protein (Figure 6.14). The flow through and washes were then concentrated by adding 80% w/v ammonium sulphate which caused the protein to precipitate. The precipitated protein was collected by centrifugation at 12000 x g for 15 minutes at 4 °C. The protein pellet was dissolved in a minimal amount of buffer, and subsequently applied to a gel filtration column with a bed volume of 300 ml (Superdex S75, GE Healthcare) equilibrated in buffer. A gel filtration step was required to remove the thrombin from the ScResA so that biochemical analysis could be performed. Protein began to elute from the column after about 100 ml and 5 ml fractions were collected while protein eluted (Figure 6.15). Eluted fractions were then analysed by SDS PAGE to identify those that contained pure ResA (Figure 6.16). After cleaving the GST:ScResA fusion protein with thrombin, to remove the GST tag, ScResA was left with an additional glycine and a serine at the N-terminal.

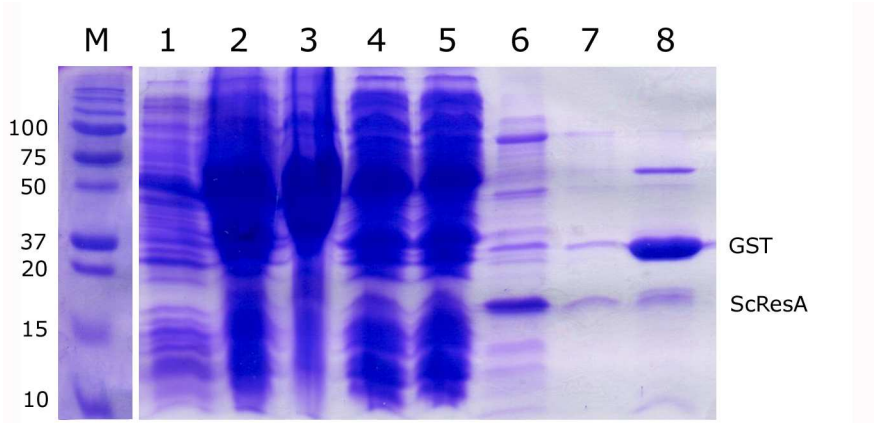

Figure 6.14. Coomassie stained SDS PAGE showing different stages of ScResA purification from *E. coli*. Lane 1, whole cell sample taken from before *ScresA* gene expression was induced with IPTG; Lane 2, whole cell sample taken 3 hours after induction with IPTG; Lane 3, Insoluble fraction after sonication of cells; Lane 4, soluble fraction after sonication of cells; Lane 5, sample of column flow through containing proteins that did not bind to the glutathione sepharose column; Lane 6, Cleaved ScResA eluted from glutathione sepharose column after thrombin treatment; Lane 7, wash to elute any remaining cleaved ScResA; Lane 8, reduced glutathione elution to clean cleaved GST tag and any remaining uncleaved GST:ScResA. ScResA cleaved from the GST tag can be seen at ~17 kDa.

There appears to be a lot of GST:ScResA in the insoluble fraction after sonication (Figure 6.10). This could be because ScResA production in the cell was so effective that the cell put protein into inclusion bodies to avoid the possibility of the protein becoming toxic to the cell. There is a large peak in the trace from the gel filtration column between 100 and 130 ml (Figure 6.11). This is caused by the large unidentified proteins contaminating ScResA which can be seen in fractions B2, B3 and B4 (Figure 6.12).

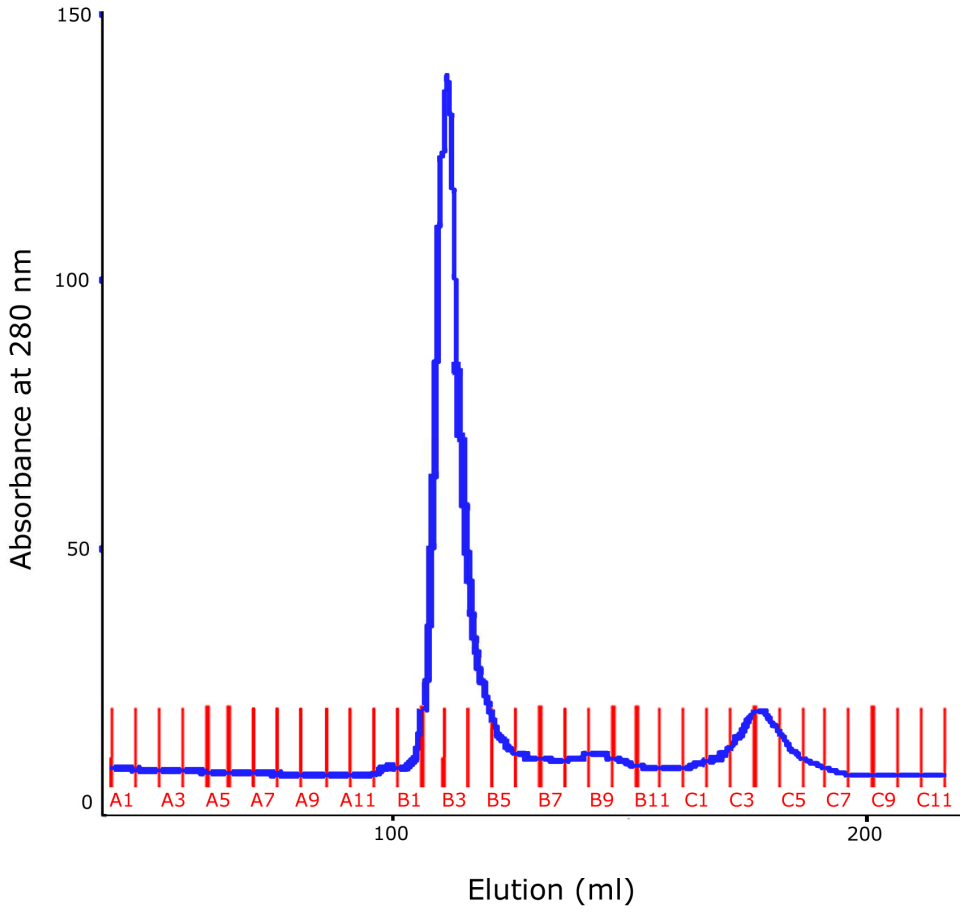

Figure 6.15. Absorbance at 280 nm from elution from gel filtration column. The column eluent was monitored at 280 nm before it was divided into fractions. The red lines denote the 5 ml fractions collected. The blue line shows absorbance of eluent at 280 nm. Samples of these fractions were examined by SDS PAGE (Figure 6.16). Pure ScResA was present in fractions C3 – C6.

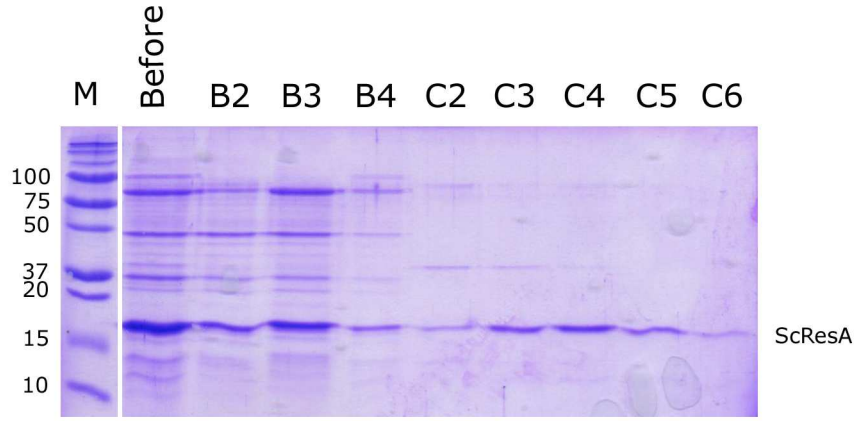

Figure 6.16. Coomassie stained SDS PAGE showing fractions eluted from S75 gel filtration column. 15 µl samples of gel filtration column eluent from fractions that showed good absorbance at 280 nm (see Figure 6.15) were analysed using SDS-PAGE. Varying amounts of ScResA appears to present in all the fractions examined but only in C3, C4 and C5 does the ScResA appear to be free of impurities. The lane labelled "Before" corresponds to a sample of what was loaded on to the gel filtration column and B2, B3, B4, C2, C3, C4, C5 and C6 refer to the fractions eluted from the gel filtration column.

6.3. Results and preliminary characterisation of the function and physiology of *S. coelicolor* ResA.

6.3.1. The *S. coelicolor* M145Δ*resA* and M145Δ*resA-C* phenotypes.

The observations made here, concerning the phenotype, are based on the ability of *S. coelicolor* M145Δ*resA* and M145Δ*resA-C* to mature cytochromes. Neither strain appeared to have any noticeable non-wild type characteristics when grown vegetatively, and both strains were able to produce viable spores. However, the spores were not subjected to any testing with regard to their ability to remain viable under extreme conditions of temperature or pH, so it cannot be concluded that these mutations do not affect growth or sporulation in any way. It should be

noted that the M145Δ*qcr* strain was slower to grow than wild type; reasons for this are discussed below.

6.3.1.1. *S. coelicolor* produces one detectable membrane associated cytochrome *c*

A strain of *S. coelicolor* M145 with the *qcr* and cytochrome *c* oxidase gene clusters knocked out was donated by Dr Matthew Hutchings. This strain is referred to here as M145Δ*qcr*. *S. coelicolor* QcrC is predicted to be 27.5 kDa, with two transmembrane helices.

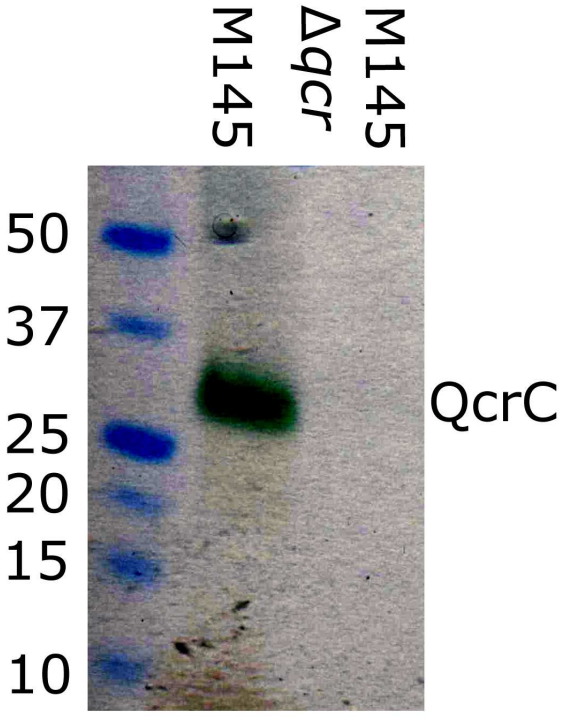

Figure 6.17. Haem stain of membranes prepared from *S. coelicolor* M145 and M145Δ*qcr*. Membrane samples from the *S. coelicolor* M145 and M145Δ*qcr* strains were prepared from 10 ml liquid culture. 100 µg of membrane sample was run by SDS-PAGE and stained for haem as described in Chapter 2. *S. coelicolor* QcrC is predicted to be 27.5 kDa. The membrane associated protein, with covalently bound haem present in the M145 wild type strain, is highly likely to be QcrC. This protein is consistent with the predicted size and location of QcrC and cannot be detected in the *qcr* deletion strain. The small mark at 50 kDa is likely to be an artefact caused by a bubble in the gel.

Membranes were prepared from cultures of wild type M145 and the M145Δ*qcr* strains. These membrane preparations were analysed by SDS-PAGE stained for haem, as described in Chapter 2. This confirmed that the cytochrome *c*, QcrC, was detectable in the membrane of M145 but not in the M145Δ*qcr* strain (Figure 6.17).

6.3.1.2. The *resA* and *res* operon deletion strains are deficient in QcrC maturation

Once it was established that *S. coelicolor* had a membrane associated cytochrome *c* that could be detected by haem staining it was possible to investigate whether *S. coelicolor* relies on the Res system to mature it.

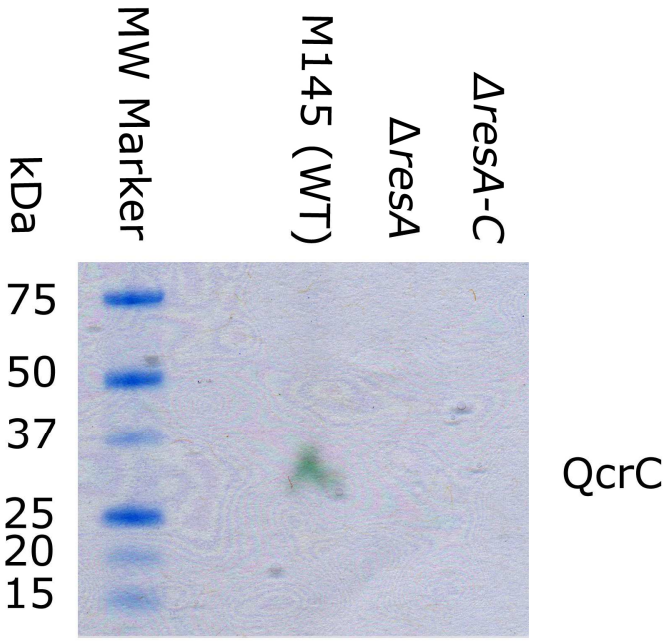

Figure 6.18. Haem stain of M145, M145Δ*resA* and M145Δ*resA-C* membranes. 100 µg of membrane samples prepared from *S. coelicolor* M145, M145Δ*resA* and M145Δ*resA-C* were analysed by SDS-PAGE gel stained for haem. Both the M145Δ*resA* and M145Δ*resA-C* strains are deficient in mature QcrC. M145 is the wild type strain, Δ*resA* and Δ*resA-C* are M145 with *resA* or the *res* operon replaced with the Apra^R disruption cassette, respectively.

Membranes were prepared from the M145Δ*resA* and M145Δ*resA-C* strains and run on an SDS-PAGE gel and stained for haem, as described in Chapter 2. Both the *resA* and the *res* operon knock out strains demonstrated a QcrC deficient phenotype, Figure 6.18.

6.3.2. Characterisation of ScResA

With a protocol for the purification of a soluble version of ScResA in place it was possible to carry out a number of experiments to characterise the biochemical properties of the protein including determining the pK_a of its active site cysteine thiol groups, the midpoint reduction potential and some preliminary observations with regard to the stability of the protein.

6.3.2.1. Determination of the extinction coefficient of ScResA at 280 nm.

In order to be able to calculate the concentration of ScResA the extinction coefficient at 280 nm was determined. An extinction coefficient at 280 nm was calculated using Protparam (http://ca.expasy.org/cgi-bin/protparam) for unfolded ScResA based on sequence analysis (and assuming all Cys residues were reduced half cysteines) as 20065 M^{-1} cm^{-1} at 280 nm. This was then used to calculate the extinction coefficient of the folded protein by spectroscopy. 0.5 µM ScResA was incubated for one hour at room temperature in 3 M guanidine hydrochloride, 50 mM potassium phosphate, pH 7 to fully unfold the protein (ScResA is very sensitive to guanidine hydrochloride unfolding, see below). The absorbance spectrum between 250 and 500 nm was recorded and compared to the spectrum of a native sample of identical concentration (Figure 6.19). The absorbance at 280 nm was used in conjunction with the extinction coefficient calculated for the

unfolded protein to calculate the extinction coefficient for the folded protein, see Equation 6.1, where A_{nat} is the absorbance of the folded protein, $A_{Gnd.HCl}$ is the absorbance of the unfolded protein and $\varepsilon_{Gdn.HCl}$ is the predicted extinction coefficient for the unfolded peptide. The measured extinction coefficient was calculated to be 22390 M^{-1} cm^{-1} at 280 nm.

$$\varepsilon = \frac{A_{nat} \cdot \varepsilon_{Gdn.HCL}}{A_{Gdn.HCL}} \qquad \text{(Equation 6.1)}$$

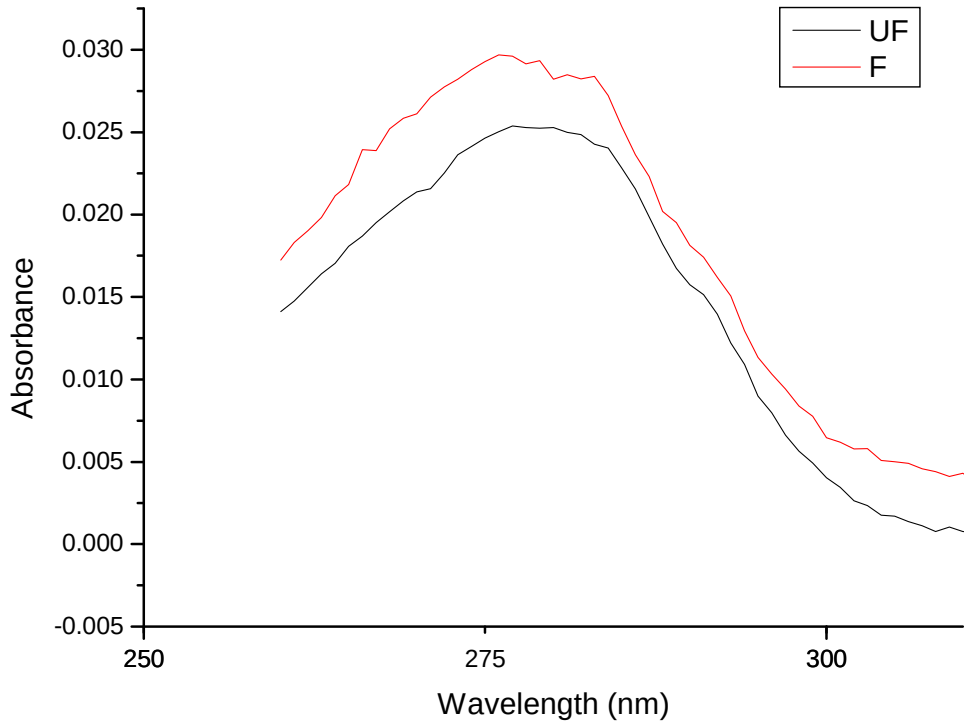

Figure 6.19. Absorbance spectra of unfolded (UF) and folded (F) ScResA used to calculate the extinction coefficient. The red and black lines represent the folded and unfolded protein, respectively. 0.5 µM protein in 50 mM potassium phosphate, pH 7 (3 M guanidine hydrochloride was present in the unfolded sample). The spectra were recorded using a Perkin Elmer lambda 800 spectrometer which is designed to be able to accurately record low absorbances from low concentrations of protein such as this.

6.3.2.2. Reduced ScResA has only one reactive thiol group at neutral pH.

Most TDORs only have one available, reactive cysteine but BsResA is different as both cysteines are solvent exposed (15). To investigate whether ScResA has similar properties 5,5'-Dithio-bis(2-nitrobenzoic acid) (DTNB) was used. DTNB reacts with thiols resulting in the release of one yellow coloured TNB^- ion per SH group, meaning that thiol reactivity can be measured spectroscopically. 100 µM DTNB was added to 5 µM ScResA in 20 µM Tris, pH 8 and the absorbance at 412 nm was measured. The reaction was too fast to follow by standard spectrophotometry and so the final A_{412} (0.091) was used to calculate that ScResA has 1.3 reactive thiols, based on an extinction coefficient of TNB^- at 412 nm of 14150 M^{-1} cm^{-1} (135). MALDI-TOF was employed to determine the ability of ScResA to react with badan, following the reaction at pH 7.5 described below. An identically treated sample without badan was also measured as a control. This experiment showed that only one molecule of badan reacted with ScResA. Unreacted protein gave a molecular weight of 17336 Da while that of the badan-reacted sample was 17555 Da, an increase of 219 Da. This was very close to the expected weight of sulphur reacted badan (212 Da). Both the DTNB and the badan experiments show that only one active site cysteine of ScResA is reactive towards modifying agents, unlike BsResA, where both cysteines are able to react (19).

6.3.2.3. pH stability of ScResA.

The pH stability of ScResA was measured to establish that the protein remains folded across the pH range used for the pK_a determination, as the unfolding of a protein will change the properties of the residue being deprotonated. 0.25 µM ScResA was added to mixed buffer (containing ammonia, potassium acetate, MES, MOPS, and Tris (10 mM each) and 200 mM KCl pH adjusted with either HCl or NaOH) pH ranging from 2-12 and allowed to equilibrate for one hour. The degree of unfolding was measured by recording fluorescence spectra between 300 and 500 nm. A scan between these wavelengths was completed three times on each sample to provide an average (Figure 6.20).

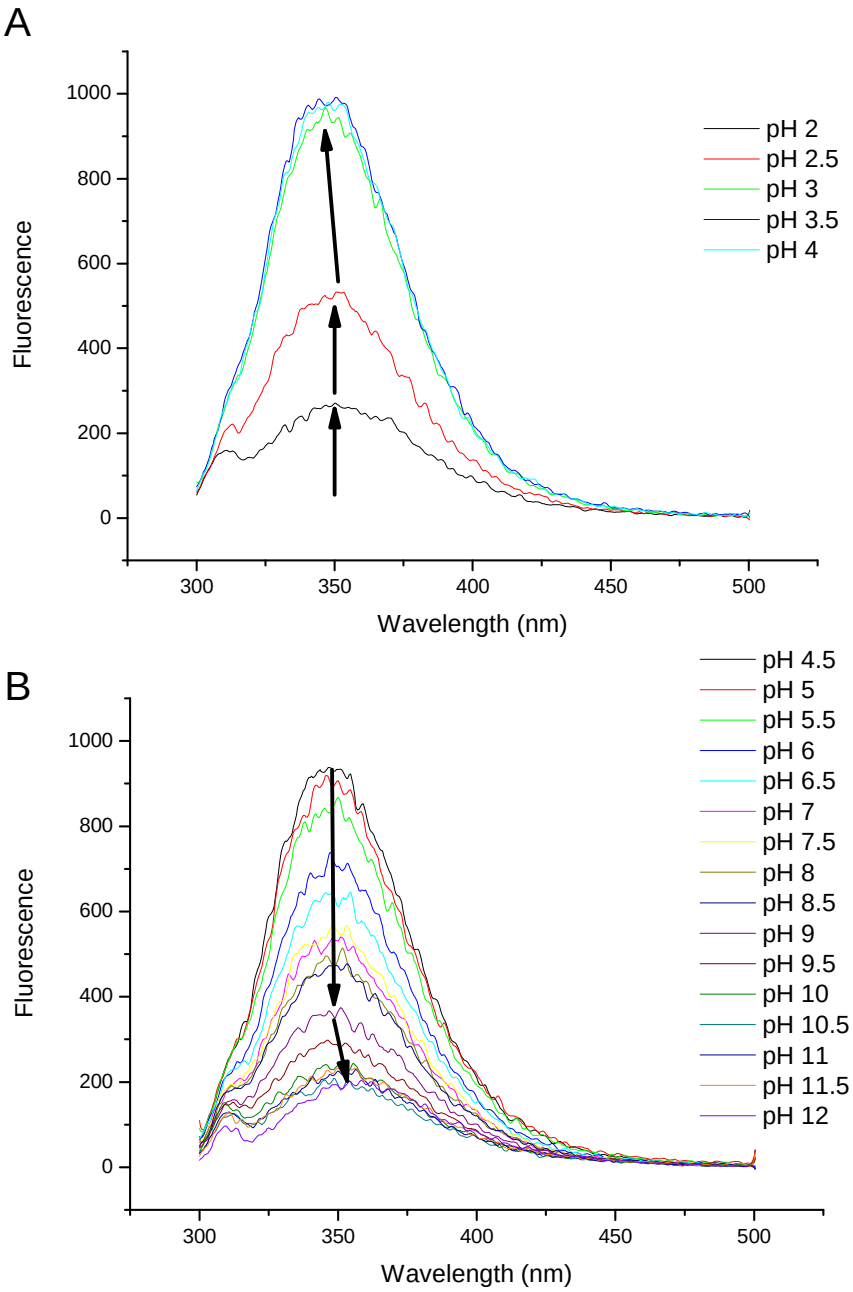

Figure 6.20. Fluorescence spectra of ScResA from pH 2 to pH 12. 0.25 µM ScResA, final concentration, was incubated for one hour in mixed buffer of stated pH. Samples were excited at 290 nm and fluorescence spectra between 300-500 nm were measured and the mean spectra for each sample are plotted. *A,* The fluorescence intensity increases and the wavelength of the maximum intensity decreases (black arrows) as the protein begins to fold as the pH increases from pH 2 to pH 4. *B*, pH 4.5-12, fluorescence intensity decreases and the wavelength of maximum increases as the protein unfolds (black arrows).

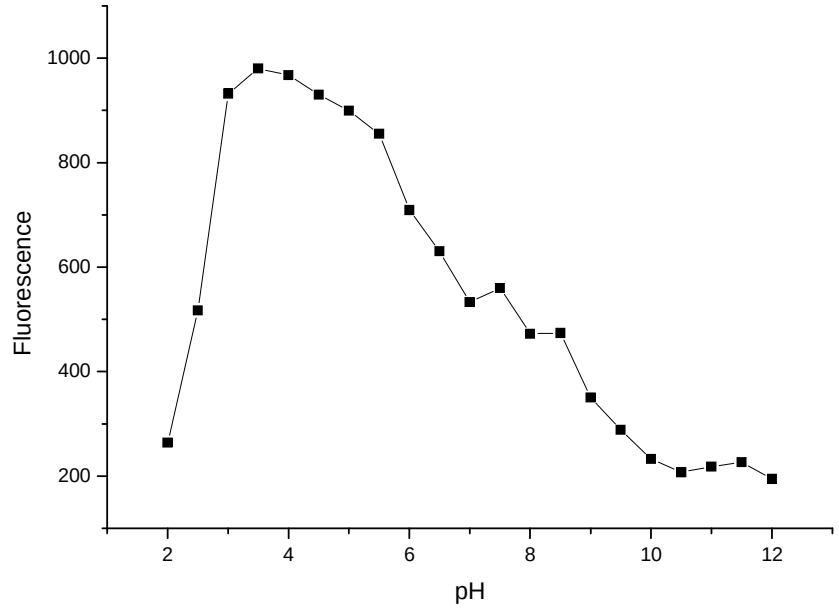

Figure 6.21. Fluorescence at 349 nm plotted as function against pH. Folded ScResA demonstrates a maximum fluorescence at 349 nm when excited at 280 nm. The intensity of fluorescence increases steeply between pH 2 and pH 4, then begins to decrease by pH 6. The wavelength where maximum fluorescence intensity occurs also changes with pH, shown in Figure 6.22.

The protein appears to have a maximum intensity around 349 nm, so the intensities at this wavelength were plotted against pH (Figure 6.21). This plot shows definite conformational changes as the protein moves from a low to high pH that may be linked to the pK_a of the exposed cysteine but makes the unfolding difficult to judge. The wavelength position of the emission maximum intensity appears to move from around 346 nm to 348 nm in the folded protein but up to 356 nm as the protein unfolds. To get a different perspective as to where the protein unfolds the position of the maximum intensity fluorescence was plotted as a function against pH (Figure 6.22). These data indicate that the protein is stable between pH 3.5 and pH 9.

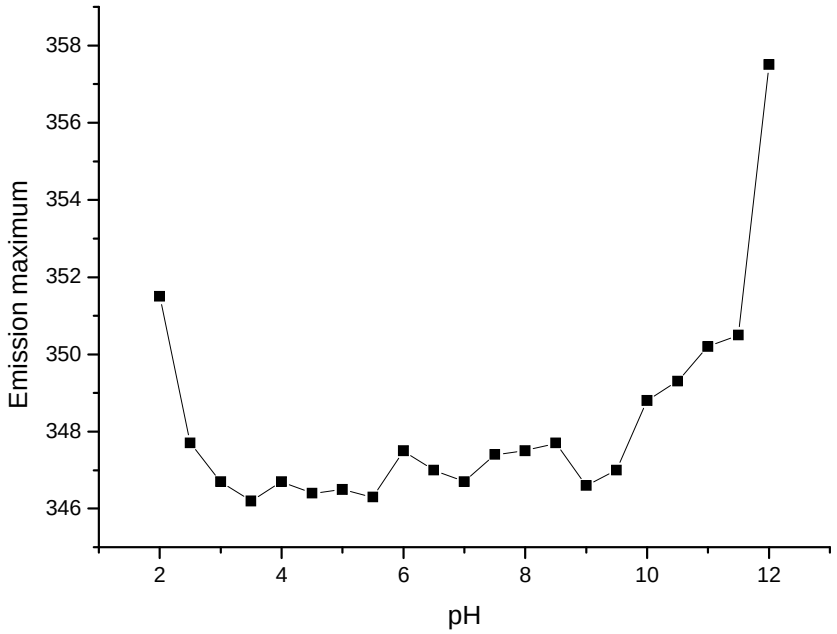

Figure 6.22. pH unfolding of ScResA. The wavelength of the maximum fluorescence intensity alters between the folded and unfolded forms of ScResA. This change was plotted as a function against pH. As ScResA unfolds the fluorescence changes the wavelength of peak maximum from between 346-348 nm in the folded protein to above 349 nm as it begins to unfold.

6.3.2.4. The reactive active site cysteine of ScResA has a pK_a of 6.9 (± 0.1).

The pK_a of the exposed thiol of ScResA was determined by monitoring the rate of reaction between ScResA and the environment sensitive fluorescent probe badan as a function of pH. The reaction between badan and ScResA was extremely fast at room temperature, so all badan fluorescence experiments were conducted at 10 °C and samples were allowed to equilibrate at this temperature before the experiment began. Experiments were carried out between the pH range of pH 4 and pH 9. Representative data at a range of pH values are shown in Figure 6.23.

The greatest increase of fluorescence was at 544 nm so datas at this wavelength were plotted against time for each pH and these datas were fitted to a single exponential function (Equation 6.2, where y is fluorescence, y_o is initial fluorescence, x is time, A_1 is the maximum increase of fluorescence during badan binding and $k1$ is the pseudo first order rate constant) in order to calculate the observed pseudo first order rate constant (k_o) (Figure 6.24).

$$y = y_0 + A_1(1 - e^{-xk1}) \qquad \text{(Equation 6.2)}$$

At pH 8 and above, the initial fluorescence increase was followed by a decrease and so an additional exponential function had to be added to Equation 6.2 to create Equation 6.3, where y is fluorescence, y_o is initial fluorescence, x is time, A_1 is the maximum increase of fluorescence during badan binding, $A2$ is the maximum decrease in fluorescence from competing process, $k1$ is the pseudo first order rate constant and $k2$ is the pseudo first order rate constant for process 2. This phenomenon was observed for BsResA and appears to be the result of localised unfolding caused by the badan group (15). The k_o values were plotted against pH and the data fitted to Equation 6.4 which is based on the Henderson Hasselbalch equation, where k_{SH} and k_S^- are the rate constants of the protonated and the deprotonated forms respectively. See Figure 6.25 for the curve fit.

$$y = y_o + A_1(1 - e^{-xk1}) + A2(1 - e^{-xk2}) \qquad \text{(Equation 6.3)}$$

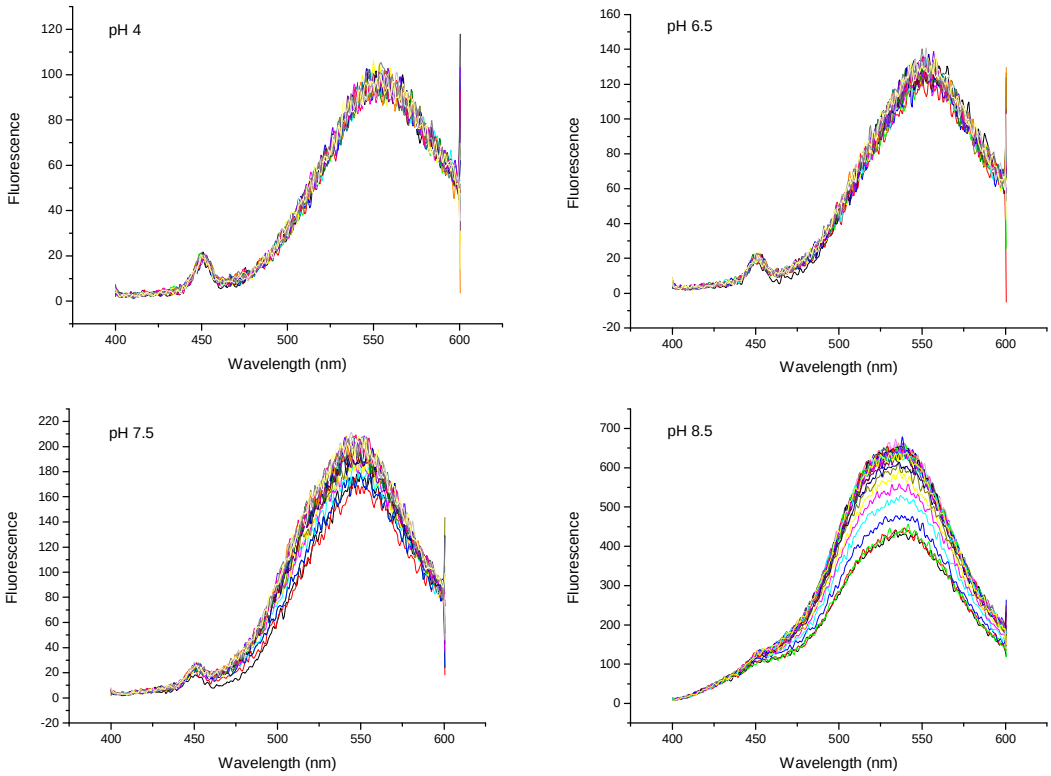

Figure 6.23. Example of Badan fluorescence between 400 and 600 nm of badan incubated with ScResA. The ratio of the exposed cysteine thiol group found in the thiolate form increases with pH allowing reaction with badan. 7 µM badan was incubated in mixed buffer at stated pH for one hour at room temperature in the dark. It was cooled to 10 ℃, excited at 391 nm and fluorescence betwee n 400 and 600 nm was recorded once before 0.25 µM ScResA was added (red). Fluorescence was then recorded once every minute, shown as coloured curves, until increases in fluorescence were no-longer detected. The maximum increase of fluorescence was observed at 544 nm.

$$k_0 = \frac{k_{SH} + k_{s^-} 10^{\mathrm{pH\text{-}p}K_a}}{1 + 10^{\mathrm{pH} - pKa}} \qquad \text{(Equation 6.4)}$$

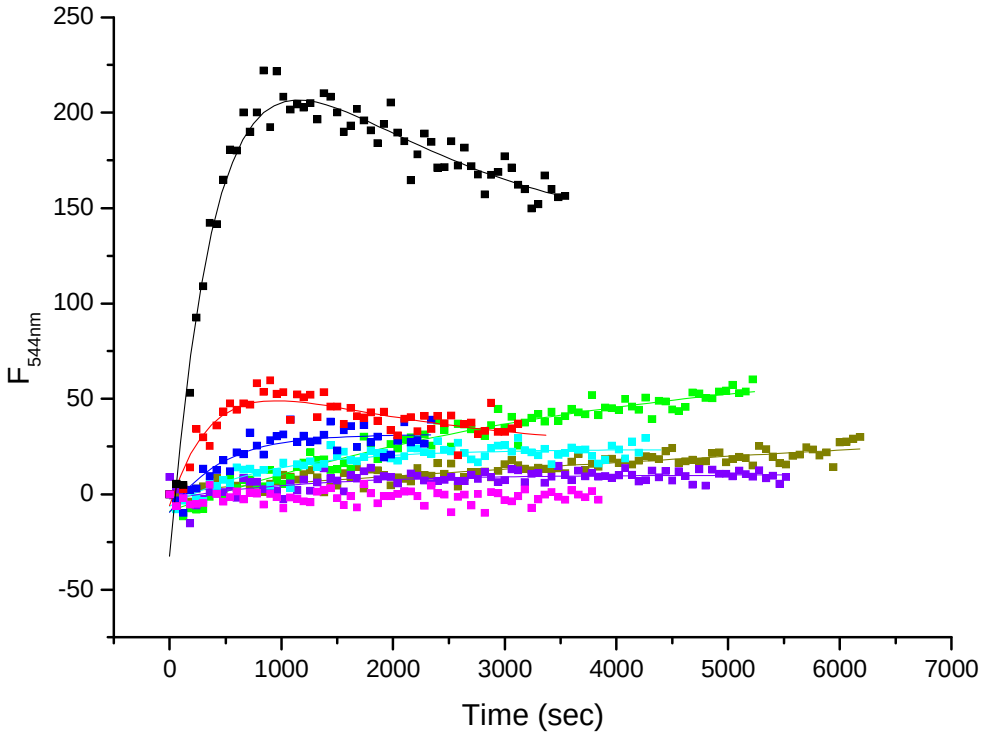

Figure 6.24. Changes in badan fluorescence intensity at 544 nm as the probe reacts with ScResA. Badan fluorescence at 544 nm was plotted as a function of time at pH 4 (magenta), pH 5 (dark yellow), pH 6 (green), pH 6.5 (violet), pH7 (cyan), pH 7.5 (blue), pH 8 (red) and pH 8.5 (black). The length of the experiment depended on the speed of the reaction. The points were fitted to a single exponential function (Equation 6.2) or, where the initial increase was followed by a decrease, a double exponential function (Equation 6.3) in order to calculate the pseudo first order rate constant. The reaction at pH 4 could not be fitted as the increase in fluorescence was minimal so the pseudo first order rate constant was set to zero.

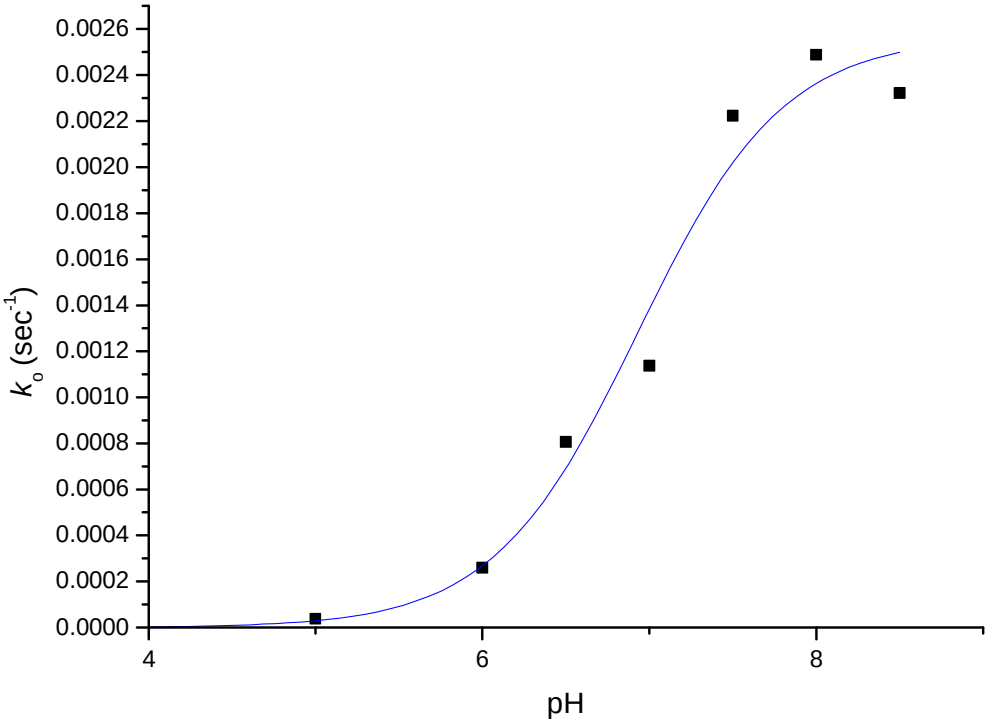

Figure 6.25. The observed pseudo first order rate constant (k_o) values plotted against pH. A curve was fitted using the Henderson Hasselbalch equation (Equation 6.4), allowing the calculation of a pK_a for the exposed cysteine as being 6.9 (± 0.1)

No reaction was observed at pH 4 and so k_o was fixed at zero. Similarly, the reaction a pH 9 was so fast and the contribution from the fluorescence decrease so large that k_o could not be determined. These data were therefore excluded. The pK_a was calculated to be 6.9 ± 0.1

6.3.2.5. Reduction potential determination for ScResA.

ScResA exhibits a small but clear difference in tryptophan fluorescence between the oxidised and reduced forms at 344 nm (Figure 6.26). The reduction potential of ScResA was measured by monitoring the difference in tryptophan fluorescence between the oxidised and reduced forms of ScResA at 344 nm.

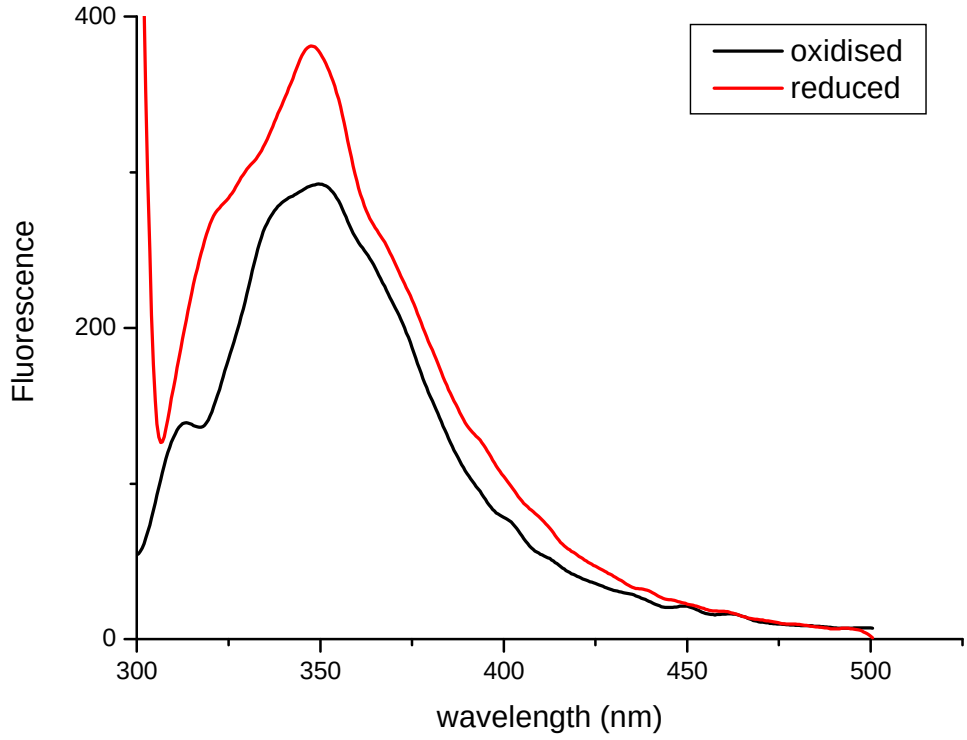

Figure 6.26. Fluorescence emission spectra of oxidised and reduced ScResA. ScResA was oxidised fully with oxidised DTT and desalted using a PD-10 gel filtration column (GE Healthcare) equilibrated with 20 mM Tris, pH 8. The sample was excited at 290 nm and the fluorescence between 300 and 500 nm was recorded (black). The sample was then reduced with 1 mM DTT and the fluorescence spectrum was recorded again (red). The largest difference in fluorescence between the oxidised and reduced samples occurs at 344 nm. This illustrates a detectable conformational change between the reduced and oxidised forms of ScResA.

0.1 µM of ScResA was incubated at room temperature over an electrochemical potential range from -330 mV to – 210 mV versus the standard hydrogen electrode (SHE) in 50 mM potassium phosphate buffer, pH 7. The fluorescence emission was recorded between 300 and 500 nm (Figure 6.27). As with BsResA, oxidised ScResA cannot be reduced with reduced glutathione (GSH) so the cell potential was generated using oxidised and reduced DTT (dithiothreitol). As oxidised DTT absorbs light in the fluorescence excitation range and can therefore

affect intensity it was kept at a constant concentration of 1 mM throughout the titration and only the concentration of reduced DTT was changed to generate the potential.

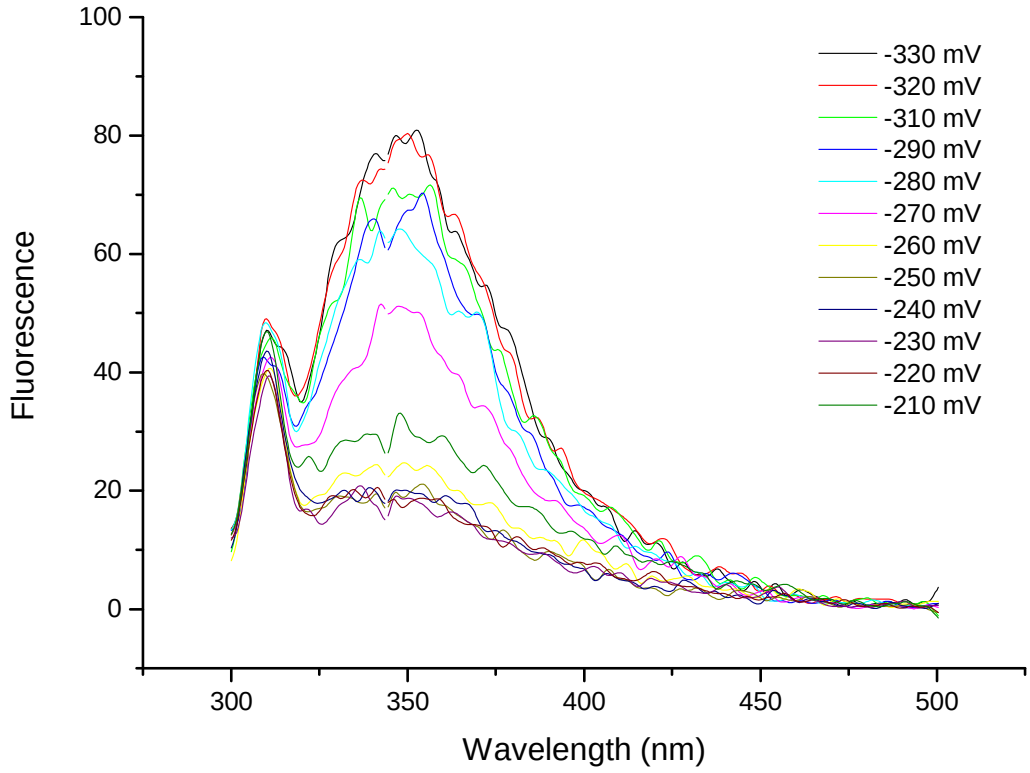

Figure 6.27. Fluorescence spectra of ScResA between -330 mV and – 210 mV. The electrochemical potential gradient was generated using oxidised and reduced DTT in 50 mM potassium phosphate buffer, pH 7. The samples were excited at 290 nm and fluorescence emission was recorded between 300 and 500 nm. The fluorescence at 344 nm increases as the electropotential decreases.

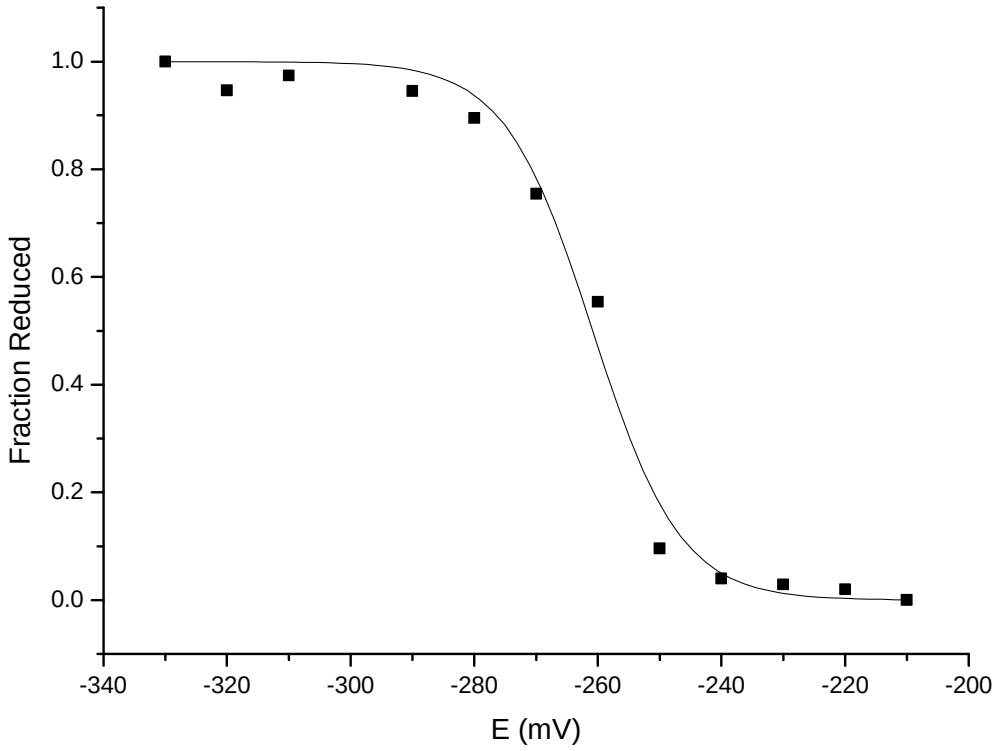

Figure 6.28. Determination of the ScResA reduction potential. Fluorescence at 344 nm was converted to fraction reduced and plotted as a function of electro potential between -330 mV and -210 mV. The fluorescence intensities at 344 nm decrease as the protein changes from the reduced to the oxidised forms. The solid line represents a fit of the data to Equation 6.5. This curve calculates that half of the protein is in the reduced form at -261 mV (±1).

The fluorescence at 344 nm was converted into fraction reduced and plotted as a function of cell electrochemical potential. This was fitted to Equation 6.5, a form of the Nernst equation, to give the reduction midpoint potential, where f_r is the fraction of the protein in the reduced form, E_h is the potential of the DTT couple, E_m is the midpoint is the midpoint potential of ScResA. The number of electrons involved in the reaction (n) was set to 2, the expected value for a TDOR. From the fit (Figure 6.28) the reduction potential of ScResA was calculated to be -261 mV (± 1) versus SHE at pH 7. This value is very close to that of BsResA, which

is -256 mV at pH 7 (19). This demonstrates that ScResA has a very low redox potential and is therefore likely to be a reducing TDOR that delivers electrons to its substrate target(s), for example, QcrC.

$$f_r = \frac{\exp((E_m - E_h)nF / RT)}{1 + \exp((E_m - E_h)nF / RT)} \qquad \text{(Equation 6.5)}$$

6.3.2.6. Stability studies of ScResA

To further investigate the stability of ScResA, guanidine hydrochloride was employed to unfold the protein in both oxidised and reduced forms. Unfolding of the protein in between 0 and 1 M guanidine was monitored through tryptophan fluorescence. ScResA was reduced with 1 mM DTT and oxidised with diamide which was removed by gel filtration before adding the protein to guanidine containing buffer. 0.1 µM of ResA was incubated for one hour in 50 mM potassium phosphate pH 7 containing between 0-1 M guanidine hydrochloride. Fluorescence spectra were measured between the wavelengths of 300 and 500 nm. As with the pH unfolding data, each measurement was repeated in triplicate. Fluorescence at 349 nm was converted to fraction folded, assuming the initial and final fluorescence intensities represented the folded and denatured forms of the protein, respectively, and plotted against guanidine hydrochloride concentration. Preliminary analysis suggested that ScResA is very sensitive to guanidine hydrochloride. In the reduced form it began to unfold as soon as the guanidine hydrochloride was added and did not begin to refold (in the reverse experiment) until guanidine hydrochloride falls to 0.1 M (Figure 6.29A). It appears that the protein is somewhat more stable in the oxidised form, where it does not begin to unfold until 0.25 M guanidine.

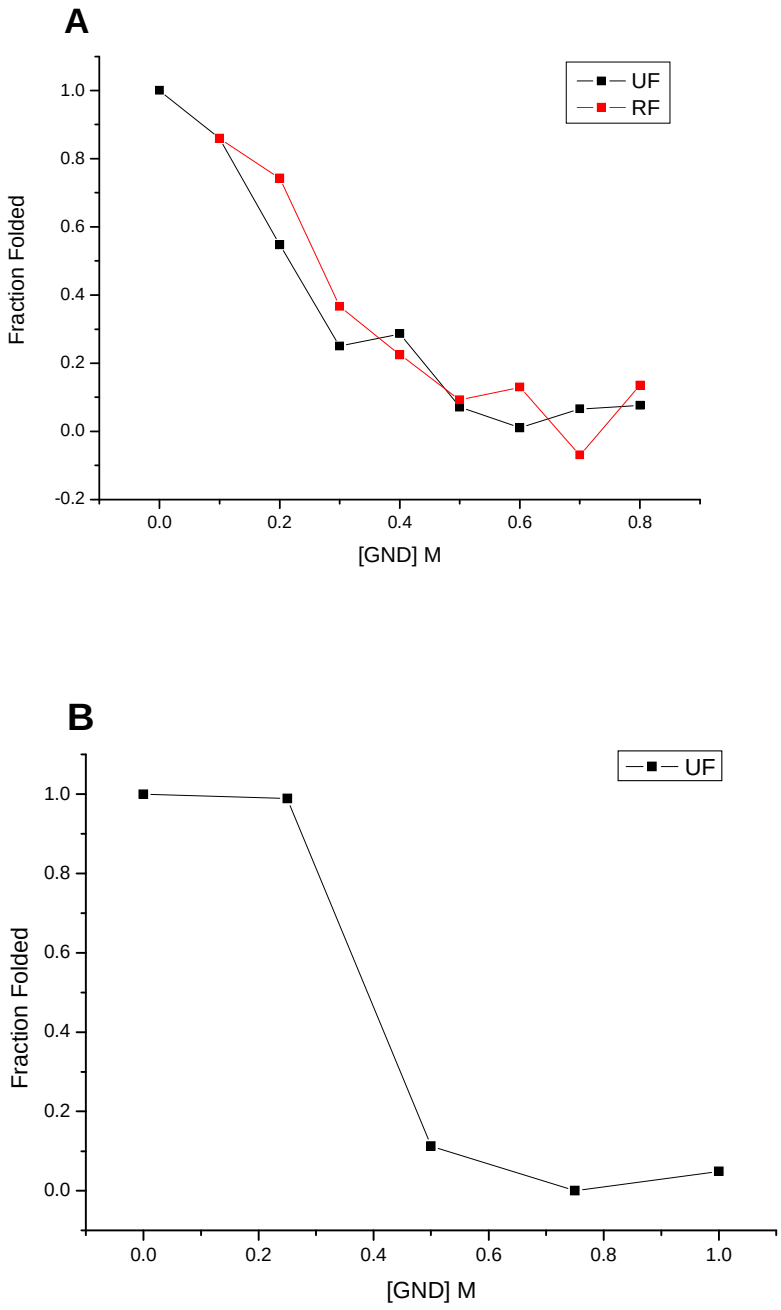

Figure 6.29. Unfolding and refolding of ScResA in guanidine hydrochloride. 0.1 µM ScResA was incubated at room temperature for one hour in 0-1 M guanidine hydrochloride (GND). The fluorescence spectra between 300-500 nm was recorded, fluorescence was most intense at 349 nm. The intensity of fluorescence at 349 nm was plotted as a function against guanidine hydrochloride concentration. Unfolding (UF) and refolding (RF) fluorescence of ScResA at 349 nm in the reduced (A) and oxidised (B) forms.

Due to a lack of protein it was not possible to repeat the unfolding or obtain data for the refolding of the oxidised protein (Figure 6.29B), This increase in stability in the oxidised form shows similarity with BsResA which is more stable in the oxidised form (14). In the case of oxidised BsResA, the increased stability of the oxidised protein contributes to the reducing power of the protein.

6.4. Discussion

It is quite clear from this work that the *res* operon is essential for the maturation of *S. coelicolor* QcrC. In *B. subtilis*, the entire *res* operon is involved in the production of cytochromes *c* but only ResB and ResC are essential; if the genes encoding these proteins are disrupted then the wild type phenotype cannot be recovered by other means (54). However, if only *resA* is inactive then the parental phenotype can be recovered by the addition of reductant to the growth medium or the inactivation of *bdbD* (12). As with *B. subtilis*, deletion of the *S. coelicolor res* genes did not affect growth or sporulation, which in turn demonstrates that QcrC is not required for growth or sporulation under laboratory conditions. However, *ccdA* was knocked out as part of the *res* operon in M145Δ*resA-C* and CcdA does play a role in spore synthesis in *B. subtilis* (8). This could suggest that CcdA in *S. coelicolor* is dedicated to CCM.

Although the M145Δ*qcr* did not grow as well or appear as healthy as wild type M145, this would appear to be due to the fact this strain is missing several genes, in addition to *qcrC*, that could be required for respiration, including several genes encoding proteins homologous to a cytochrome *c* oxidase (see Chapter 1).

A functioning cytochrome *bd* terminal oxidase would explain why the M145 was able to grow, if unhealthily, without a functioning *bc* complex or cytochrome *c* oxidase. The observed poor growth of M145Δ*qcr* suggests that *S. coelicolor* relies on cytochrome *c* oxidase more than *B. subtilis* for aerobic respiration, but further investigation of this is required.

Due to time constraints it was not possible to complement the *resA* or *res* operon deletions. Therefore, it cannot be absolutely concluded that *resA* deficiency alone is enough to block the maturation of QcrC. As the genes are arranged in an operon, it is not known whether the *resA* deletion had a polar affect on the down stream *ccdA*, *resB* and *resC* genes, blocking their transcription. Due to time restraints it was also not possible to 'flip' out the disruption cassette, leaving the 81 bps scar sequence. This would have confirmed whether deletion of *resA* alone is enough to stop maturation of QcrC, as the other genes of the operon would still be transcribed. There are many experiments remaining in order to further understand the role of Res CCM system II in *S. coelicolor*. When the disruption cassette that has replaced *resA* has been flipped out, it will be possible to complement the M145Δ*resA* with a wild type *resA* gene on a plasmid, knowing the *ccdA*, *resB* and *resC* genes are being transcribed to wild type level from the chromosome.

Attempts to over-produce and purify the soluble part of ScResA in the absence of a tag were unsuccessful. The protein was not produced at sufficiently high levels in BL21 DE3 and when enough protein was detected in the soluble, cytoplasmic fraction to warrant further purification, the protein appeared to deteriorate before

a pure sample could be obtained. The GST:ScResA construct did allow consistent overproduction and purification, but it still involved several stages and was not completely efficient. When compared with BL21 DE3, protein production was a lot greater in the specialist BL21 strains, Rosetta (Novagen) and CodonPlus(DE3)-RP (Stratagene), which can cope more easily with codons not commonly used by *E. coli* strains. Even so, there was GST:ResA to be found in the insoluble fraction after cell lysis. This could suggest that the protein was in inclusion bodies and, although protocols do exist to liberate soluble protein from inclusion bodies, there was enough ScResA available in the cytoplasm to purify and work with.

ScResA appears to have several features that are comparable to BsResA but also several surprising differences. At 6.9, the pK_a of the N-terminal cysteine of ScResA is a lot lower than that of BsResA, in which the pK_a of the N-terminal cysteine is between 8.5 and 9. In fact it is more similar to that of thioredoxin, which is in the range of 6.7-7.5 (4,6,15). ScResA only has one solvent exposed cysteine. BsResA, unlike many other TDORs, has both cysteines exposed to a degree that they can both simultaneously undergo modification with badan, although the N-terminal cysteine (C74) is more exposed than the C-terminal cysteine (C77) (15). ScResA will react with one only badan molecule, which resulted in fluorescence at about 544 nm, very close to the fluorescence of unbound badan at about 540 nm. This shows that the reactive cysteine thiol of ScResA is very well exposed. In the case of other TDORs, such as CcmG and BsResA, the N-terminal cysteine is the more exposed. This is an expected feature of ScResA as it appears to have a similar *in vivo* function. Although no

information has been revealed about the C-terminal cysteine from this study, it is likely that it has a much higher pK_a value, similar to that of thioredoxin (4).

As with BsResA, ScResA can not be reduced with glutathione, but does demonstrate a significant spectral change between the reduced and oxidised forms over an electrochemical potential gradient created with oxidised and reduced DTT. This spectral change allowed the determination of the reduction midpoint potential of ScResA as -261 mV. This very low reduction potential shows that it is likely to be a reducing protein similar to CycY from *B. japonicum* (-217 mV) and BsResA (-256 mV), which are both proposed to play similar roles in CCM, and in contrast to oxidising proteins such as *E. coli* DsbA (-89 mV) and *B. subtilis* BdbD (-75 mV) (19,27,136,137).

Guanidine-HCl unfolding studies suggested that ScResA is less stable in the reduced state, which is consistent with the findings for BsResA. But unlike BsResA, ScResA is extremely sensitive to guanidine-HCl and begins to unfold in concentrations as low 0.1 M whereas BsResA remains folded in 1 M to 1.5 M guanidine-HCl in the reduced and oxidised form respectively (19). ScResA does appear to be more stable with respect to pH, not unfolding until around pH 9, a value similar to that determined for BsResA (15). The instability of ScResA may have contributed to the failure of the early attempts to purify the protein in its native form. Several possible reasons exist for the instability of ScResA. The protein studied was engineered so as to purify it without its hydrophobic lipo-anchor; although BsResA is stable in its soluble form it is possible that the lipo-anchor domain may have a role in structural stability. It is also possible that

ResABC in *S. coelicolor* forms a tight CCM complex and ScResA needs to be in complex with ResB, ResC and possibly CcdA (which is transcribed from the same operon) for optimal stability.

Many of the unusual features that exist with BsResA, which separate it from other TDORs, are presumed to have evolved to allow the protein greater specificity toward its substrates. Many of these features do not exist with ScResA, making it in many ways more similar to the majority of known TDORs, which are often less substrate specific than BsResA. It might be that ScResA has substrates other than apo-cytochrome QcrC, and therefore must exhibit a wider substrate specificity. Alternatively, QcrC may be its only substrate and so the mechanisms by which it achieves its specificity might be distinct from those of BsResA, which must recognise four different substrates. Finally, it should also be noted that the Res proteins in *S. coelicolor* might form a super-complex that significantly affects the biophysical properties of ScResA.

Chapter 7: General discussion

This thesis describes the *in vitro* and *in vivo* properties of the TDOR ResA from both *B. subtilis* and *S. coelicolor*, which is involved in CCM in both organisms. For *B. subtilis* ResA, it has been shown that several key active-site and near active-site residues, identified through previous *in vitro* studies, are important for activity *in vivo*.

Chapter 3 describes how substitution of either/or both of the active site cysteines results in a complete loss of TDOR function and therefore CCM activity. Experiments using DTT in the growth medium to reduce the haem binding motif of the apo-cytochromes *c* to recover a *resA* deficient CCM negative phenotype in *B. subtilis* suggest that ResA may have a relatively minor role in chaperoning apo-cytochromes *c* to ResB and and ResC, the likely haem lyase apparatus. It may be that ResA, ResB and ResC form a complex and that ResA is important for the stability of this complex, therefore in the absence of ResA it could be expected that CCM would be less efficient. However, it must be concluded that the principle role of ResA in CCM is as a TDOR.

The active site amino acid residues of ResA are CEPC. Previous *in vitro* studies of the effect of substitutions of the active site residues on structure and function suggest that the proline (Pro76) is important for imparting structural rigidity within the active site, as well as having a role in maintaining the high pK_a values of the active site cysteines themselves (19). The lowered pK_a values of the active site cysteines combined with the lessened structural rigidity around the active site

in a ResA P76H mutant observed *in vitro* is likely to be the cause of a decrease in CCM observed *in vivo*. Structural observations showed that the histidine side chain of the ResA P76H variant was able to fold back into the hydrophobic cavity and interact with Glu80. Glu80 was shown to be very important for substrate recognition by ResA. Replacement of this glutamate with a glutamine (E80Q) resulted in defective CCM activity. Production of E80Q ResA in LUL9 resulted in the complete loss of detectable cytochromes *c*, QcrC, CccA and CccB, but partial maturation of CtaC was maintained. Although *in vitro* studies showed that the active site cysteines of soluble E80Q ResA had decreased pK_a values (15), this can only account for the decrease in CtaC activity and not the loss of the other three cytochromes *c* as the lowered pK_a values of the active site cysteines in P76H ResA did not appear to effect substrate specificity. CcdA and apo-cytochromes *c* are the only likely peptides that ResA will engage with via disulphide exchange. This specificity must be important for ResA function to avoid unnecessary reduction of disulphides in non-substrate proteins.

A near active site *cis*-configuration proline (Pro141) was also shown to be important for substrate recognition. LUL9 producing the Pro141 ResA variants P141S and P141T were partially defective in the maturation of CtaC and completely deficient in detectable QcrC, CccA and CccB. Pro141, like Glu80, falls within the hydrophobic cavity region, which is predicted to be important for substrate recognition from structural studies (14). The impaired substrate recognition of the ResA hydrophobic cavity variants is in agreement with this. Pro141 was shown to have an essential role in the stability of ResA due to the fact that the P141S and P141T variants degraded quickly after cell lysis. This is

in contrast to *E. coli* CcmG, in which a stable *cis*-proline variant was shown to have a similar structure but altered redox properties to the wild-type (18).

To further the understanding of the reactivity of the ResA active site it would be interesting to explore the *in vivo* activity of two other ResA active site variants, E75P and E75P/P76H. An E75P/P76H ResA variant would share the active site of *E. coli* DsbA, a highly oxidising TDOR. *In vitro* studies of the soluble form of this ResA variant demonstrated that the midpoint reduction potential was higher and pK_a values of the active cysteines were further decreased than either of the single residue variants (19), so it would be expected that E75P/P76H ResA would be less efficient than wild type ResA or the two single residue variants with regard to CCM.

ResA is attached to the external side of the cytoplasmic membrane by an N-terminal transmembrane anchor (12). Previous *in vitro* studies of ResA have been carried out on a soluble form of ResA that does not include the transmembrane anchor so very little about the importance of this region, outside of membrane attachment, is known (12,14,15,19). Chapter 4 presents data that demonstrates that the ResA N-terminal transmembrane anchor is important for efficient CCM in *B. subtilis*. A constructed protein featuring the transmembrane anchor of *B. subtilis* CccA fused to the soluble, catalytic domain of ResA demonstrated reduced CCM activity when produced in LUL9 when compared to wild type. This lowered activity occurred despite the protein being present in *B. subtilis* membranes at approximately four times the level as would be expected for ResA produced in the 1A1 wild type strain. The most likely cause for this is

that, in addition to tethering ResA to the membrane, the transmembrane anchor interacts with the integral membrane proteins ResB and ResC, which are highly likely to form a haem transport and lyase complex. ResA from *S. coelicolor* was extremely unstable under denaturing conditions leading to the conclusion that for good stability it is required to be in complex with the ResB and ResC of the *S. coelicolor* system. Although *B. subtilis* ResA is stable when purified it seems likely that precise interactions with ResB and ResC are important for efficient function, even if it is not necessary for these three proteins to form a complex. Another possible reason for the lower activity of the fusion protein compared to the wild type is the large amount produced. It was shown in Chapter 5 that over production of BdbD, an oxidising TDOR in *B. subtilis*, caused an imbalance between it and the protein responsible for maintaining its oxidised state, BdbC. In this scenario there was insufficient BdbC present in the membrane likely leading to an abnormally large amount of reduced BdbD compared to oxidised BdbD, which affected the net activity of BdbD. The ratio between ResA and CcdA would be abnormal where ResA is being produced to four times the level normally present in the wild type system, possibly leading to the proportion of oxidised ResA relative to reduced ResA having a detrimental effect on protein function. This seems plausible as wild type *resA* expressed from the same promoter as the CccA:ResA fusion protein in LUL9 led to a similar four-fold production level (12) and was demonstrated in Chapter 4 to only have about 60% activity compared to the wild type system in 1A1. If this was the case for the CccA:ResA fusion it can only account for some of the observed loss in activity.

The research presented in Chapter 5 aimed to provide *in vivo* insight into some of the key residues of *B. subtilis* BdbD. Due to the experimental system employed this was not possible but insight into the role of BdbD and the delicate balance of disulphide bond formation and reduction *in vivo* was unexpectedly gained. Over-production of BdbD in *B. subtilis* led to a phenotype similar to that of a BdbD deficient one. Experiments to test whether the over-production of BdbD would also lead to lack of competence development would be useful to further explore the over-produced BdbD phenotype as exists with a BdbD deficient phenotype (32). A different experimental system that can provide levels of BdbD production similar to that of the wild-type protein needs to be employed to investigate the *in vivo* role of BdbD.

Chapter 6 explores a homologue of *B. subtilis* ResA identified from genomic analysis in *S. coelicolor*. *S. coelicolor* has only one cytochrome *c*, a homologue of *B. subtilis* QcrC, which is produced in cells growing as mycelia in liquid medium. As *S. coelicolor* has a complex life cycle, with cells able to differentiate into different cell types, it would be very interesting to determine whether this cytochrome *c* is present at all stages of cell growth. In *B. subtilis*, cytochromes are present at their highest levels towards the end of the exponential growth phase (43). QcrC is part of the *bc* complex, similar to the bc_1 complex, which requires a second cytochrome *c* to channel electrons from it to the terminal oxidase. The mystery in *S. coelicolor* is that although it contains homologues of possible terminal oxidases, it contains no small cytochrome *c* other than QcrC. This could mean that QcrC is able to channel electrons directly to the terminal oxidase or possibly that QcrC in *S. coelicolor* is a redundant protein, an

evolutionary leftover from a no longer required *bc* complex. The *S. coelicolor qcr* knock-out used in this work did have slower growth than the wild type but this may have been due to other genes having been removed in addition to *qcrC*, including genes homologous to *B. subtilis* cytochrome *c* oxidase. This might suggest that the *S. coelicolor* cytochrome *c* oxidase is important (but not essential) and is fed electrons from a source other than the *bc* complex. Another possibility is that the *bc* complex can operate without the need for covalently bound haem. For these reasons it would be important to generate a *qcrC*-only knock-out in *S. coelicolor* to examine growth and respiration phenotypes.

Further experiments need to be carried out on the *S. coelicolor resA* and *resA-C* knock-out mutants. The *S. coelicolor res* operon also contains the *ccdA* gene suggesting that it is required for CCM only, whereas in *B. subtilis ccdA* is located elsewhere on the genome. In *B. subtilis* CcdA is required for several other functions outside of CCM, including the correct formation of the spore cortex (8). The *S. coelicolor resA-C* knock-out strain was able to produce viable spores, though these were not tested for viability after treatments that may destroy an unhealthy spore, such as heat and pH. The formation of *S. coelicolor* spores (sporophores) is distinct from the formation of the *B. subtilis* endospore but the reduction of disulphide bonds in the process may still be required to generate a fully viable sporophore.

As neither the *S. coelicolor* Δ*resA* nor the *S. coelicolor* Δ*resA-C* mutants were able to mature QcrC, further experiments are required to ensure this is a genuine phenotype. First, the *resA* and *resA-C* knock-out strains need to be

complemented with wild type *resA* or the *res* operon, respectively. Secondly, in *B. subtilis* a ResA (or CcdA) deficient phenotype can be recovered by the addition of DTT to the growth medium or deletion of *bdbD* but deficiency in either/or ResB or ResC cannot (12,24). Due to time restraints it was not possible to complement the knock-out strains or determine whether the CCM negative phenotype could be recovered by the addition of DTT or disruption to *bdbD*, even though a likely homologue of *bdbD* has been identified by sequence analysis. It would also be very interesting to see if *S. coelicolor* ResA could compliment LUL9. To minimise problems previously encountered expressing BdbD and CccA:ResA in *B. subtilis*, a hybrid proteins containing the *B. subtilis* transmembrane anchor with the solvent exposed redox active domain of *S. coelicolor* ResA should be used, expressed from pVK48 with the natural *B. subtilis resA* ribosome binding site.

Although it was demonstrated that *S. coelicolor* ResA plays a similar role to *B. subtilis* ResA in their respective organisms, *in vitro* studies of a purified soluble form of *S. coelicolor* ResA revealed some interesting differences. Both *S. coelicolor* ResA and *B. subtilis* ResA have similar low reduction potentials, -256 and -261 mV at pH 7, respectively (19). In *B. subtilis* ResA both cysteines of the active site are exposed and can simultaneously undergo modification by badan and both have pK_a values higher than 8 (15). *S. coelicolor* ResA, however, only possesses one cysteine that can undergo modification with badan and this has a pK_a of 6.9, making it more similar to *E. coli* thioredoxin, which has only the N-terminal cysteine exposed with a pK_a value between 6.7 and 7.5 (4,6).

Structural information is now required to further compare *S. coelicolor* ResA to *B. subtilis* ResA and *E. coli* thioredoxin. Many of the adaptations seen in *B. subtilis* ResA, such as the high pK_a values of the active site cysteines and the hydrophobic cavity, have been attributed to its requirement for substrate specificity, a specificity that has been demonstrated here by analysis of key residue variants of ResA *in vivo*. This specificity is required to ensure the efficient reduction of the haem binding motif of the four cytochromes *c* present in *B. subtilis*. *S. coelicolor* ResA only has one exposed cysteines, which has a lower pK_a than either of the *B. subtilis* ResA cysteines making *S. coelicolor* ResA more similar to the less-specific disulphide reducing proteins of *E. coli* and *B. subtilis*. It may be that *S. coelicolor* ResA does not share the specificity derterminants of *B. subtilis* ResA because it only needs to recognise one substrate. Structural studies would be able to identify other features of *S. coelicolor* ResA that would provide further insight into whether it might retain a similar level of specificity to its *B. subtilis* homologue, e.g. the identification of a hydrophobic cavity.

The work described here has verified the *in vivo* importance of key residues within *B. subtilis* ResA, a protein which has previously been identified as being essential to CCM in the bacterium. The identification and characterisation of the *B. subtilis* ResA homologue found in *S. coelicolor* will open a new avenue of research in CCM in *S. coelicolor*, an organism that has been well studied for its antibiotic production abilities and unusual cell differentiation but for which very little is known about its methods of respiration. The work presented here has also provided insight to CCM and the regulation of disulphide bond formation in *B. subtilis*.

8. References

1. Pan, J. L., and Bardwell, J. C. (2006) *Protein Science* **15**, 11
2. Holmgren, A., Söderberg, B. O., Eklund, H., and Brändén, C. I. (1975) *Proc Natl Acad Sci USA* **72**, 6
3. Aslund, F., Berndt, K. D., and Holmgren, A. (1997) *J Biol Chem* **272**, 30780-30786
4. Chivers, P. T., Prehoda, K. E., Volkman, B. F., Kim, B. M., Markley, J. L., and Raines, R. T. (1997) *Biochemistry* **36**, 14985-14991
5. Kallis, G. B., and Holmgren, A. (1980) *J Biol Chem* **255**, 10261-10265
6. Dillet, V., Dyson, H. J., and Bashford, D. (1998) *Biochemistry* **37**, 10298-10306
7. Moller, M. C., and Hederstedt, L. (2008) *J Bacteriol* **190**, 4660-4665
8. Schiott, T., and Hederstedt, L. (2000) *J Bacteriol* **182**, 2845-2854
9. Schiott, T., von Wachenfeldt, C., and Hederstedt, L. (1997) *J Bacteriol* **179**, 1962-1973
10. Schiott, T., Throne-Holst, M., and Hederstedt, L. (1997) *J Bacteriol* **179**, 4523-4529
11. Erlendsson, L. S., Moller, M., and Hederstedt, L. (2004) *J Bacteriol* **186**, 6230-6238
12. Erlendsson, L. S., Acheson, R. M., Hederstedt, L., and Le Brun, N. E. (2003) *J Biol Chem* **278**, 17852-17858
13. Hodson, C. T. C., Lewin, A., Hederstedt, L., and Le Brun, N. E. (2008) *J Bacteriol* **190**, 4697-4705
14. Crow, A., Acheson, R. M., Le Brun, N. E., and Oubrie, A. (2004) *J Biol Chem* **279**, 23654-23660
15. Lewin, A., Crow, A., Oubrie, A., and Le Brun, N. E. (2006) *J Biol Chem* **281**, 35467-35477
16. Kadokura, H., Tian, H., Zander, T., Bardwell, J. C., and Beckwith, J. (2004) *Science* **303**, 534-537
17. Charbonnier, J. B., Belin, P., Moutiez, M., Stura, E. A., and Quemeneur, E. (1999) *Protein Sci* **8**, 96-105
18. Ouyang, N., Gao, Y. G., Hu, H. Y., and Xia, Z. X. (2006) *Proteins* **65**, 1021-1031
19. Lewin, A., Crow, A., Hodson, C. T. C., Hederstedt, L., and Le Brun, N. E. (2008) *Biochem. J.* **414**, 81-91
20. Kortemme, T., Darby, N. J., and Creighton, T. E. (1996) *Biochemistry* **35**, 14503-14511
21. Mossner, E., Huber-Wunderlich, M., and Glockshuber, R. (1998) *Protein Sci* **7**, 1233-1244
22. Huber-Wunderlich, M., and Glockshuber, R. (1998) *Fold Des* **3**, 161-171
23. Roos, G., Garcia-Pino, A., Van Belle, K., Brosens, E., Wahni, K., Vandenbussche, G., Wyns, L., Loris, R., and Messens, J. (2007) *J Mol Biol* **368**, 800-811
24. Erlendsson, L. S., and Hederstedt, L. (2002) *J Bacteriol* **184**, 1423-1429
25. Meima, R., Eschevins, C., Fillinger, S., Bolhuis, A., Hamoen, L. W., Dorenbos, R., Quax, W. J., van Dijl, J. M., Provvedi, R., Chen, I., Dubnau, D., and Bron, S. (2002) *J Biol Chem* **277**, 6994-7001
26. Dorenbos, R., Stein, T., Kabel, J., Bruand, C., Bolhuis, A., Bron, S., Quax, W. J., and Van Dijl, J. M. (2002) *J Biol Chem* **277**, 16682-16688

27. Crow, A., Lewin, A., Hecht, O., Carlsson Moller, M., Moore, G. R., Hederstedt, L., and Le Brun, N. E. (2009) *J Biol Chem* **284**, 23719-33
28. Bardwell, J. C., McGovern, K., and Beckwith, J. (1991) *Cell* **67**, 581-589
29. Kadokura, H., Nichols, L., 2nd, and Beckwith, J. (2005) *J Bacteriol* **187**, 1519-1522
30. Bardwell, J. C., Lee, J. O., Jander, G., Martin, N., Belin, D., and Beckwith, J. (1993) *Proc Natl Acad Sci U S A* **90**, 1038-1042
31. Draskovic, I., and Dubnau, D. (2005) *Mol Microbiol* **55**, 881-896
32. Bolhuis, A., Venema, G., Quax, W. J., Bron, S., and van Dijl, J. M. (1999) *J Biol Chem* **274**, 24531-24538
33. Sone, M., Kishigami, S., Yoshihisa, T., and Ito, K. (1997) *J Biol Chem* **272**, 6174-6178
34. Kouwen, T. R., van der Goot, A., Dorenbos, R., Winter, T., Antelmann, H., Plaisier, M. C., Quax, W. J., van Dijl, J. M., and Dubois, J. Y. (2007) *Mol Microbiol* **64**, 984-999
35. Ishihara, T., Tomita, H., Hasegawa, Y., Tsukagoshi, N., Yamagata, H., and Udaka, S. (1995) *J Bacteriol* **177**, 745-749
36. Paik, S. H., Chakicherla, A., and Hansen, J. N. (1998) *J Biol Chem* **273**, 23134-23142
37. Dumoulin, A., Grauschopf, U., Bischoff, M., Thony-Meyer, L., and Berger-Bachi, B. (2005) *Arch Microbiol* **184**, 117-128
38. Piggot, P. J., and Hilbert, D. W. (2004) *Curr Opin Microbiol* **7**, 579-586
39. Crow, A., Liu, Y., Carlsson Moller, M., Le Brun, N. E., and Hederstedt, L. (2009) *J Biol Chem*
40. Eichenberger, P., Jensen, S. T., Conlon, E. M., van Ooij, C., Silvaggi, J., Gonzalez-Pastor, J. E., Fujita, M., Ben-Yehuda, S., Stragier, P., Liu, J. S., and Losick, R. (2003) *J Mol Biol* **327**, 945-972
41. Imamura, D., Kobayashi, K., Sekiguchi, J., Ogasawara, N., Takeuchi, M., and Sato, T. (2004) *J Bacteriol* **186**, 5450-5459
42. Kadokura, H., Katzen, F., and Beckwith, J. (2003) *Annu Rev Biochem* **72**, 111-135
43. von Wachenfeldt, C., and Hederstedt, L. (1992) *FEMS Microbiol Lett* **79**, 91-100
44. Giege, P., Grienenberger, J. M., and Bonnard, G. (2008) *Mitochondrion* **8**, 61-73
45. Allen, J. W., Ginger, M. L., and Ferguson, S. J. (2005) *Biochem Soc Trans* **33**, 145-146
46. Stevens, J. M., Daltrop, O., Allen, J. W., and Ferguson, S. J. (2004) *Acc Chem Res* **37**, 999-1007
47. Schagger, H. (2002) *Biochim Biophys Acta* **1555**, 154-159
48. Kranz, R., Lill, R., Goldman, B., Bonnard, G., and Merchant, S. (1998) *Mol Microbiol* **29**, 383-396
49. von Wachenfeldt, C., and Hederstedt, L. (1990) *FEBS Lett* **270**, 147-151
50. von Wachenfeldt, C., and Hederstedt, L. (1990) *J Biol Chem* **265**, 13939-13948
51. Bengtsson, J., Rivolta, C., Hederstedt, L., and Karamata, D. (1999) *J Biol Chem* **274**, 26179-26184
52. Bengtsson, J., Tjalsma, H., Rivolta, C., and Hederstedt, L. (1999) *J Bacteriol* **181**, 685-688
53. Yu, J., and Le Brun, N. E. (1998) *J Biol Chem* **273**, 8860-8866

54. Le Brun, N. E., Bengtsson, J., and Hederstedt, L. (2000) *Mol Microbiol* **36**, 638-650
55. Trumpower, B. L. (1990) *Microbiol Rev* **54**, 101-129
56. Yu, J., Hederstedt, L., and Piggot, P. J. (1995) *J Bacteriol* **177**, 6751-6760
57. Crofts, A. R., Lhee, S., Crofts, S. B., Cheng, J., and Rose, S. (2006) *Biochim Biophys Acta* **1757**, 1019-1034
58. Shin, I., Ryu, H. B., Yim, H. S., and Kang, S. O. (2005) *J Microbiol* **43**, 244-250
59. Wilson, A. C., Hoch, J. A., and Perego, M. (2009) *Mol Microbiol* **72**, 109-123
60. Santana, M., Kunst, F., Hullo, M. F., Rapoport, G., Danchin, A., and Glaser, P. (1992) *J Biol Chem* **267**, 10225-10231
61. Namslauer, A., and Brzezinski, P. (2004) *FEBS Lett* **567**, 103-110
62. Saraste, M., Metso, T., Nakari, T., Jalli, T., Lauraeus, M., and Van der Oost, J. (1991) *Eur J Biochem* **195**, 517-525
63. Liu, X., and Taber, H. W. (1998) *J Bacteriol* **180**, 6154-6163
64. Mueller, J. P., and Taber, H. W. (1989) *J Bacteriol* **171**, 4967-4978
65. Haltia, T., Saraste, M., and Wikstrom, M. (1991) *EMBO J* **10**, 2015-2021
66. Sun, G., Sharkova, E., Chesnut, R., Birkey, S., Duggan, M. F., Sorokin, A., Pujic, P., Ehrlich, S. D., and Hulett, F. M. (1996) *J Bacteriol* **178**, 1374-1385
67. Winstedt, L., and von Wachenfeldt, C. (2000) *J Bacteriol* **182**, 6557-6564
68. Daltrop, O., Allen, J. W., Willis, A. C., and Ferguson, S. J. (2002) *Proc Natl Acad Sci U S A* **99**, 7872-7876
69. Cianciotto, N. P., Cornelis, P., and Baysse, C. (2005) *Mol Microbiol* **56**, 1408-1415
70. Page, M. D., Sambongi, Y., and Ferguson, S. J. (1998) *Trends Biochem Sci* **23**, 103-108
71. Richard-Fogal, C. L., Frawley, E. R., Bonner, E. R., Zhu, H., San Francisco, B., and Kranz, R. G. (2009) *EMBO J* **28**, 2349-2359
72. Ahuja, U., and Thony-Meyer, L. (2003) *J Biol Chem* **278**, 52061-52070
73. Schulz, H., Fabianek, R. A., Pellicioli, E. C., Hennecke, H., and Thony-Meyer, L. (1999) *Proc Natl Acad Sci U S A* **96**, 6462-6467
74. Sanders, C., Boulay, C., and Daldal, F. (2007) *J Bacteriol* **189**, 789-800
75. Fabianek, R. A., Hennecke, H., and Thony-Meyer, L. (1998) *J Bacteriol* **180**, 1947-1950
76. Edeling, M. A., Ahuja, U., Heras, B., Thony-Meyer, L., and Martin, J. L. (2004) *J Bacteriol* **186**, 4030-4033
77. Rozhkova, A., Stirnimann, C. U., Frei, P., Grauschopf, U., Brunisholz, R., Grutter, M. G., Capitani, G., and Glockshuber, R. (2004) *EMBO J* **23**, 1709-1719
78. Stirnimann, C. U., Rozhkova, A., Grauschopf, U., Grutter, M. G., Glockshuber, R., and Capitani, G. (2005) *Structure* **13**, 985-993
79. Stevens, J. M., Gordon, E. H., and Ferguson, S. J. (2004) *FEBS Lett* **576**, 81-85
80. Ito, K., and Inaba, K. (2008) *Curr Opin Struct Biol* **18**, 450-458
81. Inaba, K., Murakami, S., Suzuki, M., Nakagawa, A., Yamashita, E., Okada, K., and Ito, K. (2006) *Cell* **127**, 789-801
82. Kadokura, H., and Beckwith, J. (2002) *EMBO J* **21**, 2354-2363

83. Bader, M., Muse, W., Ballou, D. P., Gassner, C., and Bardwell, J. C. (1999) *Cell* **98**, 217-227
84. Paul, S., Zhang, X., and Hulett, F. M. (2001) *J Bacteriol* **183**, 3237-3246
85. Ahuja, U., Kjelgaard, P., Schulz, B. L., Thony-Meyer, L., and Hederstedt, L. (2009) *Mol Microbiol* **73**, 1058-1071
86. Frawley, E. R., and Kranz, R. G. (2009) *Proc Natl Acad Sci U S A* **106**, 10201-10206
87. Feissner, R. E., Richard-Fogal, C. L., Frawley, E. R., Loughman, J. A., Earley, K. W., and Kranz, R. G. (2006) *Mol Microbiol* **60**, 563-577
88. Crow, A., Le Brun, N. E., and Oubrie, A. (2005) *Biochem Soc Trans* **33**, 149-151
89. Hamel, P., Corvest, V., Giege, P., and Bonnard, G. (2009) *Biochim Biophys Acta* **1793**, 125-138
90. Diekert, K., de Kroon, A. I., Ahting, U., Niggemeyer, B., Neupert, W., de Kruijff, B., and Lill, R. (2001) *EMBO J* **20**, 5626-5635
91. Bernard, D. G., Quevillon-Cheruel, S., Merchant, S., Guiard, B., and Hamel, P. P. (2005) *J Biol Chem* **280**, 39852-39859
92. Pollock, W. B., Rosell, F. I., Twitchett, M. B., Dumont, M. E., and Mauk, A. G. (1998) *Biochemistry* **37**, 6124-6131
93. Allen, J. W., Jackson, A. P., Rigden, D. J., Willis, A. C., Ferguson, S. J., and Ginger, M. L. (2008) *FEBS J* **275**, 2385-2402
94. Kuras, R., Saint-Marcoux, D., Wollman, F. A., and de Vitry, C. (2007) *Proc Natl Acad Sci U S A* **104**, 9906-9910
95. Allen, J. W., Ginger, M. L., and Ferguson, S. J. (2004) *Biochem J* **383**, 537-542
96. Fulop, V., Sam, K. A., Ferguson, S. J., Ginger, M. L., and Allen, J. W. (2009) *FEBS J* **276**, 2822-2832
97. Hopwood, D. A. (1999) *Microbiology* **145 (Pt 9)**, 2183-2202
98. Flardh, K., and Buttner, M. J. (2009) *Nat Rev Microbiol* **7**, 36-49
99. van Keulen, G., Alderson, J., White, J., and Sawers, R. G. (2005) *Biochem Soc Trans* **33**, 210-212
100. Bentley, S. D., Chater, K. F., Cerdeno-Tarraga, A. M., Challis, G. L., Thomson, N. R., James, K. D., Harris, D. E., Quail, M. A., Kieser, H., Harper, D., Bateman, A., Brown, S., Chandra, G., Chen, C. W., Collins, M., Cronin, A., Fraser, A., Goble, A., Hidalgo, J., Hornsby, T., Howarth, S., Huang, C. H., Kieser, T., Larke, L., Murphy, L., Oliver, K., O'Neil, S., Rabbinowitsch, E., Rajandream, M. A., Rutherford, K., Rutter, S., Seeger, K., Saunders, D., Sharp, S., Squares, R., Squares, S., Taylor, K., Warren, T., Wietzorrek, A., Woodward, J., Barrell, B. G., Parkhill, J., and Hopwood, D. A. (2002) *Nature* **417**, 141-147
101. Newton, G. L., Arnold, K., Price, M. S., Sherrill, C., Delcardayre, S. B., Aharonowitz, Y., Cohen, G., Davies, J., Fahey, R. C., and Davis, C. (1996) *J Bacteriol* **178**, 1990-1995
102. Stefankova, P., Perecko, D., Barak, I., and Kollarova, M. (2006) *J Basic Microbiol* **46**, 47-55
103. Stefankova, P., Maderova, J., Barak, I., Kollarova, M., and Otwinowski, Z. (2005) *Acta Crystallogr Sect F Struct Biol Cryst Commun* **61**, 164-168
104. Hutchings, M. I., Palmer, T., Harrington, D. J., and Sutcliffe, I. C. (2009) *Trends Microbiol* **17**, 13-21
105. Yanisch-Perron, C., Vieira, J., and Messing, J. (1985) *Gene* **33**, 103-119

106. Datsenko, K. A., and Wanner, B. L. (2000) *Proc Natl Acad Sci U S A* **97**, 6640-6645
107. MacNeil, D. J., Gewain, K. M., Ruby, C. L., Dezeny, G., Gibbons, P. H., and MacNeil, T. (1992) *Gene* **111**, 61-68
108. Cherepanov, P. P., and Wackernagel, W. (1995) *Gene* **158**, 9-14
109. Stragier, P., Bonamy, C., and Karmazyn-Campelli, C. (1988) *Cell* **52**, 697-704
110. Gust, B., Challis, G. L., Fowler, K., Kieser, T., and Chater, K. F. (2003) *Proc Natl Acad Sci U S A* **100**, 1541-1546
111. Redenbach, M., Kieser, H. M., Denapaite, D., Eichner, A., Cullum, J., Kinashi, H., and Hopwood, D. A. (1996) *Mol Microbiol* **21**, 77-96
112. Hoch, J. A. (1991) *Methods Enzymol* **204**, 305-320
113. Hederstedt, L. (1986) *Methods Enzymol* **126**, 399-414
114. Stoscheck, C. M. (1990) *Methods Enzymol* **182**, 50-68
115. Laemmli, U. K. (1970) *Nature* **227**, 680-685
116. Schagger, H., and von Jagow, G. (1987) *Anal Biochem* **166**, 368-379
117. Towbin, H., Staehelin, T., and Gordon, J. (1979) *Proc Natl Acad Sci U S A* **76**, 4350-4354
118. Margoliash, E. W., O.F. (1967) *Methods Enzymol* **10**, 339-349
119. van der Oost, J., von Wachenfeld, C., Hederstedt, L., and Saraste, M. (1991) *Mol Microbiol* **5**, 2063-2072
120. Kulmacz, R. J., and Lands, W. E. (1983) *Prostaglandins* **25**, 531-540
121. Lin, T. Y., and Kim, P. S. (1989) *Biochemistry* **28**, 5282-5287
122. Krause, G., and Holmgren, A. (1991) *J Biol Chem* **266**, 4056-4066
123. Reid, E., Cole, J., and Eaves, D. J. (2001) *Biochem J* **355**, 51-58
124. Colbert, C. L., Wu, Q., Erbel, P. J., Gardner, K. H., and Deisenhofer, J. (2006) *Proc Natl Acad Sci U S A* **103**, 4410-4415
125. Ahuja, U., and Thony-Meyer, L. (2006) *FEBS Lett* **580**, 216-222
126. Dailey, F. E., and Berg, H. C. (1993) *Proc Natl Acad Sci U S A* **90**, 1043-1047
127. Heras, B., Shouldice, S. R., Totsika, M., Scanlon, M. J., Schembri, M. A., and Martin, J. L. (2009) *Nat Rev Microbiol* **7**, 215-225
128. Yamanaka, H., Kameyama, M., Baba, T., Fujii, Y., and Okamoto, K. (1994) *J Bacteriol* **176**, 2906-2913
129. Aslund, F., and Beckwith, J. (1999) *J Bacteriol* **181**, 1375-1379
130. Martin, J. L., Bardwell, J. C., and Kuriyan, J. (1993) *Nature* **365**, 464-468
131. McDonald, I. R., Riley, P. W., Sharp, R. J., and McCarthy, A. J. (1995) *J Appl Bacteriol* **79**, 213-218
132. Okamoto, A., Kosugi, A., Koizumi, Y., Yanagida, F., and Udaka, S. (1997) *Biosci Biotechnol Biochem* **61**, 202-203
133. Turgeon, N., Laflamme, C., Ho, J., and Duchaine, C. (2006) *J Microbiol Methods* **67**, 543-548
134. Baudin, A., Ozier-Kalogeropoulos, O., Denouel, A., Lacroute, F., and Cullin, C. (1993) *Nucleic Acids Res* **21**, 3329-3330
135. Riddles, P. W., Blakeley, R. L., and Zerner, B. (1983) *Methods Enzymol* **91**, 49-60
136. Fabianek, R. A., Huber-Wunderlich, M., Glockshuber, R., Kunzler, P., Hennecke, H., and Thony-Meyer, L. (1997) *J Biol Chem* **272**, 4467-4473
137. Wunderlich, M., and Glockshuber, R. (1993) *Protein Sci* **2**, 717-726